

Copyright  
by  
Marshall Hunter Joyce  
2018

**The Dissertation Committee for Marshall Hunter Joyce Certifies that this is the  
approved version of the following Dissertation:**

**Physical Forces from the Extracellular Matrix Influence Breast Cancer  
Cell Response to Doxorubicin**

**Committee:**

Amy Brock, Supervisor

Marissa Nichole Rylander

Laura Suggs

Janet Zoldan

**Physical Forces from the Extracellular Matrix Influence Breast Cancer  
Cell Response to Doxorubicin**

**by**

**Marshall Hunter Joyce**

**Dissertation**

Presented to the Faculty of the Graduate School of

The University of Texas at Austin

in Partial Fulfillment

of the Requirements

for the Degree of

**Doctor of Philosophy**

**The University of Texas at Austin**

**December 2018**

## **Acknowledgements**

This thesis work would not have been possible without the combined efforts of many talented individuals. First, my mentor, Dr. Amy Brock deserves all the credit I can possibly give her for guiding me through my thesis research. She provided me the freedom to explore and solve scientific problems independently along with enough guidance to keep me focused and on track. Working with her and the students in her lab has taught me to think like a scientist. I am truly grateful for all of her assistance, guidance, and direction. I also would like to thank all the members of my dissertation committee: Dr. (Marissa) Nichole Rylander, Dr. Laura Suggs, and Dr. Janet Zoldan. Their thoughtful and constructive suggestions deepened my understanding of science and helped me avoid many potential detours in research. All of my committee members were so kind-hearted, knowledgeable, and truly wanted to help me become the best scientist possible; I couldn't have had a better group of professors supporting and challenging me. I would especially like to thank Dr. Suggs for allowing me to work in her lab and for taking the time from her busy schedule to meet with me and help me analyze data and troubleshoot problems. I'd also like to extend special thanks to Shane Allen from Dr. Suggs' lab. He trained me on many techniques and assays, and he was always happy to answer questions or lend me a hand if I was overwhelmed. I'm very fortunate to have worked with such smart and talented individuals in our lab. They were all such a joy to work with and helped me talk through the day-to-day issues that arose. I'd like to thank Grant Howard for helping me with all of my chemotherapeutic dosing and cell culture work; Kaitlyn Johnson for her immense help with the mathematical modeling in Chapter 4; Russell Durrett for helping with data analysis; Aziz Al'Khafaji, Eric Brenner, Daylin Morgan, and Millie Clark for advice and troubleshooting. There were also many undergraduates that I had the pleasure of working

with throughout my graduate studies that helped me in many facets: Carolyn Lu, Emily James, Rachel Hegab, Adán Rodríguez, Tahir Haideri, and Joshua Krachman. Last but certainly not least, I am sincerely grateful for the support from my family. They may not always have understood exactly what I was working on, but they were proud of me nonetheless and never let me get too down on myself. Without the loving support of Mom, Dad, and my wonderful girlfriend Sarah, I don't know if I would have had the mental fortitude to go on through the rough patches. Thank you all so much for your contributions and for helping me throughout my graduate studies.

## **Abstract**

### **Physical Forces from the Extracellular Matrix Influence Breast Cancer Cell Response to Doxorubicin**

Marshall Hunter Joyce, PhD

The University of Texas at Austin, 2018

Supervisor: Amy Brock

Cancer is a complex disease capable of affecting multiple organs and is driven by numerous factors. Certain ‘hallmarks of cancer’ have been identified which describe biological conditions that lead to tumor development and characteristics that often follow tumorigenesis. These hallmarks have been revisited to describe the role that the extracellular matrix (ECM) plays in each. Such observations make it evident that the ECM is an important factor in tumor initiation, progression, and metastasis and can no longer be ignored in the search for a cure. Studies aimed at characterizing the role physical cues play in tumor development have considered ligand variety, ligand density, substrate composition, and substrate stiffness. These studies frequently utilize hydrogels as a culture platform given the biological relevance and diversity achievable through such a platform. Though the stiffness of hydrogels can be attenuated at the onset of an experiment, few systems are able to alter stiffness once gelation is complete. This makes any study of progressive changes in ECM stiffness difficult and largely restricts the study of certain temporal aspects of tumor progression *in vitro*. Recently, a Matrigel-alginate hydrogel system has been described whereby progressive modulation of hydrogel stiffness can be

achieved using liposomes loaded with gold nanorods and near infrared light. In this study we utilize this hydrogel system to thoroughly investigate the role that ECM stiffness has on breast cancer response to doxorubicin. We sought to observe how progressive stiffening of the ECM affected breast cancer cell response to clinically relevant chemotherapeutics in a system that allows for minimal perturbation of cells during the stiffening process. Our results showed that breast cancer cells exhibiting a mesenchymal phenotype had a stiffness-dependent resistance to the chemotherapeutic doxorubicin. Mathematical modeling was used to determine reduced growth rate alone was not sufficient to explain this stiffness-dependent resistance, suggesting an additional mechanism associated with the mesenchymal phenotype is responsible.

## Table of Contents

List of Tables .....	xi
List of Figures .....	xii
Chapter 1: Introduction .....	1
1.1 The Extracellular Matrix.....	1
1.2 Extracellular matrix plays crucial roles in physiology, development, and disease .....	4
1.3 Cells share a reciprocal signaling relationship with their extracellular matrix.....	6
1.4 Resistance to chemotherapeutic treatments .....	6
1.5 The extracellular matrix influences how tumor cells will respond to chemotherapeutic treatment .....	8
Chapter 2: Characterization of Breast Cancer Cell Resistance to Chemotherapeutics in Alginate Hydrogels .....	25
2.1 Introduction.....	25
2.2 materials and methods .....	27
2.2.1 Cell culture.....	27
2.2.2 Hydrogel preparation .....	28
2.2.3 Rheometry.....	28
2.2.4 Dosing with chemotherapeutics.....	28
2.2.5 Isolation of cells from hydrogels .....	29
2.2.6 Measuring viability .....	29
2.3 Results.....	29
2.3.1 An alginate hydrogel platform can be used to make ECM models of varying stiffness.....	29
2.3.2 Characterization of mammary epithelial carcinoma cells to chemotherapeutic response in monolayer cultures .....	31



2.3.3 Characterization of mammary epithelial carcinoma cells to chemotherapeutic response in alginate hydrogel cultures .....	32
2.3.4 Acute responses to changes in ECM stiffness increase resistance to doxorubicin .....	32
2.4 Discussion.....	33
2.5 Conclusions.....	35
Chapter 3: Characterization of Breast Cancer Cell Response to Chemotherapeutics in Dynamic Stiffened Hydrogels.....	49
3.1 Introduction.....	49
3.2 Materials and Methods.....	51
3.2.1 Liposome preparation .....	51
3.2.2 Hydrogel preparation .....	52
3.2.3 Dynamic stiffening of alginate hydrogels.....	52
3.2.4 Statistical analysis.....	53
3.3 Results.....	53
3.4 Discussion.....	55
3.5 Conclusions.....	56
Chapter 4: Molecular Characterization of Breast Cancer Cells Cultured in Soft and Stiff Hydrogels.....	62
4.1 Introduction.....	62
4.2 Materials and Methods.....	64
4.2.1 Staining for EMT markers .....	64
4.2.2 Quantitative real-time PCR.....	64
4.2.3 Statistical Analysis and Mathematical Modeling .....	65
4.3 Results.....	65

4.3.1 Expression of EMT Markers.....	65
4.3.2 Increasing hydrogel stiffness leads to nuclear localization of YAP ....	66
4.3.3 Mathematical models suggests stiffness-induced resistance to doxorubicin is not fully explained by changes in proliferation rates.....	66
4.4 Discussion.....	67
4.5 Conclusion .....	68
Appendix.....	81
References.....	84
Chapter 1 .....	84
Chapter 2.....	96
Chapter 3.....	99
Chapter 4.....	101

## List of Tables

<b>Table 1.1 – ECM stiffness varies across tissue types.</b> Tissue stiffness measurements acquired from numerous methods are summarized here according to tissue type. The values displayed represent the tissue's measured Young's Modulus (E). Stiffness of tissue types varies drastically across the body to facilitate the differing physiological functions necessary for survival. This table is adapted from Gautier et al. <sup>38</sup> .....	10
<b>Table A1 – Doxorubicin sensitivity for MCF7 and 231 across culture conditions.</b> Dose response curves of 231 and MCF7 cells cultured in static hydrogels, dynamic hydrogels, and monolayer culture conditions following 48h exposure to Doxorubicin. Live and Dead cells were counted using a Nexcelom Cellometer with AOPI stain. ....	82

## List of Figures

- Fig. 1.1 – Canonical YAP pathway.** YAP is a component of the Hippo signaling pathway. Phosphorylated (red) YAP remains in the cell cytoplasm where it is inactive. YAP is ubiquitinated (yellow) by  $\beta$ -TrCP which signals it for proteasome degradation. If Lats1/2 is inhibited and YAP remains unphosphorylated, it translocates to the nucleus where it acts as a transcriptional co-activator. ....11
- Fig. 2.1 – Cells were cultured in hydrogels of varying stiffness before treatment with doxorubicin. a).** Hydrogel stiffness was determined by calculating Young's modulus from frequency sweep measurements obtained from a rheometer. Error bars represent a 95% confidence interval as determined by a Student's t-test distribution. The experimental protocol is outlined in **b)**. Briefly, cells were seeded onto tissue culture plastic or into hydrogels that ranged in stiffness from 450 to 2,000 Pa. After 6 days in culture, samples were exposed to doxorubicin for 48h and cell viability was determined using AOPI staining.....36
- Fig. 2.2 – Cells were cultured as a 2D monolayer and exposed to doxorubicin or paclitaxel.** MDA-MB-231 and MCF7 cells were cultured as a 2D monolayer and exposed to doxorubicin or paclitaxel for 48 h. **a)** MDA-MB-231 cultures were found to be more resistant to doxorubicin (LD50 = 26.6  $\mu$ M) than **b)** paclitaxel (LD50 = 94 nM). **c)** MCF7 cultures were also found to be more resistant to doxorubicin (LD50 = 4.4  $\mu$ M) than similar **d)** MCF7 cultures treated with paclitaxel (LD50 = 126 nM). ....37

<b>Fig. 2.3 – Additional cell lines were cultured as a 2D monolayer and challenged with doxorubicin.</b> Additional mammary epithelial carcinoma cell lines were cultured as 2D monolayers and exposed to doxorubicin for 24 and 48 h before assaying for cell viability. MDA-MB-231 and Py2T cell lines were found to be more resistant to doxorubicin than the TMEC, M6, or M6c cell lines. ....	38
<b>Fig. 2.4 – Dose response curves of a) MDA-MB-231, b) MCF7, c) M6, d) M6c, e) TMEC, f) Py2T, g) Py2T-LT following 48h exposure to Doxorubicin.</b> All cells were cultured in 450 Pa alginate-Matrigel hydrogels for 8 days before being exposed to Doxorubicin. Live and Dead cells were counted using a Nexcelom Cellometer with AOPI stain. ....	39
<b>Fig. 2.5 – Dose response curves of a) MDA-MB-231, b) MCF7, c) M6, d) M6c, e) TMEC, f) Py2T, g) Py2T-LT following 48h exposure to Doxorubicin.</b> All cells were cultured in 2,000 Pa alginate-Matrigel hydrogels for 8 days before Doxorubicin exposure. Live and Dead cells were counted using a Nexcelom Cellometer with AOPI stain. ....	40
<b>Fig. 2.6 – 231 cells have a stiffness-dependent resistance to doxorubicin.</b> Dose response curves of 231 and MCF7 cells cultured in a,b) 450 Pa hydrogel, c,d) 2,000 Pa hydrogel, and e,f) 2D monolayer following 48h exposure to Doxorubicin. Percent cell death was determined by staining samples with AOPI and counting live cells using a Nexcelom Cellometer. ....	41

**Fig. 2.7 – Shorter acclimation time gives temporary increase in doxorubicin resistance.** LD50 values of **a)** MDA-MB-231 and **b)** MCF7 cells cultured in 450 Pa hydrogel or 2,000 Pa hydrogel for 24, 72, or 120 h before a 48 h exposure to doxorubicin. Percent cell death was determined by staining samples with AOPI and counting live cells using a Nexcelom Cellometer.....42

**Fig. 2.8 – Inclusion of D-(+)-Gluconic acid  $\delta$ -lactone in hydrogel mixture does not adversely affect cell viability.** Cells were cultured as a monolayer (2D) on tissue culture plastic with culture media supplemented with concentrations of calcium carbonate and D-(+)-Gluconic acid  $\delta$ -lactone equal to those found in 450 Pa and 2,000 Pa hydrogel mixtures. Samples were seeded with the supplemented media and subsequently fed with normal culture media every other day for the remainder of the experiment to mimic the conditions that cells seeded in hydrogels would be exposed to.....43

After 5 days in culture, **a)** cell viability was assayed using acridine orange/propidium iodide (AOPI) staining, and **b)** the media was removed from samples to measure pH values. Estrella et al.<sup>40</sup> notes that the pH of a malignant tumor's microenvironment can range for pH 6.5 – 6.9. MCF10A cells cultured in presence of the 2,000 Pa hydrogel mixture conditions are the only samples to drop below this pH value causing almost complete cell death. The remaining MCF7 and 231 cell lines showed only slight deviations in pH from control conditions (normal culture media for the duration of the experiment), though all of these values fall within an acceptable range, and minimal cell death compared to control conditions.....44

**Fig. 3.1 – An alginate hydrogel platform was used to dynamically stiffen**

**hydrogels to mimic progressive ECM stiffening. a)** Cells were seeded into hydrogels and cultured for 3 days before dynamic stiffening with NIR light. After stiffening, cultures were given 1 – 5 days to acclimate to the new stiffness of the hydrogel before being exposed to doxorubicin for 2 days (48 h). Following treatment with doxorubicin, viability assays were performed to determine doxorubicin resistance. **b)** 450 Pa hydrogels were exposed to NIR light for 45 s to achieve ECM stiffness similar to 2,000 Pa static hydrogels. The same technique was used to stiffen 2,000 Pa hydrogels to 3,000 Pa. **c)** NIR light induces surface plasmon resonance in encapsulated gold nanorods (gold) to heat liposomes (pink) close to their gel-to-liquid transition temperature. This causes calcium (green) to leak from the liposomes and form additional alginate cross-links, thereby stiffening the hydrogel. The above figure was adapted from Joyce et al.<sup>26</sup> .....57



**Fig. 3.2 – MDA-MB-231 cultures have an acclimation-dependent increase in**

**resistance to doxorubicin.** a) MDA-MB-231 and b) MCF7 cells were cultured in hydrogels with an initial stiffness of 450 Pa or 2,000 Pa for 3 days. On day 3, hydrogels either remained static (450 Pa or 2,000 Pa) or were stiffened (450 → 1,600 Pa or 2,000 → 3,000 Pa) using NIR light. Samples were then given 24 h to 120 h to acclimate to the hydrogel stiffness before 48 h treatment with doxorubicin. MDA-MB-231 cells showed a higher resistance to doxorubicin as hydrogel stiffness increased and this stiffness-dependent resistance was found to be partially dependent on duration of exposure to hydrogel stiffness. Comparable MCF7 samples did not show any significant change in resistance to doxorubicin across hydrogel stiffness or acclimation time. The above figure was adapted from Joyce et al.<sup>26</sup>. \*p-value < 0.01; \*\*p-value < 0.02; \*\*\*p-value < 0.03; NS = not significant, p-value > 0.05.....58

**Fig. 4.1 – Expression of EMT markers suggests ECM stiffness promotes hybrid**

**cell state in MDA-MB-231 and MCF7 cells. a)** The expression of five EMT-related genes was examined in MDA-MB-231 (231)/MCF7 cells cultured in 450 Pa vs 2,000 Pa hydrogels using quantitative PCR (qPCR). Cells were cultured in hydrogels for 6 days before RNA was isolated from samples and prepared for qPCR. All primers were normalized to the beta-2-microglobulin (B2M) house-keeping gene. **b)** E-cadherin expression was shown to decrease when both cell lines were cultured in 2,000 Pa hydrogels vs 450 Pa hydrogels, though only the MDA-MB-231 ( $p = 0.037$ ) cultures showed a significant decrease whereas the MCF7 ( $p = 0.120$ ) cultures did not. **c)** SNAIL1 expression was shown to significantly decrease for MDA-MB-231 samples ( $p = 0.001$ ), and while expression increased in MCF7 cultures ( $p = 0.069$ ) it was not found to be statistically significant. **d)** Expression of SLUG (SNAIL2) was shown to significantly decrease for MDA-MB-231 cultures ( $p = 0.017$ ), but increase 3-fold for MCF7 cultures ( $p = 0.006$ ). **e)** ZEB1 was shown to have less expression in MDA-MB-231 cells ( $p = 0.002$ ), but were not shown to be statistically different for MCF7 cells ( $p = 0.445$ ) cultured in stiffer hydrogels. **f)** Expression of vimentin was found to be significantly decreased for both MDA-MB-231 ( $p = 0.018$ ) and MCF7 ( $p = 0.004$ ) cells cultured in 2,000 Pa hydrogels compared to their counterparts cultured in 450 Pa hydrogels. ....70

**Fig. 4.2 – Expression of EMT markers compared to epithelial cells on soft**

**hydrogels. a)** The expression of five EMT-related genes was examined in MDA-MB-231 (231)/MCF7 cells cultured in 450 Pa vs 2,000 Pa hydrogels using quantitative PCR (qPCR). All primers were normalized to the beta-2-microglobulin (B2M) house-keeping gene and compared against the MCF7 cells cultured in 450 Pa hydrogels. **b)** E-cadherin expression is much higher in MCF7 cells for both 450 Pa ( $p = 0.007$ ) and 2,000 Pa ( $p = 0.002$ ) hydrogels. **c)** SNAIL1 expression overall is much lower in MDA-MB-231 cultures ( $p = 0.002$  for 450 Pa and  $p = 0.0002$  for 2,000 Pa hydrogels). SNAIL1 further decreases in MDA-MB-231 cultures ( $p = 0.001$ ) as stiffness increases but increases with stiffness in MCF7 cultures ( $p = 0.069$ ). **d)** Expression of SLUG (SNAIL2) is much higher in MDA-MB-231 cultures ( $p = 0.0003$  for 450 Pa and  $p = 0.002$  for 2,000 Pa hydrogels). Again, SLUG further decreases in MDA-MB-231 cultures ( $p = 0.017$ ) as stiffness increases but increases with stiffness in MCF7 cultures ( $p = 0.006$ ). **e)** ZEB1 expression is much higher in MDA-MB-231 cultures overall ( $p = 0.0004$  for 450 Pa and  $p = 0.0001$  for 2,000 Pa hydrogels). Here we observe a stiffness-dependent decrease in ZEB1 for both MDA-MB-231 ( $p = 0.002$ ) and MCF7 ( $p = 0.445$ ), though differences in MCF7 cultures were not found to be statistically significant. **f)** Vimentin is dramatically more expressed in MDA-MB-231 cultures ( $p = 0.0005$  for 450 Pa and  $p = 0.0001$  for 2,000 Pa hydrogels). A stiffness-dependent decrease in vimentin was observed in both MDA-MB-231 ( $p = 0.018$ ) and MCF7 ( $p = 0.076$ ) cultures, though the difference in MCF7 cultures was not significant. ....71

**Fig. 4.3 – Stiffer ECM increases nuclear localization of YAP and decreases**

**expression of E-Cadherin.** **a)** MDA-MB-231 and **b)** MCF7 cells were cultured on 450 Pa or 2,000 Pa hydrogels for 3 days before fixation and staining with YAP (red) and actin (phalloidin-488, green) antibodies, as well as DAPI (blue). Images were captured using confocal microscopy and analysis was done in ImageJ to determine nuclear localization of YAP (n = 123 for MDA-MB-231 cells cultured in 450 Pa hydrogels, n = 119 for MDA-MB-231 cells cultured in 2,000 Pa hydrogels, n = 72 for MCF7 cells cultured in 450 Pa hydrogels, n = 90 for MCF7 cells cultured in 2,000 Pa hydrogels). There is a stiffness-dependent increase in nuclear localization of YAP for both MDA-MB-231 (p = 1.38E-22) and MCF7 (p = 0.02) cultures, though the increase in MCF7 cultures is small. MDA-MB-231 cultures showed significantly higher expression of nuclear YAP compared to similar MCF7 cultures (p = 2.37E-37 for 450 Pa and p = 4.44E-46 for 2,000 Pa). Scale bar = 50  $\mu$ m. \*p-value < 0.05; \*\*\*\*p-value << 0.001 .....72

**Fig. 4.4 – Growth dynamics of MDA-MB-231 cells in hydrogels of varying**

**stiffness before treatment with doxorubicin.** MDA-MB-231 cells were seeded into 450 (green), 900 (cyan), 1400 (blue), or 2000 (pink) Pa hydrogels and cultured for 6 days in an Incucyte S3 incubator. Images were collected every 4 h and cells were counted using the S3 on-board software.....73

**Fig. 4.5 – Growth dynamics of MDA-MB-231 cells in hydrogels of varying stiffness following treatment with doxorubicin.** Following 6 days of standard growth in 450 (green), 900 (cyan), 1400 (blue), or 2000 (pink) Pa hydrogels, cells were exposed to 10  $\mu$ M doxorubicin for 48 h. Cultures were monitored for an additional 5 days to collect growth dynamics information following treatment with doxorubicin. Images were collected every 4 h in an Incucyte S3 incubator and cells were counted using the S3 on-board software. ....74

**Fig. 4.6 – Proliferation rate of MDA-MB-231 cells decreases with increased hydrogel stiffness.** a) Data collected between 48 h and 152 h time points was fit to b) a single exponential growth model to calculate the effective growth rate for cultures pre-treatment. The cell count data from 152 h to 262 h time points, was fit to a single exponential death model to calculate the effective growth rate of cells following 48 h exposure to doxorubicin. c) Our results show that growth rate of MDA-MB-231 cells decreases as the stiffness of the hydrogel increases. The error bars shown represent the 95% confidence interval, n = 5 for each hydrogel stiffness. ....75

**Fig. 4.7 – Fitting data to a two-population EMT model shows rate of EMT**

**increases with hydrogel stiffness. a)** Growth data collected from the Incucyte S3 was fit to a two-population model that assumed populations of epithelial (E) and mesenchymal (M) were present and that they could transition from one E to M ( $k_{EM}$ ) or vice-versa ( $k_{ME}$ ). **b)** Assuming a mesenchymal growth rate ( $g_M$ ) of 0.0013 cells per hour and  $k_{ME}$  of 0.0013, we fit the data to calculate epithelial growth rate ( $g_E$ ) and  $k_{EM}$ . **c)** Our mathematical model shows that the rate of transition from E to M ( $k_{EM}$  or EMT) increases with hydrogel stiffness.....76

**Fig. 4.8 – Cells with mesenchymal phenotype have a lower death rate in response**

**to treatment with doxorubicin. a)** We fit our data to the equations in **b)** using previously calculated variables to determine the sensitivity of epithelial (E) and mesenchymal (M) populations to doxorubicin. **c)** Our model shows that mesenchymal cells are more resistant to doxorubicin. This suggests that cells undergoing transitioning from E to M ( $k_{EM}$  or EMT) would have a survival advantage and increase the overall resistance of the cell entire population.....77

**Fig. A1 – Exposure to Near Infrared (NIR) light does not significantly affect response to doxorubicin.** MDA-MB-231 cells were cultured as a monolayer (2D) on tissue culture plastic before being exposed to NIR light for 45 s. Samples were cultured an additional 2 days after lasing prior to treatment with doxorubicin. Staining with acridine orange/propidium iodide (AOPI) was used to quantify the ratio of live/dead cells. **a)** Cells that were exposed to NIR light did not show a significant difference ( $p = 0.064$ ) in resistance to doxorubicin compared to **b)** control samples that were not exposed to NIR light.  $n = 3$  .....83

## Chapter 1: Introduction<sup>1</sup>

### 1.1 THE EXTRACELLULAR MATRIX

The extracellular matrix (ECM) encompasses all the non-cellular components of a tissue that support and give structure to the cells<sup>1</sup>. It is a vital component in all animals that functions as a scaffold for cells to adhere to and a medium for transmitting biochemical and biomechanical cues. The ECM is separated into two domains: the interstitial connective tissue matrix<sup>2</sup> and the basement membrane<sup>3</sup>. Interstitial connective tissue matrix fills the interstitial space between cells and is composed primarily of collagens I, III, V, VI, VII, XII<sup>2</sup>; fibronectins<sup>4-6</sup>; and proteoglycans, mostly chondroitin sulfate<sup>7,8</sup> and heparin sulfate<sup>9,10</sup>. The basement membrane is a specialized ECM that separates epithelium from mesenchyme, guides cellular differentiation<sup>11</sup>, stores growth factors<sup>12</sup>, and plays a role in cell proliferation and migration. It is vital for epithelial cells to properly orient themselves. Epithelial cells will anchor their basal side to the basement membrane with the apical side being exposed to a fluid-filled lumen. The basement membrane is primarily composed of type IV collagen, laminin, nidogen/entactin, and perlecan. Collagen<sup>13</sup> and laminin<sup>14</sup> are the major structural components, as they are able to independently self-assemble into networks. Nidogen/entactin and perlecan further stabilize the basement membrane by binding to both collagen and laminin, thus bridging the two networks and increasing structural integrity<sup>15-18</sup>.

The early discoveries of the ECM can be attributed to mostly to gross characterization and light microscopy. Nageotte and collaborators were able to isolate what we now know to be collagen from rat tissue in the 1930's<sup>19</sup>. This substance was brought to their attention when they noted its ability to reversibly solubilize and reconstitute into fibrils. During this time, the invention of the electron microscope<sup>20</sup> and advances in x-ray diffraction<sup>21</sup> would make it possible for researchers to more fully understand the structure of ECM components and how they might interact with one

---

<sup>1</sup> Portions of this chapter were adapted from M. H. Joyce, S. Allen, L. Suggs and A. Brock, "Novel Nanomaterials Enable Biomimetic Models of the Tumor Microenvironment," *Journal of Nanotechnology*, vol. 2017, pp. 1-8, 2017. M. H. Joyce, S. Allen, L. Suggs and A. Brock wrote this review article.



another *in vivo*. Richard Bear<sup>22</sup> studied collagen fibrils using x-ray diffraction and found they had a 64 nm repeating period, and this finding was confirmed by Hall et al.<sup>23</sup> via electron microscopy. Schmitt et al.<sup>24</sup> utilized both x-ray diffraction and electron microscopy, as well as chromatography to show that collagen molecules could transition from fibrils into bundles they referred to as segment long spacings (SLS), and vice-versa. The same year, multiple groups used x-ray diffraction patterns of collagen fibrils to refine this model to the triple-chain collagen helix we know today<sup>25-27</sup>. Laminin wasn't discovered until 1979, and its characterization followed a much different path from collagen given the significant advances in technology. Laminin was first isolated from the Engelbreth-Holm-Swarm (EHS) sarcoma, a mouse tumor that was shown to produce ECM basement membrane<sup>28,29</sup>. It was identified when researchers found that neutral buffers extracted very little type IV collagen from these tumors, but a substantial amount of non-collagenous proteins. Ion exchange chromatography was used to determine the amino acid composition, polyacrylamide gel electrophoresis was used to determine approximate molecular weight, and immunofluorescence was used to localize laminin to the basement membrane<sup>29</sup>.

The exact composition of the ECM depends on a number of factors that also influence resident cell phenotype such as mechanical forces, biochemical signals, oxygen requirements, and pH. Such factors vary across species and even across tissue types within species, so the ECM composition is highly tailored to the tissue type that it is found in. Tailoring the ECM is one control mechanism the tissue as a whole has on regulating local cell phenotype, migration, and proliferation<sup>30-33</sup>. Collagen is the major insoluble fibrous protein in the ECM<sup>34</sup>, and the main structural element of the ECM<sup>1</sup>, however there are numerous types that help shape the physical characteristics of a tissue type. Types I and III collagens have tremendous tensile strength, which makes them the ideal components for the ECM of tendons that connect muscle to bone<sup>34</sup>. On the other hand, type II collagen fibrils are smaller in diameter and orient randomly, giving the ECM of cartilage tissues their compressibility and resistance to deformations in shape<sup>34</sup>. These differences in ECM composition extend beyond variation in collagen types; the proteoglycan profile of skeletal muscle tissue, for example, is dominated by the small leucine-rich proteoglycan

family<sup>35</sup>, whereas chondroitin sulfate proteoglycan constitutes the major population of proteoglycans in the central nervous system<sup>36</sup>. Glycosaminoglycans (GAGs) are the primary polysaccharide found in vertebrate ECM, however chitin (poly-N-acetylglucosamine) and cellulose are the main polysaccharides found in insect and plant ECM, respectively<sup>37</sup>.

ECM composition contributes significantly to the overall physical properties of the tissue, including its stiffness, viscoelasticity, and pore size. **Table 1.1** shows stiffness measurements of various tissue types and illustrates the contribution of ECM to the stiffness of each tissue. The measurements listed in **Table 1.1** were collected primarily using atomic force microscopy (AFM) and magnetic resonance elastography (MRE)<sup>38</sup>. Atomic force microscopy is a form of scanning probe microscopy<sup>39</sup> that skims along the surface of a sample and, by tracking the deflection of laser light off the probe tip, can apply indentations along a samples and calculate the force required to do so and approximately how stiff the material must be to resist that force<sup>40</sup>. Magnetic resonance elastography works by inducing mechanical shear waves into the tissue, imaging with phase-contrast MRI techniques, and processing the wave images to calculate a measurement of stiffness<sup>41</sup>. Tissue viscoelasticity is dependent on the structural proteins of the ECM, crosslinking<sup>42,43</sup>, folding/unfolding of ECM proteins<sup>44,45</sup>, and flow of fluid through the ECM<sup>43</sup>. This property is especially important in softer materials and tissues, as compliant samples can lead to inaccurate measurements of stiffness when using techniques like nanoindentation<sup>46</sup>. Measurements of the viscoelasticity of ECM or ECM substitutes is typically performed using a rheometer to measure shear stresses and strains that are applied to the sample<sup>47</sup>. The porosity of the ECM helps dictate what size molecules and cells can move through the ECM. Since the pore size can be as small as a few nanometers, electron microscopy is a method commonly used to measure the average pore size and porosity of ECM.

## **1.2 EXTRACELLULAR MATRIX PLAYS CRUCIAL ROLES IN PHYSIOLOGY, DEVELOPMENT, AND DISEASE**

During embryogenesis and early development, cells rely on physical cues, chemical gradients, and electrical signals for differentiation and morphogenesis. The ECM provides physical cues and facilitates chemical signaling during normal tissue development<sup>48</sup>. This is probably most evident in cardiomyocytes and myoepithelial cells lining blood vessels, which are highly sensitive to stretch and tension. Myocardial cells have been shown to increase their size and protein production upon exposure to cyclical stress, as opposed to myocardial cells that are grown in a static environment<sup>49</sup>. Cyclical stretching of cardiomyocytes induces phosphorylation of pathways involved in differentiation and proliferation such as ERK, JNK, FAK, and p38 MAPK<sup>50</sup>. Chondrocytes also require mechanical tension for proper development and maturation. Wong et al.<sup>51</sup> demonstrated that cyclical tension activates the Cbfa1/MMP-13 pathway and increases expression of terminal differentiation hypertrophic markers such as COMP and lubricin. Even neurons and glial cells respond to the mechanical properties of the tissue microenvironment to maintain normal physiological function<sup>52-57</sup>. Landmark studies in the field of neuronal development have shown how tension along axons and other mechanical cues contribute to organization of the nervous system<sup>58-60</sup>.

Dysregulation of structure, function, or composition of the ECM contributes to many various diseases and conditions<sup>61</sup>. The mechanical properties of tissues vary widely among different physiological and pathological states<sup>62,63</sup>. Fibronectin has been shown to play a role in cardiovascular disease and tumor metastasis<sup>64,65</sup>. In the liver, hepatic fibrosis will cause stiffening of the ECM<sup>66,67</sup>. Similarly, patients with chronic obstructive pulmonary disease (COPD) have been reported to have decreased elastin<sup>68-70</sup> and proteoglycans<sup>71</sup> with increased collagen content in the alveoli, leading to a stiffening of the lung tissue and decreased elasticity. A detailed analysis of the ECM composition of COPD patients further showed decreased expression of type I collagen in the large and small airways, lower versican fractional area in distal parenchyma regions, and higher fractional areas of fibronectin and tenascin in large and small airways<sup>72</sup>.

Tumors are typically stiffer than their surrounding healthy tissue and this is due, in part, to increased ECM deposition, ECM remodeling, and increased contractility of cells in the tumor microenvironment<sup>73-75</sup>. Tumor cells also secrete matrix metalloproteases (MMPs)<sup>76,77</sup> that break down surrounding basement membrane, releasing sequestered growth factors such as vascular endothelial growth factor (VEGF)<sup>77,78</sup> from the matrix. VEGF promotes the branching growth of blood vessels through angiogenesis, which further increases interstitial tissue pressure through added cell density. This leads to a positive feedback loop where tumor-associated stiffening causes the release of growth factors, which leads to increased interstitial pressure from proliferation, angiogenesis, and cellular contractility<sup>73,79-81</sup>. Similar changes have been observed in ECM of mammary tissue progressing through the stages of breast cancer<sup>82-88</sup>. Healthy mammary gland tissue is characterized as have a basement membrane composed of laminins, type IV collagen, nidogens, and perlecan with an interstitial ECM composed of fibrillar collagens (types I, III, and V), fibronectin, decorin, and biglycan. During cancer progression, MMPs and other ECM remodeling enzymes breakdown the basement membrane<sup>89</sup> leading to decreased levels of type IV collagen<sup>83,84</sup> and laminin-111<sup>90</sup>. The surrounding interstitial ECM gradually stiffens due to increased deposition of fibrillar collagen (types I, III, and V) and fibronectin along with elevated LOX activity<sup>74</sup>. Matricellular proteins that promote tumor cell survival including tenascin C, periostin, osteopontin, SPARC, and thrombospondin-1 are upregulated<sup>91</sup>, as are the versican<sup>92</sup>, syndecan-1<sup>93</sup>, and glypican-1 proteoglycans<sup>94</sup>. These changes in mammary tissue ECM composition promote tumor growth and progression, which leads to a positive feedback loop that leads to further tissue stiffening and disease progression.

The difference in stiffness between healthy tissue and tumors may be significant and may be detectable by physical palpation. In fact, palpation remains a time-tested diagnostic tool for physicians as a means of quickly scanning the body for differences in the mechanical properties that would signify healthy or abnormal tissue. It is still used as a standard medical test to detect breast tumors<sup>95</sup> and liver tumors<sup>96</sup>.

### **1.3 CELLS SHARE A RECIPROCAL SIGNALING RELATIONSHIP WITH THEIR EXTRACELLULAR MATRIX**

The ECM exists in a state of dynamic equilibrium, as cells are constantly breaking down components of the ECM and secreting new ECM proteins<sup>31</sup>. Fibroblasts secrete and organize type I and III collagens, elastin, fibronectin, tenascin, hyaluronic acid, decorin, and additional proteoglycans to ensure structural integrity of interstitial ECM<sup>1</sup>. Conversely, cells also produce MMPs to break down ECM to facilitate cell migration and the release of growth factors that are sequestered in the ECM. Cells and their surrounding ECM are tailor made for one another. For example, smooth muscle cells assume an elongated cell shape based on interactions with the  $\alpha_v\beta_3$  integrin receptor and tenascin-C, which promotes EGF-dependent survival<sup>97</sup>. Roskelley et al.<sup>98</sup> further describe a dynamic signaling hierarchy that occurs during mammary gland development. First they describe how a mammary cell must detach from its rigid substrate to allow for changes in cytoskeletal and nuclear architecture. This leads to integrin-dependent biochemical signals (FAK phosphorylation, MAP kinase activation, and transient increase in AP1 transcription factor activity) which activate ECM-responsive elements such as BCE-1. Signals initiating in the cell nucleus are conveyed to the surface membrane where changes to the ECM are executed; this might involve increasing MMP production to breakdown ECM or increasing secretion of structural ECM proteins. Tumor cells have also been shown to take advantage of this reciprocal relationship between cells and ECM. Fullár et al.<sup>99</sup> found that cancer-associated fibroblasts (CAFs) produced significant amounts of laminin-1 in response to signals sent from cervical cancer cells (CSCC7) that predominantly migrated towards and produced integrin receptors ( $\alpha_6\beta_4$ ) for laminin.

### **1.4 RESISTANCE TO CHEMOTHERAPEUTIC TREATMENTS**

Breast cancer is the second leading cause of cancer death among women<sup>100</sup>. It is estimated that breast cancer will have seen 268,670 new cases emerge and caused 41,400 deaths in 2018 in the U.S. alone<sup>100</sup>. One of the most challenging aspects of treating cancer is the fact that small populations of cancer cells may be resistant treatment and persist after treatment has finished. These cells survive the initial round of treatments, continue to proliferate, repopulate the tumor

(disease relapse), and may metastasize to other regions. Only 10% of malignant tumor types can be eradicated by chemotherapy, leaving the other 90% with varying degrees of improved survivability<sup>101</sup>. Current treatment regimens will usually include administering a cocktail of chemotherapeutics to the patient prior to (neoadjuvant) or immediately following (adjuvant) surgical resection of the tumor in an attempt to fully eradicate the disease. However, nearly 50% of all cancer patients are afflicted with a malignancy that is intrinsically resistant to chemotherapeutic treatment<sup>101</sup>. Most of the remaining half will stop responding to treatment as tumor cells acquire resistance to the chemotherapeutics being used. Intrinsically resistant tumor cells have pre-existing mutations that confer a survival advantage during initial treatment, whereas cells with acquired resistance (also known as therapy-induced resistance) undergo changes in response to treatment that ultimately decrease the effectiveness of the drug. A good example of intrinsic resistance is seen in tumor cells that carry the BRAF V600E mutation, which renders those tumor cells resistant to BRAF inhibitors<sup>102,103</sup>. Studies that selected for resistant populations through progressively increased dosing with topoisomerase II poisons (daunorubicin, doxorubicin, melphalan ) showed that the surviving cells overexpressed the multi-drug resistance 1 (MDR1) gene which increased cell resistance through P-170-mediated MDR<sup>104-106</sup>. The molecular mechanisms behind cancer cell resistance to chemotherapeutic treatment include transporter pumps, activation of oncogenes, suppression of tumor suppressor genes, mitochondrial alteration, DNA repair, autophagy, epithelial-mesenchymal transition (EMT), cancer stemness, and exosomes<sup>107-109</sup>. In the present study, we focus primarily on the chemotherapeutic drug, doxorubicin (trade name Adriamycin®). This anthracycline functions by disrupting topoisomerase-II-mediated DNA repair<sup>110,111</sup>, generating free radicals to damage cellular membranes<sup>112,113</sup>, and inducing histone eviction<sup>114</sup>. It has proved useful as a broad-spectrum chemotherapeutic in neoadjuvant breast tumor therapies, but it is known to induce resistant cells that can cause disease relapse. Mechanisms of doxorubicin resistance may involve ABCB1 (MDR1, Pgp)<sup>115</sup>, ABCC1 (MRP1)<sup>116-118</sup>, ABCC2<sup>118</sup>, ABCC3<sup>118</sup>, ABCG2, and RALBP1<sup>119</sup> transporters, as well as amplification of TOP2A<sup>120-122</sup>. Another chemotherapeutic agent used in

this study is paclitaxel (trade name Taxol®), a member of the taxane class. This is a microtubule stabilizer that kills cancer cells by polymerizing and stabilizing mitotic spindles in dividing cells, thus preventing them from clearing the mitotic checkpoint<sup>123</sup>. Resistance to paclitaxel has been shown to arise through a variety of mechanisms. The mechanisms that are most well-studied include alterations to expression of IL-6 and IL-8 cytokines, alterations in  $\beta$ -tubulin, alterations in genes involved in apoptosis (BCL-2, BCL-XL, BAX, BAD, and p53), and overexpression of P-glycoprotein<sup>124</sup>. Many other mechanisms of paclitaxel resistance have been proposed as well including changes in fibroblastic growth factors<sup>125</sup>, increased expression of transmembrane receptors<sup>126,127</sup>, increased expression of adhesion molecules<sup>128</sup>, increased expression of certain cell signaling molecules<sup>128-134</sup>, increased expression of nuclear proteins<sup>134-136</sup>, and the switch from apoptotic to autophagic cell death<sup>137</sup>. This list is by no means exhaustive, but illustrates the complex nature of treating cancer patients with modern chemotherapeutics.

## **1.5 THE EXTRACELLULAR MATRIX INFLUENCES HOW TUMOR CELLS WILL RESPOND TO CHEMOTHERAPEUTIC TREATMENT**

Cancer is a complex disease capable of affecting multiple organs and is driven by numerous factors. Hanahan and Weinberg<sup>138,139</sup> have summarized and defined certain ‘hallmarks of cancer’ which describe biological conditions that lead to tumor development and characteristics that often follow tumorigenesis. Pickup et al.<sup>140</sup> revisited these hallmarks and described the role that the extracellular matrix (ECM) plays in each. Such observations make it evident that the ECM is an important factor in tumor initiation, progression, and metastasis and can no longer be ignored in the search for a cure. Studies aimed at characterizing the role physical cues play in tumor development have considered ligand variety, ligand density, substrate composition, and substrate stiffness<sup>141-147</sup>. More recent studies are focusing on understanding how the physical cues from the microenvironment affect how cancer cells will respond to chemotherapeutic treatment. Shin & Mooney<sup>144</sup> investigated how ECM stiffness would affect chemosensitivity of myeloid leukemia cells lines by culturing them within alginate hydrogels that not only varied in stiffness, but in

functionalizing peptide. What they were able to show was that the myeloid leukemia cell lines challenged with varying chemotherapeutics would fall into one of three categories: ligand sensitive, ligand and matrix stiffness sensitive, or mechanics independent. Zusiak et al.<sup>148</sup> cultured multiple cancer cell lines on top of collagen-coated polyacrylamide hydrogels that ranged from 1 – 100 kPa in stiffness. These samples were treated with paclitaxel to observe how ECM stiffness would modulate drug sensitivity. Their results showed only found HeLa and SY5Y cell lines to have a stiffness-dependent resistance to paclitaxel out of the 10 cell lines tested, however their study was limited in that the cells were cultured on top of the hydrogels and not embedded within them. Rice et al.<sup>149</sup> performed a very similar study with pancreatic ductal adenocarcinoma (PDAC) cell lines cultured on 1, 4, and 25 kPa polyacrylamide hydrogels. In their study, they found that the PDAC cell lines they used had a stiffness-dependent increase in resistance to paclitaxel. To uncover the mechanism behind the observed stiffness-dependent resistance, they measured total expression of vimentin and nuclear localization of YAP/TAZ. Their results showed that the PDAC cells they cultured on stiffer hydrogels increased expression of vimentin and had higher levels of nuclear localized YAP/TAZ.

YAP (yes-associated protein) and TAZ (transcriptional co-activator with PDZ-binding motif) are functionally similar transcriptional co-activators capable of inducing EMT<sup>150</sup>. As the Hippo pathway effector, YAP has been shown to promote metastasis through its TEAD-interaction domain<sup>151</sup> and upregulation of EGF receptor<sup>152</sup> (**Fig 1.1**). LATS1/2 kinases are members of the Hippo pathway that will phosphorylate, and thus inhibit, YAP<sup>153,154</sup>. When YAP is phosphorylated, it will remain in the cytoplasm of the cell where it will eventually be marked for proteasome degradation. Once translocated to the nucleus, however, it can perform its role as a transcriptional co-activator that regulates organ size, cell proliferation, and EMT. YAP has been shown to drive these effects through targeting of ABCB1, ANKRD, CAT, GPATCH4, LMNB2, PTGS2, TXN, WSB2, and more specifically AXL, CDKN2C, CTGF, CYR61, DAB2, DLC1, TSTL1, LHFP, SDPR, SERPINE1, SLIT2, TGFB2, and THBS1 in breast tumor samples<sup>155,156</sup>.



Tissue	Elastic Modulus (E, Pa)	References
Brain, white matter	$(\sim 2.25) \times 10^2$	Christ et al. <sup>155</sup>
Brain, gray matter	$(\sim 3.4) \times 10^2$	Christ et al. <sup>155</sup>
Breast, normal	$(0.25 - 1) \times 10^3$	Sinkus et al. <sup>156</sup> Lorenzen et al. <sup>157</sup> Chen et al. <sup>158</sup> Griesenaur et al. <sup>159</sup>
Endothelium, aortic	$(0.1 - 2) \times 10^3$	Sato et al. <sup>160</sup>
Breast, cancerous	$\sim (1.5 - 3.5) \times 10^3$	Sinkus et al. <sup>156</sup> Lorenzen et al. <sup>157</sup> Chen et al. <sup>158</sup>
Liver	$(12.88) \times 10^3$	Tay et al. <sup>161</sup>
Muscle tissue	$(12 - 24) \times 10^3$	Engler et al. <sup>162</sup> Mathur et al. <sup>163</sup>
Articular cartilage	$(0.4 - 200) \times 10^6$	Nemir and West <sup>164</sup>
Bone	$(0.008 - 40) \times 10^9$	Nemir and West <sup>164</sup>

**Table 1.1 – ECM stiffness varies across tissue types.** Tissue stiffness measurements acquired from numerous methods are summarized here according to tissue type. The values displayed represent the tissue's measured Young's Modulus (E). Stiffness of tissue types varies drastically across the body to facilitate the differing physiological functions necessary for survival. This table is adapted from Gautier et al.<sup>38</sup>

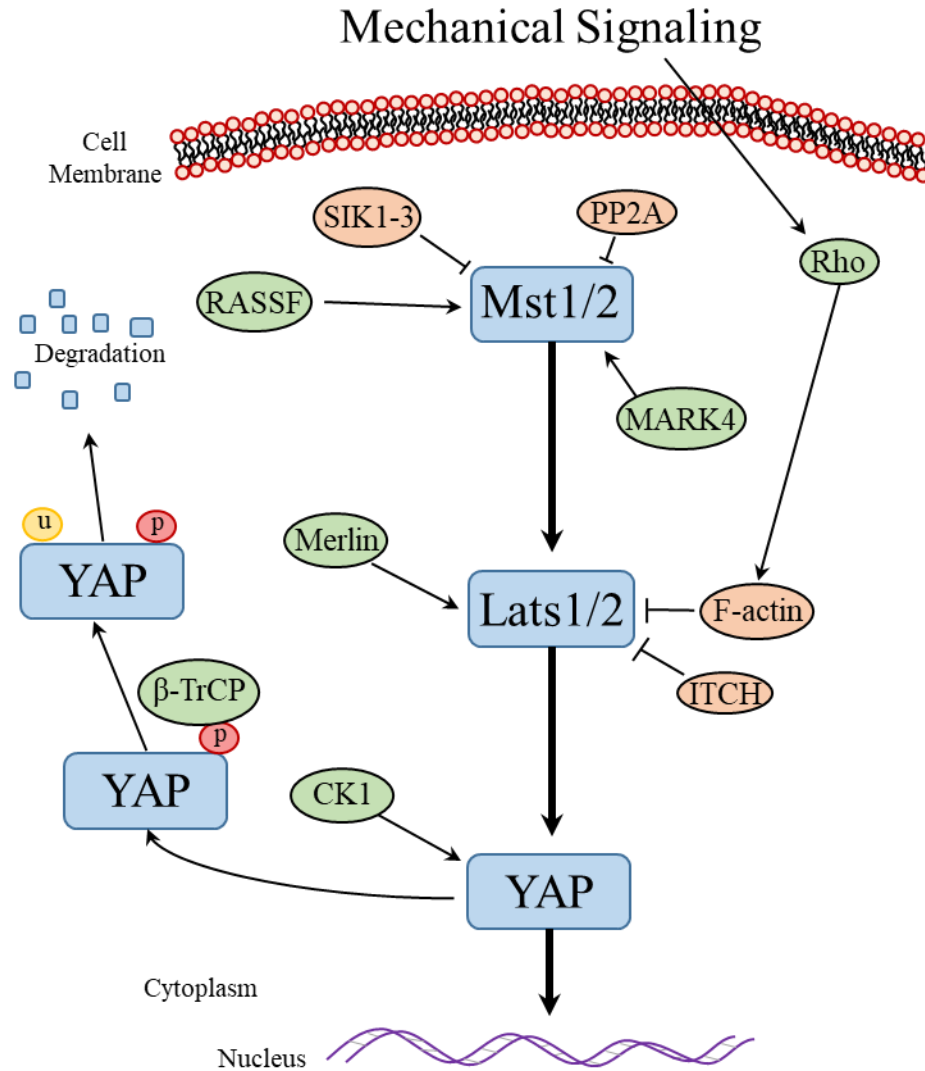


**Fig. 1.1 – Canonical YAP pathway.** YAP is a component of the Hippo signaling pathway. Phosphorylated (red) YAP remains in the cell cytoplasm where it is inactive. YAP is ubiquitinated (yellow) by  $\beta$ -TrCP which signals it for proteasome degradation. If Lats1/2 is inhibited and YAP remains unphosphorylated, it translocates to the nucleus where it acts as a transcriptional co-activator.

1. C. Frantz, K. M. Stewart and V. M. Weaver, "The Extracellular Matrix at a Glance," *Journal of Cell Science*, vol. 123, no. 24, pp. 4195 LP-4200, 2010.
2. T. F. Lisenmayer, "Collagen," in *Cell Biology of Extracellular Matrix*, E. D. Hay, Ed., New York, Plenum Press, 1991, pp. 7-44.
3. R. Timpl, "Structure and biological activity of basement membrane proteins," *Eur J Biochem*, vol. 180, no. 3, pp. 487-502, 1989.
4. E. Ruoslahti, E. G. Hayman, M. Pierschbacher and E. Engvall, "Fibronectin: purification, immunochemical properties, and biological activities," *Methods Enzymol*, vol. 82, pp. 803-831, 1982.
5. R. O. Hynes, *Fibronectins*, New York: Springer-Verlag, 1990.
6. K. M. Yamada, "Fibronectin and other cell interactive glycoproteins," in *Cell Biology of Extracellular Matrix*, E. D. Hay, Ed., New York, Plenum Press, 1991, pp. 111-146.
7. M. J. Brennan, A. Oldberg, M. D. Pierschbacher and E. Ruoslahti, "Chondroitin/dermatan sulfate proteoglycan in human fetal membranes. Demonstration of an antigenically similar proteoglycan in fibroblast," *Journal of Biological Chemistry*, vol. 259, no. 22, pp. 13742-13750, 1984.
8. B. Voss, J. Glössl, Z. Cully and H. Kresse, "Immunocytochemical investigation on the distribution of small chondroitin sulfate-dermatan sulfate proteoglycan in the human," *Journal of Histochemistry and Cytochemistry*, vol. 34, no. 8, pp. 1013-1019, 1986.
9. L. Cöster, I. Carlstedt, S. Kendall, A. Malmström, A. Schmidtchen and L.-Å. Fransson, "Structure of proteoglycan sulfates from fibroblasts. Confluent and proliferating fibroblasts produce at least three types of proteoglycan sulfates with functionally different core proteins," *Journal of Biological Chemistry*, vol. 261, no. 26, pp. 12079-12088, 1986.
10. A. Heremans, B. V. D. Schueren, B. D. Cock, M. Paulsson, J.-J. Cassiman, H. V. D. Berghe and G. David, "Matrix-associated heparan sulfate proteoglycan: core protein-specific monoclonal antibodies decorate the pericellular matrix of connective tissue cells and the stromal side of basement membranes," *Journal of Cell Biology*, vol. 109, pp. 3199-3211, 1989.
11. J. Perry, S. Tam, K. Zheng, Y. Sado, H. Dobson, B. Jefferson, R. Jacobs and P. S. Thorner, "Type IV collagen induces podocytic features in bone marrow stromal stem cells in vitro," *J Am Soc Nephrol*, vol. 17, pp. 66-76, 2006.
12. R. Jayadev and D. R. Sherwood, "Basement membranes," *Current Biology*, vol. 27, no. 6, pp. R207-R211, 2017.
13. E. Poschl, U. Schlotzer-Schrehardt, B. Brachvogel, K. Saito, Y. Ninomiya and U. Mayer, "Collagen IV is essential for basement membrane stability but dispensable for initiation

- of its assembly during early development," *Development*, vol. 131, pp. 1619-1628, 2004.
14. J. H. Miner, C. Li, J. L. Mudd, G. Go and A. E. Sutherland, "Compositional and structural requirements for laminin and basement membranes during mouse embryo implantation and gastrulation," *Development*, vol. 131, pp. 2247-2256, 2004.
  15. A. C. Erickson and J. R. Couchman, "Still more complexity in mammalian basement membranes," *J Histochem Cytochem*, vol. 48, pp. 1291-1306, 2000.
  16. A. E. Chung, L. J. Dong, C. Wu and M. E. Durkin, "Biological functions of entactin," *Kidney Int*, vol. 43, pp. 13-19, 1993.
  17. P. D. Yurchenco and J. J. O'Rear, "Basal lamina assembly," *Curr Opin Cell Biol*, vol. 6, pp. 674-681, 1994.
  18. M. Paulsson, "Basement membrane proteins: structure, assembly, and cellular interactions," *Crit Rev Biochem Mol Biol*, vol. 27, pp. 93-127, 1992.
  19. J. Nageotte and L. Guyon, "Reticulin," *American Journal of Pathology*, vol. 6, no. 6, pp. 631-653, 1930.
  20. C. W. Oatley, "The early history of the scanning electron microscope," *Journal of Applied Physics*, vol. 53, no. 2, pp. R1-R13, 1982.
  21. T. M. Weiss, "Small Angle Scattering: Historical Perspective and Future Outlook," in *Biological Small Angle Scattering: Techniques, Strategies and Tips*, vol. 1009, B. Chaudhuri, I. Muñoz, S. Qian and V. Urban, Eds., Singapore, Springer, Singapore, 2017, pp. 1-10.
  22. R. S. Bear, "Long x-ray diffraction spacings of collagen," *J Am Chem Soc*, vol. 64, no. 3, pp. 727-727, 1942.
  23. C. E. Hall, M. A. Jakus and F. O. Schmitt, "Electron microscope observations of collagen," *J Am Chem Soc*, vol. 64, no. 5, pp. 1234-1234, 1942.
  24. F. O. Schmitt, J. Gross and J. H. Highberger, "A new particle type in certain connective tissue extracts," *Proc Natl Acad Sci USA*, vol. 39, no. 6, pp. 459-470, 1953.
  25. A. Rich and F. H. C. Crick, "The structure of collagen," *Nature*, vol. 176, pp. 593-595, 1955.
  26. G. N. Ramachandran and G. Kartha, "Structure of collagen," *Nature*, vol. 176, pp. 593-595, 1955.
  27. P. Cowan, S. McGavin and A. North, "The polypeptide chain configuration of collagen," *Nature*, vol. 176, no. 4492, pp. 1062-1064, 1955.

28. R. Orkin, P. Gehron, E. McGoodwin, G. Martin, T. Valentine and R. Swarm, "A murine tumor producing a matrix of basement membrane," *J Exp Med*, vol. 145, no. 1, pp. 204-220, 1977.
29. R. Timpl, H. Rohde, P. G. Robey, S. I. Rennard, J.-M. Foidart and G. R. Martin, "Laminin - A Glycoprotein from Basement Membranes," *Journal of Biological Chemistry*, vol. 254, no. 19, pp. 9933-9937, 1979.
30. S. Baker and J. Southgate, "Towards control of smooth muscle cell differentiation in synthetic 3D scaffolds," *Biomaterials*, vol. 29, no. 23, pp. 3357-3366, 2008.
31. M. Bissell, H. Hall and G. Parry, "How does the extracellular matrix direct gene expression?," *J Theor Biol*, vol. 99, no. 1, pp. 31-68, 1982.
32. N. Boudreau, C. Myers and M. Bissell, "From laminin to lamin: regulation of tissue-specific gene expression by the ECM," *Trends Cell Biol*, vol. 5, no. 1, pp. 1-4, 1995.
33. D. Ingber, "Extracellular matrix and cell shape: potential control points for inhibition of angiogenesis," *J Cell Biochem*, vol. 47, no. 3, pp. 236-241, 1991.
34. H. Lodish, A. Berk and S. Zipursky, "Collagen: The Fibrous Proteins of the Matrix," in *Molecular Cell Biology*, New York, W. H. Freeman, 2000.
35. A. R. Gillies and R. L. Lieber, "Structure and Function of the Skeletal Muscle Extracellular Matrix," *Muscle Nerve*, vol. 44, no. 3, pp. 318-331, 2011.
36. H. Cui, C. Freeman, G. A. Jacobson and D. H. Small, "Proteoglycans in the central nervous system: Role in development, neural repair, and Alzheimer's disease," *IUBMB Life*, vol. 65, no. 2, pp. 108-120, 2013.
37. B. Alberts, A. Johnson and J. Lewis, "The Extracellular Matrix of Animals," in *Molecular Biology of the Cell*, New York, Garland Science, 2002.
38. H. O. Gautier, A. J. Thompson, S. Achouri, D. E. Koser, K. Holtzmann, E. Moeendarbary and K. Franze, "Atomic force microscopy-based force measurements on animal cells and tissues," in *Biophysical Methods in Cell Biology*, E. K. Paluch, Ed., Elsevier, 2015, pp. 211-235.
39. G. Binnig, C. Quate and C. Gerber, "Atomic force microscope," *Physical Review Letters*, vol. 56, no. 9, pp. 930-933, 1986.
40. G. Thomas, N. A. Burnham, T. A. Camesano and Q. Wen, "Measuring the Mechanical Properties of Living Cells Using Atomic Force Microscopy," *J Vis Exp*, vol. 76, p. e50497, 2013.
41. Y. K. Mariappan, K. J. Glaser and R. L. Ehman, "Magnetic Resonance Elastography: A Review," *Clin Anat*, vol. 23, no. 5, pp. 497-511, 2010.

42. S. Nam, K. H. Hu, M. J. Butte and O. Chaudhuri, "Strain-enhanced stress relaxation impacts nonlinear elasticity in collagen gels," *Proc Natl Acad Sci USA*, vol. 113, no. 20, pp. 5492-5497, 2016.
43. X. Zhao, N. Huebsch, D. J. Mooney and Z. Suo, "Stress-relaxation behavior in gels with ionic and covalent crosslinks," *J Appl Phys*, vol. 107, no. 6, p. 063509, 2010.
44. X. Zhao, "Multi-scale multi-mechanism design of tough hydrogels: building dissipation into stretchy networks," *Soft Matter*, vol. 10, pp. 672-687, 2014.
45. A. E. Brown, R. I. Litvinov, D. E. Discher, P. K. Purohit and J. W. Weisel, "Multiscale Mechanics of Fibrin Polymer: Gel Stretching with Protein Unfolding and Loss of Water," *Science*, vol. 325, no. 5941, pp. 741-744, 2009.
46. C.-S. Han, S. H. Sanei and F. Alisafaei, "On the origin of indentation size effects and depth dependent mechanical properties of elastic polymers," *J Polym Eng*, vol. 36, no. 1, pp. 103-111, 2015.
47. O. Chaudhuri, "Viscoelastic hydrogels for 3D cell culture," *Biomaterials Science*, vol. 5, pp. 480-1490, 2017.
48. G. Davis and D. Senger, "Endothelial extracellular matrix: biosynthesis, remodeling, and functions during vascular morphogenesis and neovessel stabilization," *Circ Res*, vol. 97, no. 11, pp. 1093-1107, 2005.
49. V. Gupta and K. J. Grande-Allen, "Effects of static and cyclic loading in regulating extracellular matrix synthesis by cardiovascular cells," *Cardiovascular Research*, vol. 72, no. 3, pp. 375-383, 2006.
50. S. Y. N. Takahashi, K. Tobe, T. Kadowaki and Y. Yazaki, "Pulsatile stretch activates mitogen-activated protein kinase (MAPK) family members and focal adhesion kinase (p125FAK) in cultured rat cardiac myocytes," *Biochem Biophys Res Commun*, vol. 259, no. 1, pp. 8-14, 1999.
51. M. Wong, M. Siegrist and K. Goodwin, "Cyclic tensile strain and cyclic hydrostatic pressure differentially regulate expression of hypertrophic markers in primary chondrocytes," *Bone*, vol. 33, no. 4, pp. 685-693, 2003.
52. D. Discher, P. Janmey and Y. Wang, "Tissue cells feel and respond to the stiffness of their substrate," *Science*, vol. 310, pp. 1139-1143, 2005.
53. L. Flanagan, Y. Ju, B. Marg, M. Osterfield and P. Janmey, "Neurite branching on deformable substrates," *Neuroreport*, vol. 13, pp. 2411-2415, 2002.
54. P. Georges, W. Miller, D. Meaney, E. Sawyer and P. Janmey, "Matrices with compliance comparable to that of brain tissue select neuronal overglial growth in mixed cortical cultures," *Biophysical Journal*, vol. 90, pp. 3012-3018, 2006.

55. X. Jiang, P. Georges, B. Li, Y. Du, M. Kutzinger, M. Previtera, N. Langrana and B. Firestein, "Cell growth in response to mechanical stiffness is affected by neuron-astroglia interactions," *The Open Neuroscience Journal*, vol. 1, pp. 7-14, 2007.
56. F. Jiang, B. Yurke, B. Firestein and N. Langrana, "Neurite outgrowth on a DNA crosslinked hydrogel with tunable stiffnesses," *Annals of Biomedical Engineering*, vol. 36, pp. 1565-1579, 2008.
57. K. Franze, J. Gerdemann, M. Weick, T. Betz, S. Pawlizak, M. Lakadamyali, J. Bayer, K. Rillich, M. Gogler, Y. Lu, A. Reichenback, P. Janmey and J. Kas, "Neurite branch retraction is caused by a threshold-dependent mechanical impact," *Biophysical Journal*, vol. 97, pp. 1883-1890, 2009.
58. D. Bray, "Axonal growth in response to experimentally applied mechanical tension," *Developmental Biology*, vol. 102, pp. 379-389, 1984.
59. D. Van Essen, "A tension-based theory of morphogenesis and compact wiring in the central nervous system," *Nature*, vol. 385, pp. 313-318, 1997.
60. S. Heidemann and R. Buxbaum, "Mechanical tension as a regulator of axonal development," *Neurotoxicology*, vol. 15, pp. 95-107, 1994.
61. A. Naba, O. M. Pearce, A. D. Rosario, D. Ma, H. Ding, V. Rajeeve, P. R. Cutillas, F. R. Balkwill and R. O. Hynes, "Characterization of the Extracellular Matrix of Normal and Diseased Tissues Using Proteomics," *Journal of Proteome Research*, vol. 16, no. 8, pp. 3083-3091, 2017.
62. F. A. Duck, "Mechanical Properties of Tissue," in *Physical Properties of Tissues: A Comprehensive Reference Work*, San Diego, Academic Press Limited, 1990, pp. 137-165.
63. A. Sarvazyan, A. Skovoroda, S. Emelianov, J. Fowlkes, J. Pipe, R. Adler, R. Buxton and P. Carson, "Biophysical Bases of Elasticity Imaging," in *Acoustical Imaging*, Boston, Springer, 1995, pp. 223-240.
64. T. Rozario and D. DeSimone, "The extracellular matrix in development and morphogenesis: a dynamic view," *Dev Biol*, vol. 341, pp. 126-140, 2010.
65. K. Tsang, M. Cheung, D. Chan and K. Cheah, "The development roles of the extracellular matrix: beyond structure to regulation," *Cell Tissue Res*, vol. 339, pp. 93-110, 2010.
66. S. Venkatesh, M. Yin, J. Glockner, N. Takahashi, P. Araoz, J. Talwalkar and R. Ehman, "MR elastography of liver tumors: preliminary results," *AJR Am J Roentgenol*, vol. 190, no. 6, pp. 1534-1540, 2008.

67. M. Yin, J. Talwalkar, K. Glaser, A. Manduca, R. Grimm, P. Rossman, J. Fidler and R. Ehman, "Assessment of hepatic fibrosis with magnetic resonance elastography," *Clin Gastroenterol Hepatol*, vol. 5, no. 10, pp. 1207-1213, 2007.
68. R. Wright, "Elastic tissue of normal and emphysematous lungs: a tridimensional histologic study," *Am J Pathol*, vol. 39, pp. 355-367, 1961.
69. P. Chrzanowski, S. Keller and J. Cerreta, "Elastin content of normal and emphysematous lung parenchyma," *Am J Med*, vol. 69, pp. 351-359, 1980.
70. M. Merrilees, P. Ching and B. Beaumont, "Changes in elastin, elastin binding protein and versican in alveoli in chronic obstructive pulmonary disease," *Respir Res*, vol. 9, p. 41, 2008.
71. J. van Straaten, W. Coers and J. Noordhoek, "Proteoglycan changes in the extracellular matrix of lung tissue from patients with pulmonary emphysema," *Mod Pathol*, vol. 12, pp. 697-705, 1999.
72. R. Annoni, T. Lanças, R. Tanigawa, M. Matsushita, S. Fernezlian, A. Bruno, L. Silva, P. Roughley, S. Battaglia, M. Dolhnikoff, P. Hiemstra, P. Sterk, K. Rabe and T. Mauad, "Extracellular matrix composition in COPD," *Eur Respir J*, vol. 40, pp. 1362-1373, 2012.
73. D. Butcher, T. Alliston and V. Weaver, "A tense situation: forcing tumor progression," *Nat Rev Cancer*, vol. 9, pp. 108-122, 2009.
74. K. R. Levental, H. Yu, L. Kass, J. N. Lakins, M. Egeblad, J. T. Erler, S. F. Fong, K. Csiszar, A. Giaccia, W. Weninger, M. Yamauchi, D. L. Gasser and V. M. Weaver, "Matrix crosslinking forces tumor progression by enhancing integrin signaling," *Cell*, vol. 139, no. 5, pp. 891-906, 2009.
75. R. Jain, J. Martin and T. Stylianopoulos, "The Role of Mechanical Forces in Tumor Growth and Therapy," in *Annual Review of Biomedical Engineering*, Vol 16, M. Yarmush, Ed., Palo Alto, Annual Reviews, 2014, pp. 321-346.
76. O. De Wever, P. Demetter, M. Mareel and M. Bracke, "Stromal myofibroblasts are drivers of invasive cancer growth," *Int J Cancer*, vol. 123, pp. 2229-2238, 2008.
77. K. Kessenbrock, V. Plaks and Z. Werb, "Matrix metalloproteinases: regulators of the tumor microenvironment," *Cell*, vol. 141, pp. 52-67, 2010.
78. F. T. Bosman and I. Stamenkovic, "Functional structure and composition of the extracellular matrix," *Journal of Pathology*, vol. 200, no. 4, pp. 423-428, 2003.
79. J. Erler and V. Weaver, "Three-dimensional context regulation of metastasis," *Clin Exp Metastasis*, vol. 26, pp. 35-49, 2009.
80. M. Paszek and V. Weaver, "The tension mounts: mechanics meets morphogenesis and malignancy," *J Mammary Gland Biol Neoplasia*, vol. 9, pp. 325-342, 2004.



81. M. Paszek, N. Zahir, K. Johnson, J. Lakins, G. Rozenberg, A. Gefen, C. Reinhart-King, S. Margulies, M. Dembo, D. Boettiger, D. Hammer and V. Weaver, "Tensional homeostasis and the malignant phenotype," *Cancer Cell*, vol. 8, no. 3, pp. 241-254, 2005.
82. Insua-Rodríguez and T. Oskarsson, "The extracellular matrix in breast cancer," *Advanced Drug Delivery Reviews*, vol. 97, pp. 51-55, 2016.
83. T. Oskarsson, "Extracellular matrix components in breast cancer progression and metastasis," *The Breast*, vol. 22, no. Supplement 2, pp. S66-S72, 2013.
84. A. Lochter and M. Bissell, "Involvement of extracellular matrix constituents in breast cancer," *Semin Cancer Biol*, vol. 6, pp. 165-173, 1995.
85. P. Lu, K. Takai, V. Weaver and Z. Werb, "Extracellular matrix degradation and remodeling in development and disease," *Cold Spring Harb Perspect Biol*, vol. 3, no. 12, 2011.
86. P. Schedin, J. O'Brien, M. Rudolph, T. Stein and V. Borges, "Microenvironment of the involuting mammary gland mediates mammary cancer progression," *J Mammary Gland Biol Neoplasia*, vol. 12, pp. 71-82, 2007.
87. J. O'Brien, L. Vanderlinden, P. Schedin and K. Hansen, "Rat mammary extracellular matrix composition and response to ibuprofen treatment during postpartum involution by differential GeLC-MS/MS analysis," *J Proteome Res*, vol. 11, pp. 4894-4905, 2012.
88. P. Schedin, "Pregnancy-associated breast cancer and metastasis," *Nat Rev Cancer*, vol. 6, pp. 281-291, 2006.
89. M. Duffy, T. Maguire, A. Hill, E. McDermott and N. O'Higgins, "Metalloproteinases: role in breast carcinogenesis, invasion and metastasis," *Breast Cancer Res*, vol. 2, no. 4, pp. 252-257, 2000.
90. T. Gudjonsson, L. Ronnov-Jessen, R. Villadsen, F. Rank, M. Bissell and O. Petersen, "Normal and tumor-derived myoepithelial cells differ in their ability to interact with luminal breast epithelial cells for polarity and basement membrane deposition," *J Cell Sci*, vol. 115, pp. 39-50, 2002.
91. H. Chong, C. Tan, R. Huang and N. Tan, "Matricellular proteins: a sticky affair with cancers," *Journal of Oncology*, vol. 2012, pp. 1-17, 2012.
92. A. Yee, M. Akens, B. Yang, J. Finkelstein, P. Zheng, Z. Deng and B. Yang, "The effect of versican G3 domain on local breast cancer invasiveness and bony metastasis," *Breast Cancer Res*, vol. 9, p. R47, 2007.
93. M. Leivonen, J. Lundin, S. Nordling, K. von Boguslawski and C. Haglund, "Prognostic value of syndecan-1 expression in breast cancer," *Oncology*, vol. 67, pp. 11-18, 2004.

94. K. Matsuda, H. Maruyama, F. Guo, J. Kleeff, J. Itakura, Y. Matsumoto, A. Lander and M. Korc, "Glypican-1 is overexpressed in human breast cancer and modulates the mitogenic effects of multiple heparin-binding growth factors in breast cancer cells," *Cancer Res*, vol. 61, pp. 5562-5569, 2001.
95. M. Barton, R. Harris and S. Fletcher, "The rational clinical examination. Does this patient have breast cancer? The screening clinical breast examination: should it be done? How?," *JAMA*, vol. 282, no. 13, pp. 1270-1280, 1999.
96. D. Elias, L. Sideris, M. Pocard, T. de Baere, C. Dromain, N. Lassau and P. Lasser, "Incidence of unsuspected and treatable metastatic disease associated with operable colorectal liver metastases discovered only at laparotomy (and not treated when performing percutaneous radiofrequency ablation)," *Ann Surg Oncol*, vol. 12, no. 4, pp. 298-302, 2005.
97. P. L. Jones, J. Crack and M. Rabinovitch, "Regulation of tenascin-C, a Vascular Smooth Muscle Cell Survival Factor that Interacts with the  $\alpha$ V $\beta$ 3 Integrin to Promote Epidermal Growth Factor Receptor Phosphorylation and Growth," *J Cell Biol*, vol. 139, pp. 279-293, 1997.
98. C. D. Roskelley, A. Srebrow and M. J. Bissell, "A hierarchy of ECM-mediated signalling regulates tissue-specific gene expression," *Current Opinion in Cell Biology*, vol. 7, pp. 736-747, 1995.
99. A. Fullár, J. Dudás, L. Oláh, P. Hollósi, Z. Papp, G. Sobel, K. Karászi, S. Paku, K. Baghy and I. Kovalszky, "Remodeling of extracellular matrix by normal and tumor-associated fibroblasts promotes cervical cancer progression," *BMC Cancer*, vol. 15, pp. 256-271, 2015.
100. American Cancer Society, "Cancer Facts & Figures 2018," American Cancer Society, Atlanta, 2018.
101. H. Verheul and H. Pinedo, "Clinical implications of drug resistance," in *Drug Resistance in the Treatment of Cancer*, H. Pinedo and G. Giaccone, Eds., Cambridge, Cambridge University Press, 2006, pp. 199-231.
102. A. Prahallad, "Unresponsiveness of colon cancer to BRAF(V600E) inhibition through feedback activation of EGFR," *Nature*, vol. 483, pp. 100-103, 2012.
103. C. Sun, L. Wang, S. Huang, G. Heynen, A. Prahallad, C. Robert, J. Haanen, C. Blank, J. Wesseling, S. Willems, D. Zecchin, S. Hobor, P. Bajpe, C. Lieftink, C. Mateus, S. Vagner, W. Gernrum, I. Hofland, A. Schlicker, L. Wessels, R. Beijersbergen and e. al, "Reversible and adaptive resistance to BRAF(V600E) inhibition in melanoma," *Nature*, vol. 508, no. 7494, pp. 118-122, 2014.
104. J. Riordan and V. Ling, "Genetic and biochemical characterization of multidrug resistance," *Pharmacol Ther*, vol. 28, no. 1, pp. 51-75, 1985.

105. L. Liu, "DNA topoisomerase poisons as antitumor drugs," *Annu Rev Biochem*, vol. 58, pp. 351-375, 1989.
106. S. Hasegawa, T. Abe, S. Naito, S. Kotoh, J. Kumazawa, D. Hipfner, R. Deeley and S. K. M. Cole, "Expression of multidrug resistance-associated protein (MRP), MDR1 and DNA topoisomerase II in human multidrug-resistant bladder cancer cell lines," *Br J Cancer*, vol. 71, no. 5, pp. 907-913, 1995.
107. K. Brasseur, N. Gévry and E. Asselin, "Chemoresistance and targeted therapies in ovarian and endometrial cancers," *Oncotarget*, vol. 8, pp. 4008-4042, 2017.
108. C. Lu and A. Shervington, "Chemoresistance in gliomas," *Mol Cell Biochem*, vol. 312, pp. 71-80, 2008.
109. E. A. O'Reilly, L. Gubbins, S. Sharma, R. Tully, M. H. Z. Guang, K. Weiner-Gorzel, J. McCaffrey, M. Harrison, F. Furlong, M. Kell and A. McCann, "The fate of chemoresistance in triple negative breast cancer (TNBC)," *BBA Clinical*, vol. 3, pp. 257-275, 2015.
110. D. Gewirtz, "A critical evaluation of the mechanisms of action proposed for the antitumor effects of the anthracycline antibiotics adriamycin and daunorubicin," *Biochem Pharmacol*, vol. 57, pp. 727-741, 1999.
111. K. Tewey, T. Rowe, L. Yang, B. Halligan and L. Liu, "Adriamycin-induced DNA damage mediated by mammalian DNA topoisomerase-II," *Science*, vol. 226, pp. 466-468, 1984.
112. J. Doroshow, "Role of hydrogen peroxide and hydroxyl radical formation in the killing of Ehrlich tumor cells by anticancer quinones," *Proc Natl Acad Sci USA*, vol. 83, pp. 4514-4518, 1986.
113. S. Fogli, P. Nieri and M. Breschi, "The role of nitric oxide in anthracycline toxicity and prospects for pharmacologic prevention of cardiac damage," *FASEB J*, vol. 18, pp. 664-675, 2004.
114. F. Yaquub, "Mechanism of action of anthracycline drugs," *The Lancet Oncology*, vol. 14, no. 8, p. e296, 2013.
115. U. Germann, "P-glycoprotein: a mediator of multidrug resistance in tumour cells," *Eur J Cancer*, vol. 32A, pp. 927-944, 1996.
116. S. Cole, G. Bhardwaj, J. Gerlach, J. Mackie, C. Grant, K. Almquist, A. Stewart, E. Kurz, A. Duncan and R. Deeley, "Overexpression of a transporter gene in a multidrug-resistant human lung cancer cell line," *Science*, vol. 258, no. 5088, pp. 1650-1654, 1992.

117. S. Lal, A. Mahajan, W. Chen and B. Chowbay, "Pharmacogenetics of target genes across doxorubicin disposition pathway: a review," *Curr Drug Metab*, vol. 11, pp. 115-128, 2010.
118. L. Young, B. Campling, S. Cole, R. Deeley and J. Gerlach, "Multidrug resistance proteins MRP3, MRP1, and MRP2 in lung cancer: correlation of protein levels with drug response and messenger RNA levels," *Clin Cancer Res*, vol. 7, pp. 1798-1804, 2001.
119. S. Singhal, J. Singhal, R. Sharma, S. Singh, P. Zimniak and Y. A. S. Awasthi, "Role of RLIP76 in lung cancer doxorubicin resistance: I. The ATPase activity of RLIP76 correlates with doxorubicin and 4-hydroxynonenal resistance in lung cancer cells.," *Int J Oncol*, vol. 22, no. 2, pp. 365-375, 2003.
120. D. Burgess, J. Doles, L. Zender, W. Xue, B. Ma, W. McCombie, G. Hannon, S. Lowe and M. Hemann, "Topoisomerase levels determine chemotherapy response in vitro and in vivo," *Proc Natl Acad Sci USA*, vol. 105, no. 26, pp. 9053-9058, 2008.
121. C. Oakman, E. Moretti, F. Galardi, L. Santarpia and L. A. Di, "The role of topoisomerase-IIalpha and HER-2 in predicting sensitivity to anthracyclines in breast cancer patients," *Cancer Treat Rev*, vol. 35, pp. 662-667, 2009.
122. K. Pritchard, H. Messersmith, L. Elavathil, M. Trudeau, F. O'Malley and B. Dhesy-Thind, "HER-2 and topoisomerase II as predictors of response to chemotherapy," *J Clin Oncol*, vol. 26, pp. 736-744, 2008.
123. B. A. Weaver, "How Taxol/paclitaxel kills cancer cells," *Mol Biol Cell*, vol. 25, no. 18, pp. 2677-2681, 2014.
124. R. Yusuf, Z. Duan, D. Lamendola, R. Penson and M. Seiden, "Paclitaxel Resistance: Molecular Mechanisms and Pharmacologic Manipulation," *Current Cancer Drug Targets*, vol. 3, no. 1, pp. 1-19, 2005.
125. T. Strobel, L. Swanson, S. Korsmeyer and S. Cannistra, "BAX Enhances Paclitaxel-Induced Apoptosis through a p53-Independent Pathway," *Proc Natl Acad Sci USA*, vol. 93, pp. 14094-14099, 1996.
126. T. Strobel, Y. Tai, S. Korsmeyer and S. Cannistra, "BAD Partly Reverses Paclitaxel Resistance in Human Ovarian Cancer Cells," *Oncogene*, vol. 17, pp. 2419-2427, 1998.
127. D. Luo, S. Cheng, H. Xie and Y. Xie, "Effects of Bcl-2 and Bcl-XL Protein Levels On Chemoresistance Of Hepatoblastoma Hepg2 Cell Line," *Biochem Cell Biol*, vol. 78, pp. 119-126, 2000.
128. B. Ogretmen and A. Safa, "Down-Regulation of Apoptosis-Related Bcl-2 but not Bcl-Xl or Bax Proteins in Multidrug-Resistant MCF-y/Adr Human Breast Cancer Cells," *Int J Cancer*, vol. 67, pp. 608-614, 1996.

129. Z. Duan, D. Lamendola, R. Penson, K. Kronish and M. Seiden, "Overexpression of IL-6 but not IL-8 Increases Paclitaxel Resistance of u-2os Human Osteosarcoma Cells," *Cytokine*, vol. 17, pp. 234-242, 2002.
130. S. Song, M. Wientjes, Y. Gan and J. Au, "Fibroblast Growth Factors: An Epigenetic Mechanism of Broad Spectrum Resistance to Anticancer Drugs," *Proc Natl Acad Sci USA*, vol. 97, pp. 8658-8663, 2000.
131. D. Yu and M. Hung, "Role of ErbB2 in Breast Cancer Chemosensitivity," *Bioessays*, vol. 22, pp. 673-680, 2000.
132. J. Mendelsohn and J. Baselga, "The EGF Receptor Family as Targets for Cancer Therapy," *Oncogene*, vol. 19, pp. 6550-6565, 2000.
133. F. Aoudjit and K. Vuori, "Integrin Signaling Inhibits Paclitaxel-Induced Apoptosis in Breast Cancer Cells," *Oncogene*, vol. 20, pp. 4995-5004, 2001.
134. K. Luker, C. Pica, R. Schreiber and D. Piwnica-Worms, "Overexpression of IRF9 Confers Resistance to Antimicrotubule Agents in Breast Cancer Cells," *Cancer Res*, vol. 61, pp. 6540-6547, 2001.
135. E. Dolci, R. Abramson, Y. Xuan, J. Siegfried, K. Yuenger, D. Yassa and T. Tritton, "Anomalous Expression Of P-Glycoprotein in Highly Drug-Resistant Human KB Cells," *Int J Cancer*, vol. 54, pp. 302-308, 1993.
136. P. Cesaro, E. Raiteri, M. Demoz, R. Castino, F. Baccino, G. Bonelli and C. Isidoro, "Expression of protein kinase C beta1 confers resistance to TNFalpha- and paclitaxel-induced apoptosis in HT-29 colon carcinoma cells," *Int J Cancer*, vol. 93, no. 2, pp. 179-184, 2001.
137. G. Ajabnoor, T. Crook and H. Coley, "Paclitaxel resistance is associated with switch from apoptotic to autophagic cell death in MCF-7 breast cancer cells," *Cell Death and Disease*, vol. 3, no. 1, p. e260, 2012.
138. D. Hanahan and R. Weinberg, "The hallmarks of cancer," *Cell*, vol. 100, pp. 57-70, 2000.
139. D. Hanahan and R. Weinberg, "Hallmarks of cancer: the next generation," *Cell*, vol. 144, pp. 646-674, 2011.
140. M. Pickup, J. Mouw and V. Weaver, "The extracellular matrix modulates the hallmarks of cancer," *EMBO Rep*, vol. 15, no. 12, pp. 1243-1253, 2014.
141. V. Weaver, O. Petersen, F. Wang, C. Larabell, P. Briand, C. Damsky and M. Bissell, "Reversion of the Malignant Phenotype of Human Breast Cells in Three-Dimensional Culture and In Vivo by Integrin Blocking Antibodies," *Journal of Cell Biology*, vol. 137, no. 1, pp. 231-245, 1997.

142. P. Provenzano, D. Inman, K. Eliceiri, J. Knittel, L. Yan, C. Rueden, J. White and P. Keely, "Collagen density promotes mammary tumor initiation and progression," *BMC Medicine*, vol. 6, no. 11, 2008.
143. P. Provenzano, D. Inman, K. Eliceiri and P. Keely, "Matrix density-induced mechanoregulation of breast cell phenotype, signaling and gene expression through a FAK-ERK linkage," *Oncogene*, vol. 28, no. 49, pp. 4326-4343, 2009.
144. J.-W. Shin and D. J. Mooney, "Shin, J.-W., & Mooney, D. J. (2016). Extracellular matrix stiffness causes systematic variations in proliferation and chemosensitivity in myeloid leukemias," *Proceedings of the National Academy of Sciences of the United States of America*, vol. 113, no. 43, pp. 12126-12131, 2016.
145. H. Abu-Tayeh, K. Weidenfeld, A. Zhilin-Roth, S. Schif-Zuck, S. Thaler, C. Cotarelo, T. Tan, J. Thiery, J. Green, G. Klorin, E. Sabo, J. Sleeman, M. Tzukerman and D. Barkan, "'Normalizing' the malignant phenotype of luminal breast cancer cells via alpha(v)beta(3)-integrin," *Cell Death and Disease*, vol. 7, p. e2491, 2016.
146. S. Carey, K. Martin and C. Reinhart-King, "Three-dimensional collagen matrix induces a mechanosensitive invasive epithelial phenotype," *Scientific Reports*, vol. 7, p. 42088, 2017.
147. S. Gopal, L. Veracini, D. Grall, C. Butori, S. Schaub, S. Audebert, L. Camoin, E. Baudalet, A. Radwanska, S. Divonne, S. Violette, P. Weinreb, S. Rekima, M. Ilie, A. Sudaka, P. Hofman and E. Obberghen-Schilling, "Fibronectin-guided migration of carcinoma collectives," *Nature Communications*, vol. 8, p. 14105, 2017.
148. S. Zusiak, R. Nossal and D. Sackett, "Multiwell Stiffness Assay for the Study of Cell Responsiveness to Cytotoxic Drugs," *Biotechnology and Bioengineering*, vol. 111, no. 2, pp. 396-403, 2014.
149. A. Rice, E. Cortes, D. Lachowski, B. Cheung, S. Karim, J. Morton and A. d. R. Hernández, "Matrix stiffness induced epithelial-mesenchymal transition and promotes chemoresistance in pancreatic cancer cells," *Oncogenesis*, vol. 6, p. e352, 2017.
150. T. Moroishi, C. Hansen, K. Guan and S. Diego, "The emerging roles of YAP and TAZ in cancer," *Nat Rev Cancer*, vol. 15, pp. 73-79, 2015.
151. J. M. Lamar, P. Stern, H. Liu, J. W. Schindler, Z.-G. Jiang and R. O. Hynes, "The Hippo pathway target, YAP, promotes metastasis through its TEAD-interaction domain," *PNAS*, vol. 109, no. 37, pp. E2441-E2450, 2012.
152. Y. Liu, K. He, Y. Hu, X. Guo, D. Wang, W. Shi, J. Li and J. Song, "YAP modulates TGF-beta1-induced simultaneous apoptosis and EMT through upregulation of the EGF receptor," *Scientific Reports*, vol. 7, p. 45523, 2017.
153. C. Badouel and H. McNeill, "SnapShot: The Hippo Signaling Pathway," *Cell*, vol. 145, no. 3, pp. 484-484, 2011.

154. D. Pan, "The Hippo Signaling Pathway in Development and Cancer," *Dev Cell*, vol. 19, no. 4, pp. 491-505, 2010.
155. H. J. J. van Rensburg and X. Yang, "The roles of the Hippo pathway in cancer metastasis," *Cellular Signalling*, vol. 28, pp. 1761-1772, 2016.
156. W. Lehmann, D. Mossmann, J. Kleemann, K. Mock, C. Meisinger, T. Brummer, R. Herr, S. Brabletz, M. P. Stemmler and T. Brabletz, "ZEB1 turns into a transcriptional activator by interacting with YAP1 in aggressive cancer types," *Nat Comm*, vol. 7, pp. 1-15, 2016.

## Chapter 2: Characterization of Breast Cancer Cell Resistance to Chemotherapeutics in Alginate Hydrogels<sup>2</sup>

### 2.1 INTRODUCTION

The extracellular matrix (ECM) plays a critical role in the control of cell processes including cell survival, proliferation and apoptosis<sup>1-3</sup>. Cancer cells as well as normal cells integrate signals from ECM and may initiate different signaling programs in response to microenvironmental cues<sup>4-6</sup>. Understanding the contribution of mechanical signals from the 3D ECM in the tumor microenvironment is therefore important for predicting tumor progression and response to therapeutics.

There are many methods and platforms that can be used to grow and maintain cells as 3D cultures *in vitro*. One such method is to harvest matrix proteins such as collagens, laminins, or fibrins to construct a scaffold on which cells can grow. The primary advantage of using collagen and other native matrix proteins is their ability to closely mimic the fibril formation and a viscoelastic properties of their native environment<sup>7</sup>. Provenzano et al.<sup>8</sup> made use of this approach in studies of mouse mammary carcinoma cells cultured in dense collagen hydrogels to simulate mammographically dense breast tissue, a major risk factor for developing breast carcinomas<sup>9-12</sup>. However, this study also highlights one of the difficulties of using collagen hydrogels, namely that pure collagen hydrogels are typically of low stiffness (< 1 kPa) and stiffening collagen hydrogels comes at the cost of increasing overall collagen density or requires extensive chemical crosslinking.

Matrigel is a commercially available basement membrane extract consisting primarily of laminin, type IV collagen, entactin, and various growth factors<sup>13</sup>. The milieu of native matrix components and growth factors make it an appealing option for hydrogel cultures. However, Matrigel preparations are produced from basement membrane extracts from Engelbreth-Holm-

---

<sup>2</sup> Portions of this chapter were adapted from M. H. Joyce, C. Lu, E. R. James, R. Hegab, S. C. Allen, L. J. Suggs and A. Brock, "Phenotypic Basis for Matrix Stiffness-Dependent Chemoresistance of Breast Cancer Cells to Doxorubicin," *Front Oncol*, vol. 8, p. 337, 2018. A. B. and M. J. were responsible for the planning of the study and writing of the manuscript; C. L., E. J., M. J., R. H., and S. A. conducted the experiments; all authors were involved with the analysis of the manuscript.



Swarm mouse sarcoma tumors, meaning they are of tumorigenic origin and subject to significant batch-to-batch variation. This is an important factor for technologies and studies that require Good Manufacturing Processes (GMP) enforced by the Federal Drug Administration (FDA); it may also impact many studies that require a higher degree of precision in matrix composition.

Hyaluronic acid (HA) also falls in the native matrix component category. It is an anionic non-sulfated glycosaminoglycan distributed throughout connective, epithelial, and neural tissues. HA is an essential component of vertebrae ECM during growth, repair, and neoplasia<sup>14-16</sup>. It can be isolated from animal tissues or produced through microbial fermentation in *Escherichia coli*. Unmodified HA is not compatible with integrin-mediated cell adhesion, but rather facilitates cell adhesion through cell surface markers such as CD44 and CD168<sup>17</sup>. However, HA can be modified to present functional groups that allow for a broad range of crosslinking chemistries and can be further processed to form films (2D) or hydrogels (3D)<sup>18</sup>. Researchers have made use of this flexibility to investigate cellular mechanotransduction<sup>19,20</sup>.

Non-native biological materials have also been shown to be suitable for mimicking ECM. Shin and Mooney<sup>21</sup> have previously used alginate-based hydrogels to mimic matrix stiffness conditions that would be physiologically relevant for myeloid leukemia cells. Using ionic cross-linking, it was feasible to produce hydrogels that model a range of microenvironments, from stiff bone marrow (Young's modulus  $E = 3$  kPa) to low shear blood ( $E = 40$  cP). The alginate-based system proved ideal for these conditions, as the stiffness of hydrogel cultures could be tuned by including increasing concentrations of calcium sulfate to achieve stiffer hydrogels. In these studies, hydrogels as soft as  $E = 75$  Pa could be fabricated with the cross-linking agent (calcium sulfate), and fluid cultures ( $E = 40$  cP) could be maintained when no cross-linking agent was added. This platform allowed Shin and Mooney to study matrix mechanics of myeloid leukemias subtypes in ECM mimicking diverse *in vivo* environments.

Synthetic polymers can also be used to facilitate 3D cultures. Polyethylene glycol (PEG), acrylamide, and custom polypeptides are examples of polymers that can be used to create hydrogels. Zustiak et al.<sup>22</sup> used collagen-coated polyacrylamide hydrogels to form hydrogels from

$E = 1 \text{ kPa} - 100 \text{ kPa}$ . These hydrogels provide a very broad range of potential stiffness making them ideal for testing stiffness-dependence across many orders of magnitude. However, they must be coated with peptides or coupled with other matrix proteins to promote cell adhesion, and they are not a good representation of the fibrous networks that make up the ECM *in vivo*.

In this chapter, we utilize an alginate hydrogel model developed by Stowers et al.<sup>23</sup>, to culture breast carcinoma cells in engineered microenvironments with specific stiffness properties. We investigate whether ECM stiffness in these hydrogels affects cell response to cytotoxic chemotherapeutic treatments. We explore two types of therapeutics, with different mechanisms of action, and compare their action in multiple human breast carcinoma and mouse mammary carcinoma models.

## **2.2 MATERIALS AND METHODS**

### **2.2.1 Cell culture**

MCF7 cells were cultured in Minimum Essential Media (MEM, Life Technologies, REF: 11095-080, 89%) supplemented with Fetal Bovine Serum (FBS, Life Technologies, REF: 10437-028, 10%) and Penicillin/Streptomycin (P/S, Life Technologies, REF: 15070-063, 1%). Py2T cells were cultured in Dulbecco's Modified Eagle's Medium (DMEM, Life Technologies, REF: 10569-010, 89%) supplemented with FBS (Life Technologies, REF: 10437-028, 10%) and P/S (Life Technologies, REF: 15070-063, 1%). MDA-MB-231, TMEC, and M6 cells were cultured in Dulbecco's Modified Eagle's Medium (DMEM, Life Technologies, REF: 10569-010, 94%) supplemented with FBS (Life Technologies, REF: 10437-028 5%) and P/S (Life Technologies, REF: 15070-063, 1%). All cultures maintained in a tissue culture incubator set to 37 °C with 5% CO<sub>2</sub>. For 2D cultures, cells were grown as a monolayer in 12- (TrueLine, TR5000) or 96-well (Falcon, REF: 353072) plates. Studies done in 12-well plates have an  $n = 3$  for each condition, while studies using 96-well plates have an  $n = 5$  for each condition.

### **2.2.2 Hydrogel preparation**

The system described in these studies is a Matrigel-alginate based system. Hydrogels were prepared by mixing the following ingredients in the order described with thorough mixing after addition of each ingredient: 4% alginate (1.6% final concentration, 40% total volume; ProNova UP MVG), 5 – 20 mM calcium carbonate (5% total volume), 100 mM NaCl + 1mM HEPES buffer (20% total volume), cells (5% total volume), 10 – 40 mM D-(+)-Gluconic acid  $\delta$ -lactone (5% total volume), and Matrigel (25% total volume; VWR International). Once mixed, 50  $\mu$ L of the gel solution was pipetted into each well of a 96-well plate and placed in an incubator (37 °C, 5% CO<sub>2</sub>) for one hour to promote gelation. After gelation, 100  $\mu$ L of media was added to each sample and placed back in an incubator. Optimal cell seeding density was found to be within the range of 8,000,000 cells/mL to 16,000,000 cells/mL; this seeding density ensured a sufficient amount of cells were cultured for data analysis without overcrowding the available growth area within hydrogels. For a 50  $\mu$ L hydrogel this equates to approximately 25,000 to 50,000 cells per gel, respectively. Each condition will have an  $n = 3$ .

### **2.2.3 Rheometry**

To determine hydrogel stiffness, a hydrogel solution was prepared following the protocol outlined in section 2.2.2, and approximately 50  $\mu$ L of hydrogel solution was pipetted into an 8 mm diameter PDMS mold. Samples were then incubated overnight in a tissue culture incubator (37°C, 5% CO<sub>2</sub>) before being measured on a Physica MCR 101 Rheometer using an 8 mm geometry (Anton Paar, Cat.#: 5681). Frequency sweep measurements were taken from 0.05 rad/s to 500 rad/s using Rheoplus (v3.40) software with 5% initial strain.

### **2.2.4 Dosing with chemotherapeutics**

Samples were exposed to doxorubicin (Sigma-Aldrich, Cat.#: D1515) or paclitaxel (Sigma-Aldrich, Cat.#: T7402) for 48 h. A broad range (1 nM – 200  $\mu$ M) of doses was used to determine the drug sensitivity.

### **2.2.5 Isolation of cells from hydrogels**

To extract the cells cultured in hydrogels for analysis, each 50  $\mu$ L gel was soaked in 100  $\mu$ L of 50 mM sodium citrate (Fisher Scientific, Cat#: BP327) for 15 m at room temperature. Gels were then mechanically disrupted by pipetting until the alginate dissolved to a liquid solution. Each sample was transferred to a microcentrifuge tube and centrifuged at 600 x g for 10 m to pellet.

### **2.2.6 Measuring viability**

Viability measures was assessed using acridine orange/propidium iodide (AOPI, Nexcelom, Cat#: CS2-0106) stain and MTS reagent (Promega, REF: G3580). Samples treated with AOPI were pelleted, resuspended in AccuMAX (Innovative Cell Technologies, Cat.#: AM-105), and mixed 1:1 with AOPI stain. Samples were then assayed using a Nexcelom Cellometer Vision. MTS assays were performed following the manufacturer's instructions. Briefly, all cell media was removed and replaced with MTS reagent mixed with media at 1:6 ratio, or 20  $\mu$ L of MTS reagent with 100  $\mu$ L of cell media per well of a 96-well plate. Samples were then incubated at 37 °C (5% CO<sub>2</sub>) for 1 – 2 h before reading their absorbance at 490 nm on a plate-reader. The data gathered from both cell viability assays was fit to a sigmoid function in Microsoft Excel and used to calculate drug sensitivity, as measured by LD50 value.

## **2.3 RESULTS**

### **2.3.1 An alginate hydrogel platform can be used to make ECM models of varying stiffness**

This study sought to investigate how the ECM stiffness might affect breast cancer cell response to chemotherapeutic treatment. To this end, we employed an alginate hydrogel model developed by Stowers et al.<sup>23</sup>. This system was chosen because of the broad range of achievable stiffness, uniformity of stiffness throughout the hydrogel, ability to dynamically tune hydrogel stiffness (discussed in Chapter 3), and unique ability to isolate the effects of ECM stiffness on cells.

Stowers et al.<sup>23</sup> have shown the capability of this system to form hydrogels as soft as 40 Pa and as stiff as 20,000 Pa. The stiffness of this hydrogel system is driven by ionic calcium ( $\text{Ca}^{2+}$ ) cross-linking G-blocks on alginate polymers. As additional cross-links are formed, the hydrogel will become progressively stiffer. The binding affinity of ionic calcium ( $\text{Ca}^{2+}$ ) to these G-blocks is high enough<sup>24</sup> to cause almost immediate cross-linking. Attempting to mix ionic calcium ( $\text{Ca}^{2+}$ ) with alginate will result in poor diffusion of calcium through the alginate and cause highly localized cross-linking. This system instead uses calcium carbonate ( $\text{CaCO}_3$ ), which prevents immediate cross-linking by keeping ionic calcium ( $\text{Ca}^{2+}$ ) bound to a carbonate ( $\text{CO}_3$ ) molecule. To achieve cross-linking, glucono- $\delta$ -lactone (GDL) is added to the mixture with calcium carbonate and alginate. GDL is pH neutral, but hydrolyses in water to gluconic acid, which is subsequently buffered by the carbonate ( $\text{CO}_3$ ) from the calcium carbonate ( $\text{CaCO}_3$ ), thus allowing ionic calcium ( $\text{Ca}^{2+}$ ) to bind to alginate G-blocks and form cross-links. This extends the cross-linking process such that it occurs over the span of hours rather than seconds, thus allowing gelation to occur evenly across the hydrogel.

Alginate is the major contributing factor to the hydrogel stiffness in this system, however alginate is bioinert<sup>25</sup> so Matrigel was added to provide cells with a substrate for the formation of cell-matrix adhesions and attachment sites. In this approach, cells are unable to directly rearrange the hydrogel and alter its stiffness. Such a system allowed us to further isolate the effects of stiffness on breast cancer cell resistance with limited dependence on cell adhesion type.

Hydrogels were prepared with 5 – 20 mM calcium carbonate and oscillatory shear stress rheometry was used to measure hydrogel stiffness. To collect stress and strain measurements, a hydrogel solution was prepared following the protocol outlined in section 2.2.2. Briefly, approximately 50  $\mu\text{L}$  of hydrogel solution was pipetted into an 8 mm diameter PDMS mold. Samples were then incubated overnight in a tissue culture incubator (37°C, 5%  $\text{CO}_2$ ) before being measured on a Physica MCR 101 Rheometer using an 8 mm geometry (Anton Paar, Cat.#: 5681). Frequency sweep measurements were taken from 0.05 rad/s to 500 rad/s using Rheoplus (v3.40) software with 5% initial strain. The elastic modulus was calculated for each frequency measured

within this range. Our results show that we were able to make gels ranging from 450 – 2,000 Pa (5 mM = 228 Pa, n = 3; 10 mM = 910 Pa, n = 1; 15 mM = 1,368, n = 8; 20 mM = 1,958 Pa, n = 5; **Fig. 2.1a**) by varying the concentration of calcium carbonate added to the initial gel mixture.

### **2.3.2 Characterization of mammary epithelial carcinoma cells to chemotherapeutic response in monolayer cultures**

We began our study by challenging breast cancer cell lines with two clinically relevant chemotherapeutics – doxorubicin and paclitaxel. MDA-MB-231 and MCF7 cells were cultured as a monolayer on tissue culture plastic (2D) and challenged with each drug as a single agent (**Fig. 2.1b**). After 48 h exposure the chemotherapeutic was removed and replaced with MTS reagent mixed into culture medium at a 1:6 ratio. Samples were incubated at 37C for 2 h, to allow for sufficient metabolism of the MTS reagent, and immediately placed on a plate-reader to measure 490 nm absorbance. These readings were used to calculate cell viability and fit to a sigmoidal function to determine the 50% lethal dose (LD50) for each drug-cell combination. The results outlined in **Fig. 2.2** show that MDA-MB-231 cells were more resistant to doxorubicin (LD50 = 26.6  $\mu$ M, **Fig. 2.2a**) than paclitaxel (LD50 = 94 nM, **Fig. 2.2b**). MCF7 cells showed a similar response with cells being more resistant to doxorubicin (LD50 = 4.4  $\mu$ M, **Fig. 2.2c**) than paclitaxel (LD50 = 126 nM, **Fig. 2.2d**).

Given that these cells lines had similar responses to paclitaxel but not doxorubicin when cultured as monolayers (2D), we expanded our study to evaluate the response of additional cell lines to doxorubicin (**Fig. 2.3**). TMEC, M6, M6c, and Py2T cell lines were all cultured as a monolayer and challenged for 48 h with doxorubicin. We observed that the MDA-MB-231 and Py2T cell lines had a significant advantage over the MCF7, M6, and M6c cell lines when exposed to doxorubicin.

### 2.3.3 Characterization of mammary epithelial carcinoma cells to chemotherapeutic response in alginate hydrogel cultures

Our experiments with monolayer cultures have shown that mammary epithelial carcinoma cell lines can have differing responses to treatment with doxorubicin. It has previously been shown that growing cells in 3D cultures can increase their resistance to chemotherapeutic drugs<sup>26-28</sup>. We sought to explore this with mammary epithelial carcinoma cell lines cultured in the previously described alginate hydrogel system. Samples were cultured for six days in either 450 Pa (**Fig. 2.4**) or 2,000 Pa (**Fig. 2.5**) hydrogels before treatment with doxorubicin; this was done to allow cultures plenty of time to form microstructures before exposure to treatment. Our goal was to determine if cells grown in 3D cultures would respond differently to the chemotherapeutics, and if so, to quantify these differences. We observed that chemoresistance of MDA-MB-231 cells to doxorubicin was 3-fold higher in the stiff ECM environment (LD50 = 10  $\mu$ M in 450Pa hydrogel cultures vs. LD50 = 32  $\mu$ M in 2,000Pa cultures;  $p = 0.002$ ; **Fig. 2.6a,c**). MCF7 cells did not display any significant ( $p = 0.134$ ; **Fig. 2.6b,d**) differences in resistance across substrates of increasing stiffness.

### 2.3.4 Acute responses to changes in ECM stiffness increase resistance to doxorubicin

Following our experiments that showed differing responses of mammary carcinoma cell lines to doxorubicin in alginate hydrogels, we questioned if the time a cell was exposed to their ECM would affect their response to treatment with doxorubicin. Our hypothesis was that cells exposed to stiffer ECM for longer would have increased resistance to doxorubicin. To test this hypothesis, we cultured MDA-MB-231 (**Fig. 2.7a**) and MCF7 (**Fig. 2.7b**) cells in 450 Pa or 2,000 Pa alginate hydrogels for 4 (3 days + 24 h), 6 (3 days + 72 h), or 8 (3 days + 120 h) days before challenging them with a 48 h exposure to doxorubicin.

Our results showed that MDA-MB-231 cells cultured in either 450 Pa or 2,000 Pa for 4 days had no significant difference in resistance to doxorubicin ( $p = 0.822$ , **Fig. 2.7a**). However, after 6 days ( $p = 0.002$ , **Fig. 2.7a**) and 8 days ( $p = 0.0005$ , **Fig. 2.7a**) MDA-MB-231 cells cultured in 2,000 Pa hydrogels showed an increase in resistance to doxorubicin compared to similar cultures

in 450 Pa hydrogels. MCF7 cells also showed no significant difference in doxorubicin resistance at 4 days ( $p = 0.575$ , **Fig. 2.7b**), 6 days ( $p = 0.134$ , **Fig. 2.7b**), or 8 days ( $p = 0.333$ , **Fig. 2.7b**) when comparing 450 Pa cultures to 2,000 Pa cultures. However, there was a significant decrease in resistance for 450 Pa cultures ( $p = 0.001$ , **Fig. 2.7b**) and 2,000 Pa cultures ( $p = 0.046$ , **Fig. 2.7b**) between the 4 day and 6 day time-point. No significant difference was found between 450 Pa cultures ( $p = 0.064$ , **Fig. 2.7b**) and 2,000 Pa cultures ( $p = 0.965$ , **Fig. 2.7b**) between the 6 day and 8 day time-point.

Viability assays were performed on cells that were cultured in 450 Pa or 2,000 Pa hydrogels at 48 h post-seeding and 1 week post-seeding (**Fig. 2.8a**). The results were compared to similar cells grown on tissue culture plastic, and we found that the total viability was similar for both MDA-MB-231 and MCF7 cells grown in all conditions. The culture media of these samples was also collected and measured for pH at the same time as viability testing (**Fig. 2.8b**). We found all pH measures to be within acceptable ranges given the values of the 2D (control) samples and previous findings in the literature stating that a malignant tumor's microenvironment can range from pH 6.5 – 6.9<sup>29</sup>.

## 2.4 DISCUSSION

Using the alginate hydrogel model described by Stowers et al.<sup>23</sup>, we optimized conditions to generate hydrogels mimicking the ECM stiffness of biologically healthy (~450 Pa) to early stage breast tumors (~2,000 Pa)<sup>30</sup>. We used this experimental model to determine how ECM mimicking both normal and early stage tumor tissue affects mammary epithelial carcinoma cell response to treatment with chemotherapeutics. Initially, we challenged samples with doxorubicin and paclitaxel. Doxorubicin, also known by the trade name Adriamycin, is a common chemotherapeutic used to treat neoadjuvant breast cancer. It works by intercalating into DNA and inhibiting progression of topoisomerase II after it has broken the DNA double helix for replication<sup>31</sup>. This prevents the DNA strands from resealing, thereby stopping DNA replication and ultimately leading to cell death after accumulation of enough unrepaired fragments. Paclitaxel



(sold under the trade name Taxol) is a member of the taxane family of drugs which work by disrupting microtubule function<sup>32</sup>. Microtubules in the mitotic spindle are normally highly dynamic, growing and shrinking to facilitate segregation of chromosomes to daughter cells during mitosis<sup>33</sup>. Paclitaxel functions as a microtubule-stabilizing agent, binding to  $\beta$ -tubulin near the M loop and increasing affinity for tubulin molecules, ultimately suppressing microtubule dynamics<sup>34,35</sup>. It has been shown to cause cell death by trapping cells in the metaphase/anaphase transition of mitosis, and thus acts preferentially on cancer cells due to their increased mitotic activity<sup>36,37</sup>.

Our results showed very similar LD50s for both MDA-MB-231 and MCF7 cells to paclitaxel in 2D cultures, but MDA-MB-231 cells had a 6-fold higher LD50 to doxorubicin compared to MCF7 cells. The differing response of these two mammary epithelial carcinoma lines to the same drug led us to challenge a panel of mammary epithelial carcinoma lines. This panel of cells was cultured both as monolayers (2D) and in hydrogels (3D) and challenged with doxorubicin. We found that cells displaying a mesenchymal phenotype (MDA-MB-231, Py2T-LT, TMEC) showed a stiffness-dependent increase in resistance to doxorubicin, whereas cell types displaying epithelial phenotypes (MCF7, M6, M6c) did not. This finding is similar to myeloid leukemia subtypes described by Shin & Mooney<sup>38</sup>. They cultured two myeloid leukemia cell lines in alginate hydrogels of varying stiffness and functionalized with varying ligands and proceeded to challenge cultures with chemotherapeutics commonly used to treat myeloid leukemia. Their results showed three subtypes of myeloid leukemia – class I being cells that were ligand sensitive, class II being cells that were ligand and matrix stiffness sensitive, and class III being cells that were mechanics independent. Our results indicate that the mesenchymal lines we tested would fall under the class II subtype, with the epithelial lines falling under the class III subtype. This is further supported by Lovitt et al.<sup>39</sup> who showed in their 2018 study that functional inhibition of  $\beta$ 1-integrin signaling in 3D cultures of MDA-MB-231 cells has a dose-dependent increase in sensitivity to doxorubicin.

We next sought to determine if the duration of exposure to ECM stiffness would affect resistance to doxorubicin. By culturing cells for varying periods of time in defined ECM environments, we explored the temporal dynamics of ECM-stiffness mediated responses. Our results indicate that there is an acute response to ECM changes, but this response levels out after approximately 4 days in the hydrogel. This area is currently understudied, but is an important consideration when screening for drug sensitivity or efficacy.

## **2.5 CONCLUSIONS**

Here we have shown that mammary epithelial carcinoma cell lines will respond differently when cultured in hydrogels (3D) as opposed to monolayers. Our results shed light on the importance of ECM stiffness and duration of exposure to ECM stiffness when evaluating drug sensitivities of mammary epithelial carcinoma cells. We believe that giving more attention to ECM stiffness and exposure to ECM stiffness prior to treatment will lead to more accurate simulations of drug efficacy.

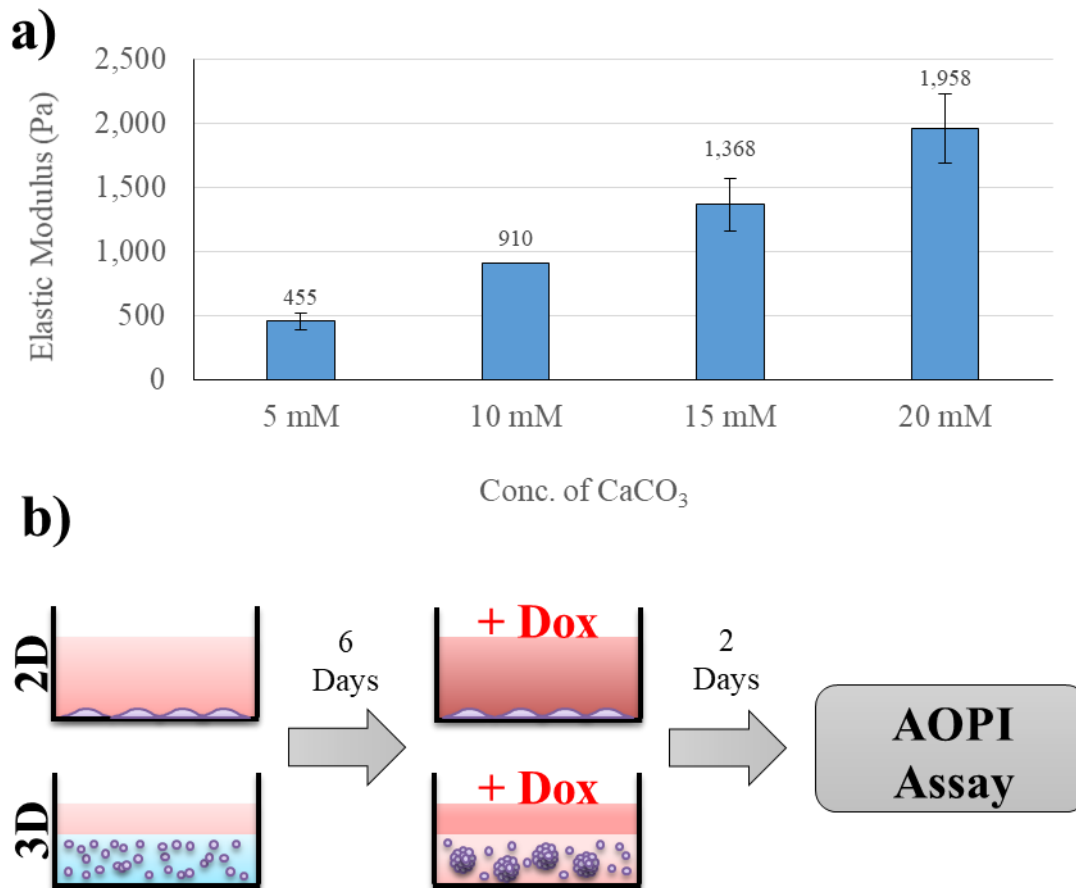


**Fig. 2.1 – Cells were cultured in hydrogels of varying stiffness before treatment with doxorubicin. a).** Hydrogel stiffness was determined by calculating Young’s modulus from frequency sweep measurements obtained from a rheometer. Error bars represent a 95% confidence interval as determined by a Student’s t-test distribution. The experimental protocol is outlined in **b).** Briefly, cells were seeded onto tissue culture plastic or into hydrogels that ranged in stiffness from 450 to 2,000 Pa. After 6 days in culture, samples were exposed to doxorubicin for 48h and cell viability was determined using AOPI staining.

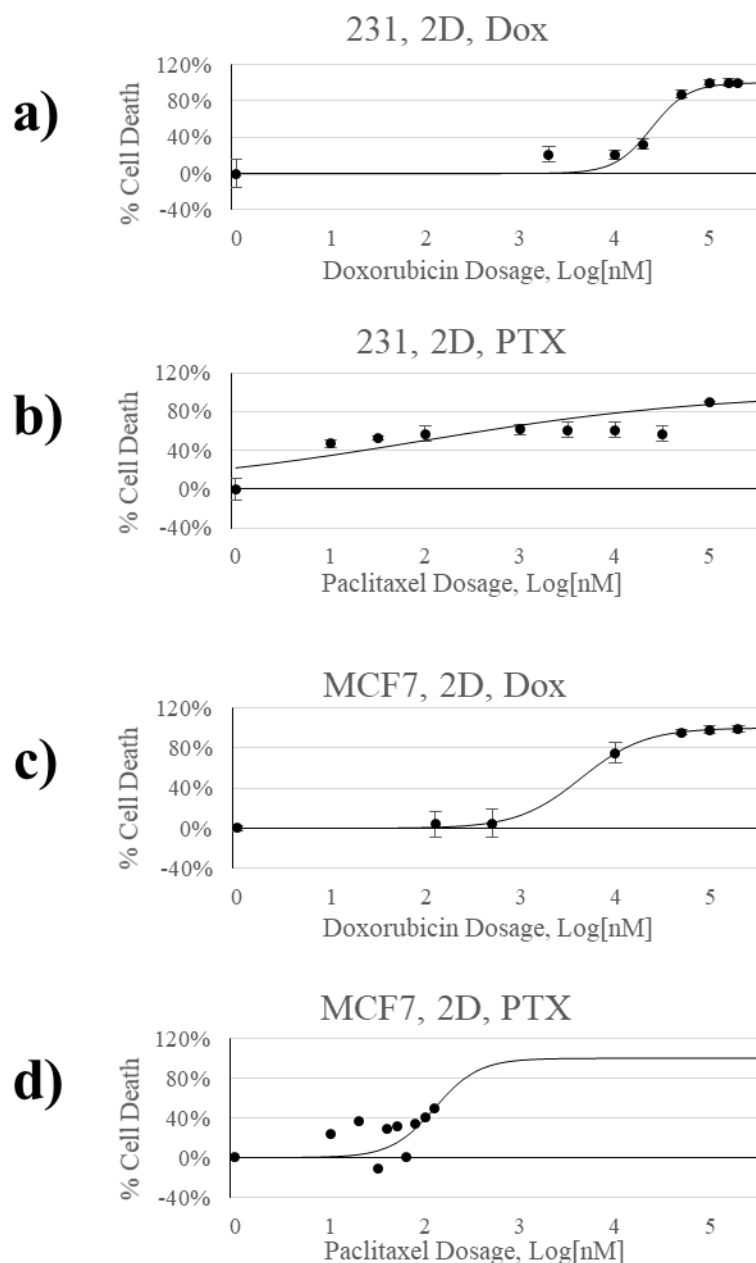


**Fig. 2.2 – Cells were cultured as a 2D monolayer and exposed to doxorubicin or paclitaxel.** MDA-MB-231 and MCF7 cells were cultured as a 2D monolayer and exposed to doxorubicin or paclitaxel for 48 h. **a)** MDA-MB-231 cultures were found to be more resistant to doxorubicin (LD50 = 26.6  $\mu$ M) than **b)** paclitaxel (LD50 = 94 nM). **c)** MCF7 cultures were also found to be more resistant to doxorubicin (LD50 = 4.4  $\mu$ M) than similar **d)** MCF7 cultures treated with paclitaxel (LD50 = 126 nM).

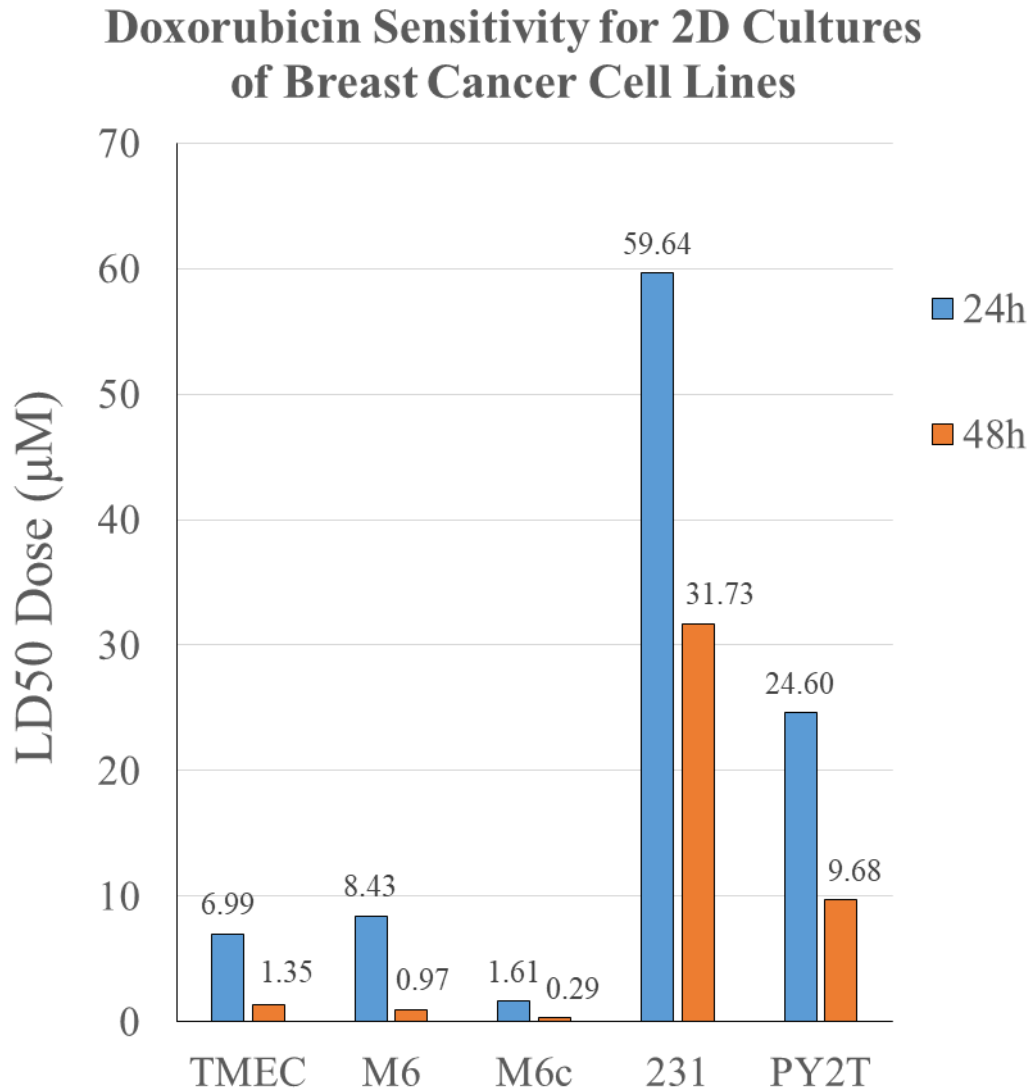


**Fig. 2.3 – Additional cell lines were cultured as a 2D monolayer and challenged with doxorubicin.** Additional mammary epithelial carcinoma cell lines were cultured as 2D monolayers and exposed to doxorubicin for 24 and 48 h before assaying for cell viability. MDA-MB-231 and Py2T cell lines were found to be more resistant to doxorubicin than the TMEC, M6, or M6c cell lines.

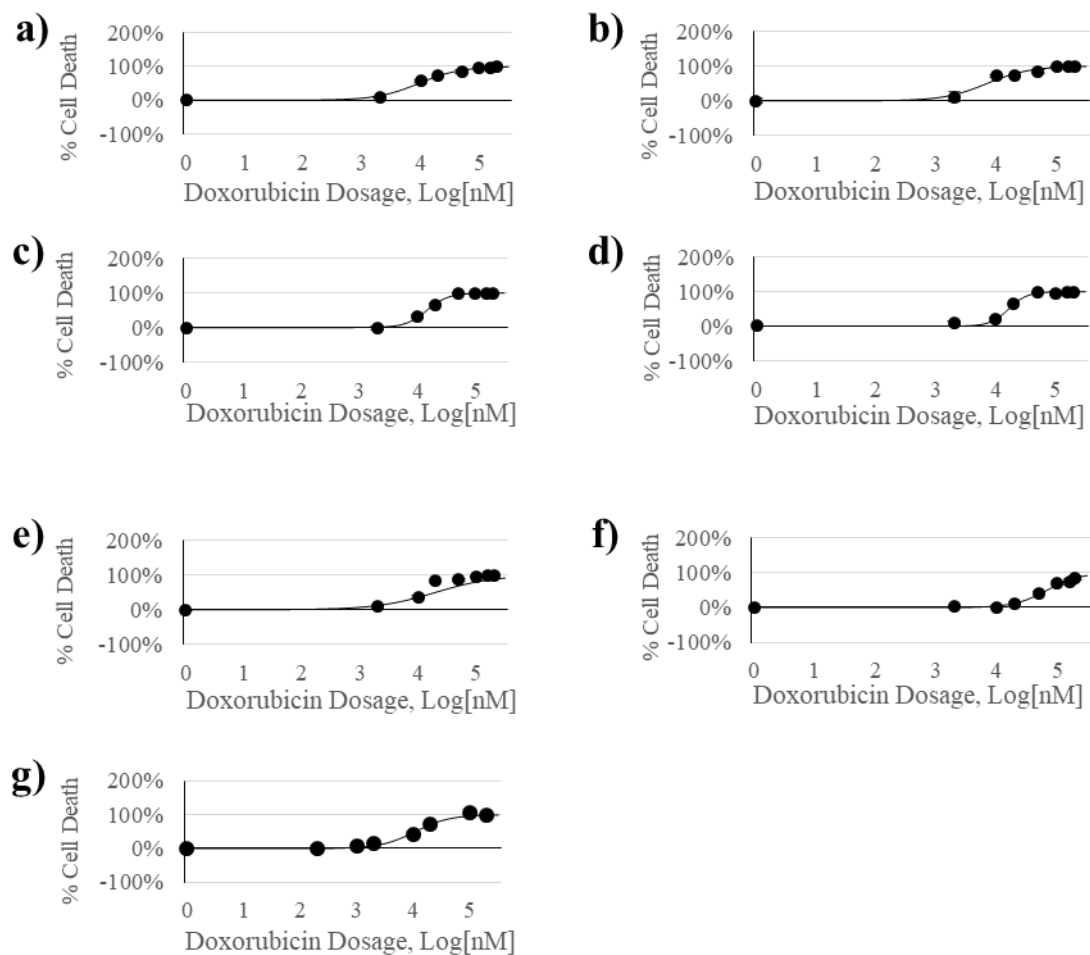


**Fig. 2.4** – Dose response curves of **a)** MDA-MB-231, **b)** MCF7, **c)** M6, **d)** M6c, **e)** TMEC, **f)** Py2T, **g)** Py2T-LT following 48h exposure to Doxorubicin. All cells were cultured in 450 Pa alginate-Matrigel hydrogels for 8 days before being exposed to Doxorubicin. Live and Dead cells were counted using a Nexcelom Cellometer with AOPI stain.

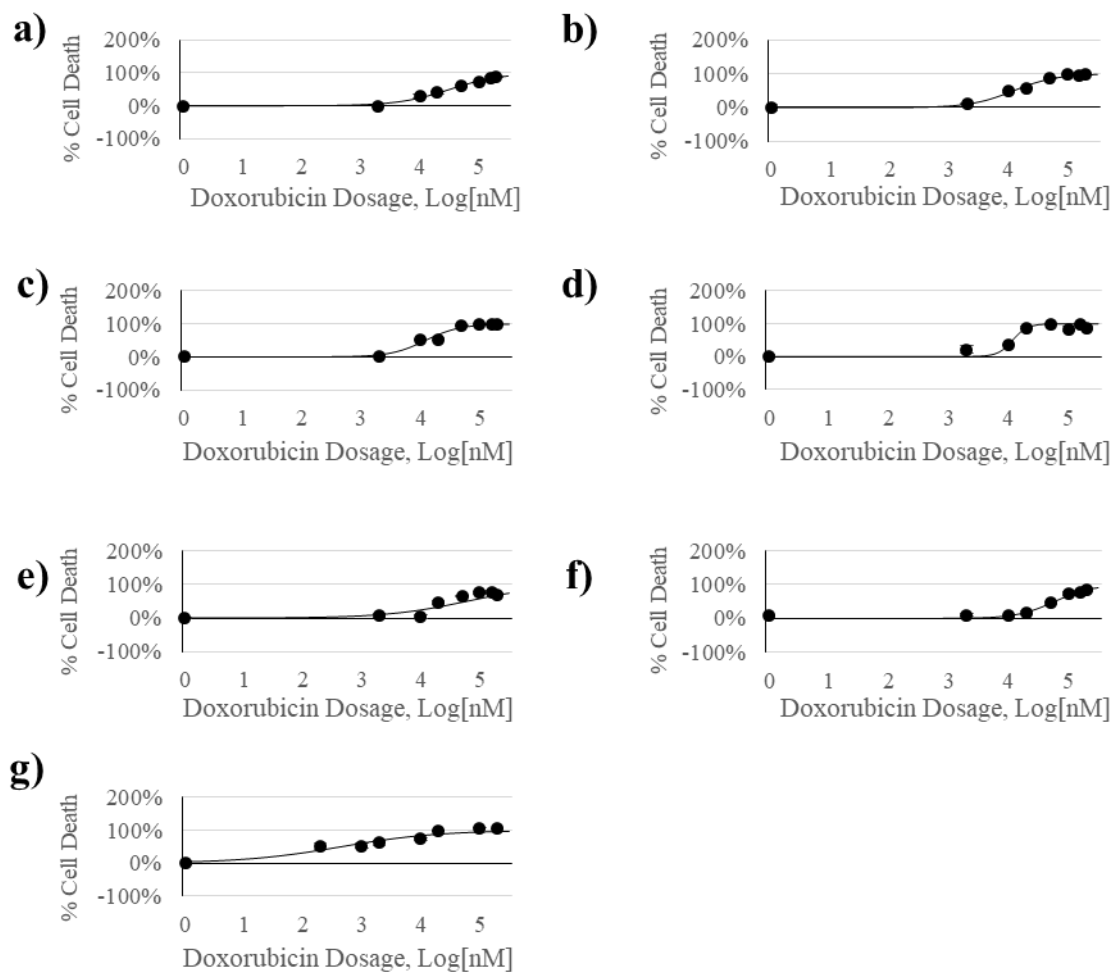


**Fig. 2.5** – Dose response curves of **a)** MDA-MB-231, **b)** MCF7, **c)** M6, **d)** M6c, **e)** TMEC, **f)** Py2T, **g)** Py2T-LT following 48h exposure to Doxorubicin. All cells were cultured in 2,000 Pa alginate-Matrigel hydrogels for 8 days before Doxorubicin exposure. Live and Dead cells were counted using a Nexcelom Cellometer with AOPI stain.

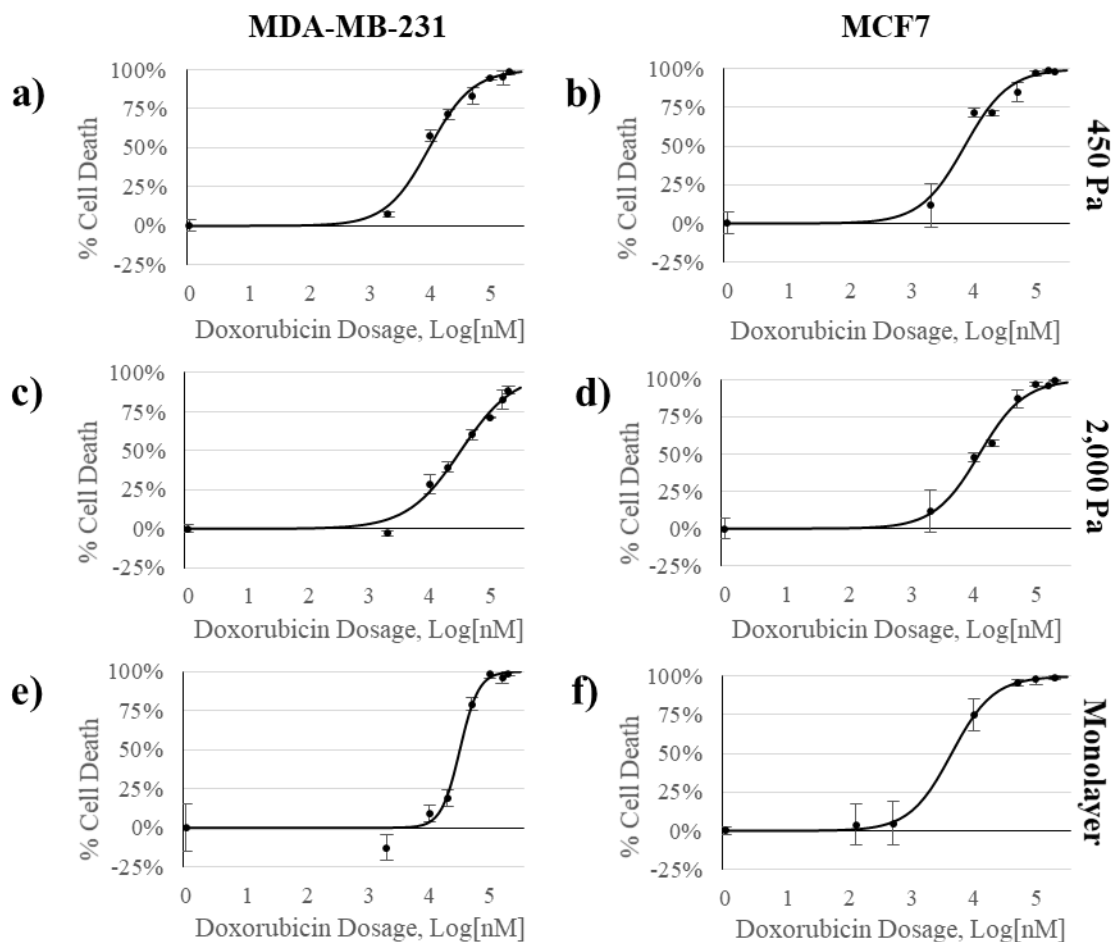


**Fig. 2.6 – 231 cells have a stiffness-dependent resistance to doxorubicin.** Dose response curves of 231 and MCF7 cells cultured in **a,b)** 450 Pa hydrogel, **c,d)** 2,000 Pa hydrogel, and **e,f)** 2D monolayer following 48h exposure to Doxorubicin. Percent cell death was determined by staining samples with AOPI and counting live cells using a Nexcelom Cellometer.



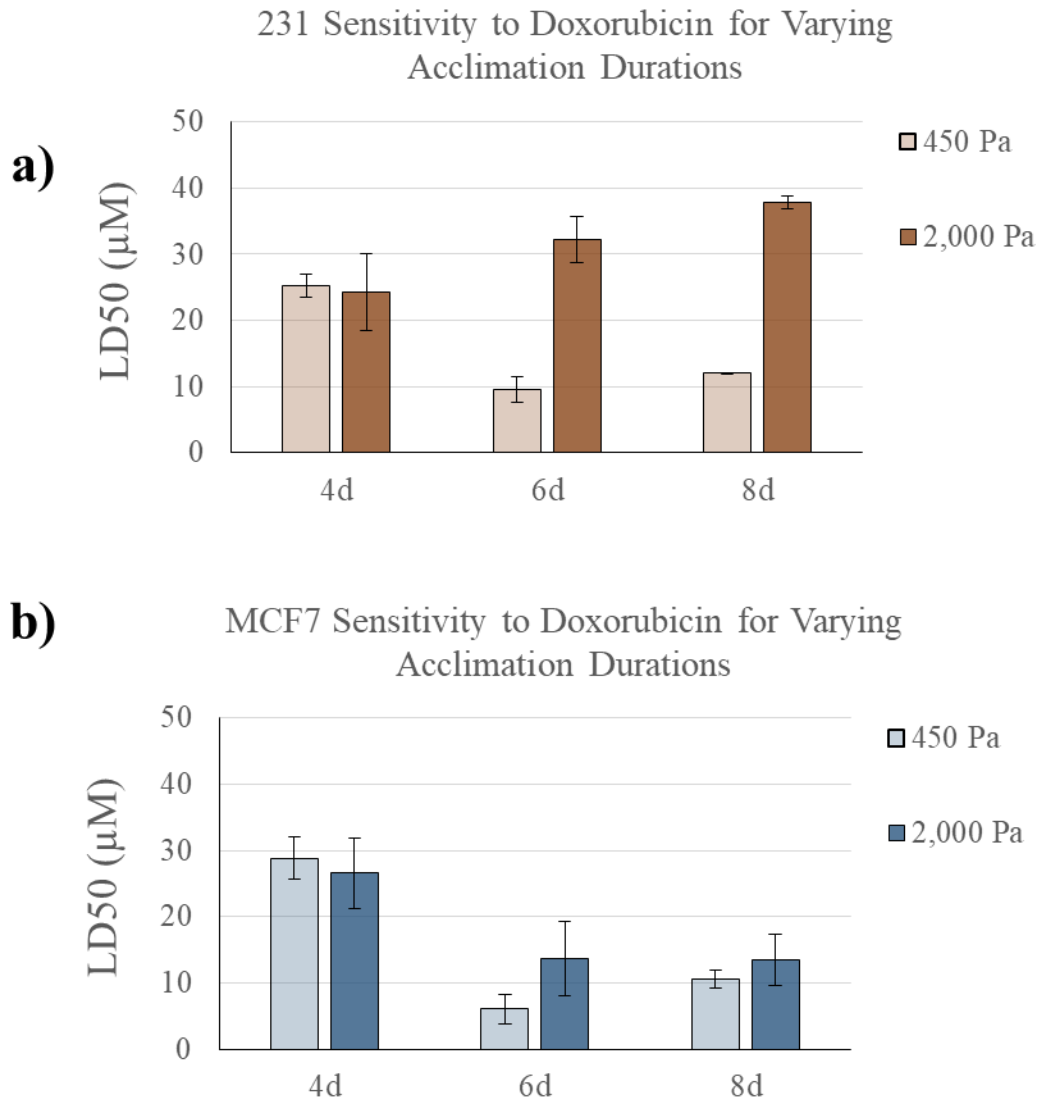
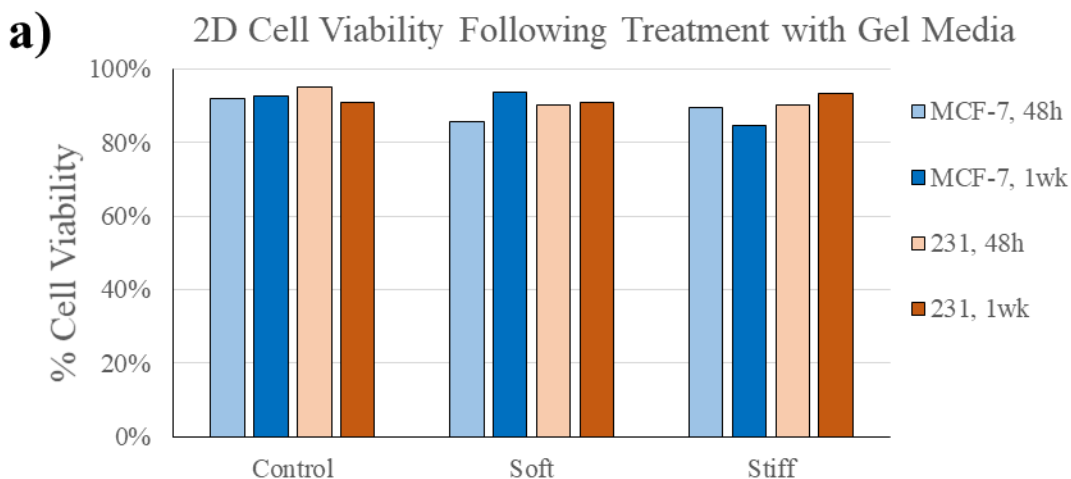


**Fig. 2.7 – Shorter acclimation time gives temporary increase in doxorubicin resistance.**

LD50 values of **a)** MDA-MB-231 and **b)** MCF7 cells cultured in 450 Pa hydrogel or 2,000 Pa hydrogel for 24, 72, or 120 h before a 48 h exposure to doxorubicin. Percent cell death was determined by staining samples with AOPI and counting live cells using a Nexcelom Cellometer.



**b)**

Cell Type	Media	pH (48h)	pH (1wk)
MCF7	Control	8.28	7.85
	450 Pa	7.85	7.87
	2,000 Pa	6.95	7.95
231	Control	8.09	7.6
	450 Pa	7.9	7.62
	2,000 Pa	7.16	7.95

**Fig. 2.8 – Inclusion of D-(+)-Gluconic acid  $\delta$ -lactone in hydrogel mixture does not adversely affect cell viability.** Cells were cultured as a monolayer (2D) on tissue culture plastic with culture media supplemented with concentrations of calcium carbonate and D-(+)-Gluconic acid  $\delta$ -lactone equal to those found in 450 Pa and 2,000 Pa hydrogel mixtures. Samples were seeded with the supplemented media and subsequently fed with normal culture media every other day for the remainder of the experiment to mimic the conditions that cells seeded in hydrogels would be exposed to.

After 5 days in culture, **a)** cell viability was assayed using acridine orange/propidium iodide (AOPI) staining, and **b)** the media was removed from samples to measure pH values. Estrella et al.<sup>40</sup> notes that the pH of a malignant tumor's microenvironment can range for pH 6.5 – 6.9. MCF10A cells cultured in presence of the 2,000 Pa hydrogel mixture conditions are the only samples to drop below this pH value causing almost complete cell death. The remaining MCF7 and 231 cell lines showed only slight deviations in pH from control conditions (normal culture media for the duration of the experiment), though all of these values fall within an acceptable range, and minimal cell death compared to control conditions.

1. T. Rozario and D. W. DeSimone, "The extracellular matrix in development and morphogenesis: A dynamic view," *Developmental Biology*, vol. 341, no. 2010, pp. 126-140, 2010.
2. S. L. Bowers, I. Banerjee and T. A. Baudino, "The Extracellular Matrix: At the Center of it All," *J Mol Cell Cardiol*, vol. 48, no. 3, pp. 474-482, 2010.
3. C. Bonnans, J. Chou and Z. Werb, "Remodelling the extracellular matrix in development and disease," *Nat Rev Mol Cell Biol*, vol. 15, no. 12, pp. 786-801, 2014.
4. P. Jones, J. Crack and M. Rabinovitch, "Regulation of tenascin-C, a Vascular Smooth Muscle Cell Survival Factor that Interacts with the  $\alpha$ V $\beta$ 3 Integrin to Promote Epidermal Growth Factor Receptor Phosphorylation and Growth," *J Cell Biol*, vol. 139, pp. 279-293, 1997.
5. C. Roskelley, A. Srebrow and M. Bissell, "A hierarchy of ECM-mediated signalling regulates tissue-specific gene expression," *Current Opinion in Cell Biology*, vol. 7, pp. 736-747, 1995.
6. A. Fullár, J. Dudás, L. Oláh, P. Hollósi, Z. Papp, G. Sobel, K. Karászi, S. Paku, K. Baghy and I. Kovalszky, "Remodeling of extracellular matrix by normal and tumor-associated fibroblasts promotes cervical cancer progression," *BMC Cancer*, vol. 15, pp. 256-271, 2015.
7. S. Caliali and J. Burdick, "A Practical Guide to Hydrogels for Cell Culture," *Nat Methods*, vol. 13, no. 5, pp. 405-414, 2016.
8. P. Provenzano, D. Inman, K. Eliceiri, J. Knittel, L. Yan, C. Rueden, J. White and P. Keely, "Collagen density promotes mammary tumor initiation and progression," *BMC Med*, p. 11, 2008.
9. V. McCormack and S. dos Santos, "Breast density and parenchymal patterns as markers of breast cancer risk: a meta-analysis," *Cancer Epidemiol Biomarkers Prev*, pp. 1159-1169, 2006.
10. N. Boyd, G. Lockwood, J. Byng, D. Tritchler and M. Yaffe, "Mammographic densities and breast cancer risk," *Cancer Epidemiol Biomarkers Prev*, pp. 1133-1144, 1998.
11. N. Boy, L. Martin, J. Stone, C. Greenberg, S. Minkin and M. Yaffe, "Mammographic densities as a marker of human breast cancer risk and their use in chemoprevention," *Curr Oncol Rep*, pp. 314-321, 2001.
12. N. Boyd, G. Dite, J. Stone, A. Gunasekara, D. English, M. McCredie, G. Giles, D. Tritchler, A. Chiarelli, M. Yaffe and J. Hopper, "Heritability of mammographic density, a risk factor for breast cancer," *N Engl J Med*, pp. 886-894, 2002.

13. H. Kleinman and G. Martin, "Matrigel: basement membrane matrix with biological activity," *Semin Cancer Biol.*, vol. 15, pp. 378-386, 2005.
14. B. Toole, "Hyaluronan in morphogenesis," *Semin Cell Dev Biol*, vol. 12, no. 2, pp. 79-87, 2001.
15. B. Toole, "Hyaluronan: from extracellular glue to pericellular cue," *Nat Rev Cancer*, vol. 4, no. 7, pp. 528-539, 2004.
16. R. Stern, Ed., *Hyaluronan in cancer biology*, 1st ed., San Diego, CA: Elsevier, 2009.
17. K. Dicker, L. Gurski, S. Pradhan-Bhatt, R. Witt, M. Farach-Carson and X. Jia, "Hyaluronan: a simple polysaccharide with diverse biological functions," *Acta Biomater.*, vol. 10, no. 4, pp. 1558-1570, 2014.
18. J. Burdick and D. Glenn, "Hyaluronic Acid Hydrogels for Biomedical Applications," *Adv Mater*, vol. 23, no. 12, pp. H41-H56, 2011.
19. S. Khetan, M. Guvendiren, W. Legant, D. Cohen, C. CS and J. Burdick, "Degradation-mediated cellular traction directs stem cell fate in covalently crosslinked three-dimensional hydrogels," *Nat Mater*, vol. 12, no. 5, pp. 458-465, 2013.
20. M. Guvendiren and J. Burdick, "Stiffening hydrogels to probe short- and long-term cellular responses to dynamic mechanics," *Nat Commun*, vol. 3, p. 792, 2012.
21. S. Mooney and J. Shin, "Extracellular matrix stiffness causes systematic variations in proliferation and chemosensitivity in myeloid leukemias.," *Proceedings of the National Academy of Sciences of the United States of America*, pp. 12126-12131, 2016.
22. S. Zustiak, R. Nossal and D. Sackett, "Multiwell Stiffness Assay for the Study of Cell Responsiveness to Cytotoxic Drugs," *Biotechnology and Bioengineering*, vol. 111, no. 2, pp. 396-403, 2014.
23. R. Stowers, S. Allen and L. Suggs, "Dynamic phototuning of 3D hydrogel stiffness," *Proceedings of the National Academy of Sciences*, pp. 1953-1958, 2015.
24. X. Wang and H. G. Spencer, "Calcium alginate gels: formation and stability in the presence of an inert electrolyte," *Polymer*, vol. 39, no. 13, pp. 2759-2764, 1998.
25. N. Genes, J. Rowley, D. Mooney and L. Bonassar, "Effect of substrate mechanics on chondrocyte adhesion to modified alginate surfaces," *Archives of Biochemistry and Biophysics*, vol. 422, no. 2, pp. 161-167, 2004.
26. M. Wästfelt, B. Fadeel and J. Henter, "A journey of hope: Lessons learned from studies on rare diseases and orphan drugs," *J Intern Med*, vol. 260, pp. 1-10, 2006.
27. Y. Uchida, S. Tanaka, A. Aihara, R. Adikrisna, K. Yoshitake, S. Matsumura, Y. Mitsunori, A. Murakata, N. Noguchi, T. Irie, A. Kudo, N. Nakamura, P. Lai and S. Aii,

- "Analogy between sphere forming ability and stemness of human hepatoma cells," *Oncol Rep*, vol. 24, no. 5, pp. 1147-1151, 2010.
28. H. Dhiman, A. Ray and A. Panda, "Three-dimensional chitosan scaffold-based MCF-7 cell culture for the determination of the cytotoxicity of tamoxifen," *Biomaterials*, vol. 26, pp. 979-986, 2005.
  29. V. Estrella, T. Chen, M. Lloyd, J. Wojtkowiak, H. Cornnell, A. Ibrahim-Hashim, K. Bailey, Y. Balagurunathan, J. Rothberg, B. Sloane, J. Johnson, R. Gatenby and R. Gillies, "Acidity generated by the tumor microenvironment drives local invasion," *Cancer Res*, vol. 73, no. 5, pp. 1524-1535, 2013.
  30. D. T. Butcher, T. Alliston and V. M. Weaver, "A tense situation: forcing tumour progression," *Nature Reviews Cancer*, vol. 9, pp. 108-122, 2009.
  31. O. Tacar, P. Sriamornsak and C. Dass, "Doxorubicin: an update on anticancer molecular action, toxicity and novel drug delivery systems," *Journal of Pharmacy and Pharmacology*, vol. 65, pp. 157-170, 2012.
  32. M. Jordan and L. Wilson, "Microtubules as a target for anticancer drugs," *Nat. Rev. Cancer*, vol. 4, no. 4, pp. 356-265, 2004.
  33. C. Walczak and R. Heald, "Mechanisms of mitotic spindle assembly and function," in *International Review of Cytology*, vol. 265, K. W. Jeon, Ed., San Diego, California: Elsevier, 2008, pp. 111-158.
  34. E. Nogales, S. Wolf, I. Khan, R. Luduena and K. Downing, "Structure of tubulin at 6. 5Å and location of the taxol-binding site," *Nature*, vol. 375, pp. 424-427, 1995.
  35. E. Nogales, "Structural insights into microtubule function," *Annu. Rev. Biochem.*, vol. 69, pp. 277-302, 2000.
  36. B. Long and C. Fairchild, "Paclitaxel inhibits progression of mitotic cells to G1 phase by interference with spindle formation without affecting other microtubule functions during anaphase and telephase," *Cancer Res*, vol. 54, no. 16, pp. 4355-4361, 1994.
  37. M. Jordan, K. Wendell, S. Gardiner, W. Derry, H. Copp and L. Wilson, "Mitotic block induced in HeLa cells by low concentrations of paclitaxel (Taxol) results in abnormal mitotic exit and apoptotic cell death," *Cancer Res*, vol. 56, no. 4, pp. 816-825, 1996.
  38. J.-W. Shin and D. J. Mooney, "Shin, J.-W., & Mooney, D. J. (2016). Extracellular matrix stiffness causes systematic variations in proliferation and chemosensitivity in myeloid leukemias," *Proceedings of the National Academy of Sciences of the United States of America*, vol. 113, no. 43, pp. 12126-12131, 2016.
  39. C. J. Lovitt, T. B. Shelper and V. M. Avery, "Doxorubicin resistance in breast cancer cells is mediated by extracellular matrix proteins," *BMC Cancer*, vol. 18, no. 1, p. 41, 2018.

40. V. Estrella, T. Chen, M. Lloyd, J. Wojtkowiak, H. Cornnell, A. Ibrahim-Hashim, K. Bailey, Y. Balagurunathan, J. Rothberg, B. Sloane, J. Johnson, R. Gatenby and R. Gillies, "Acidity generated by the tumor microenvironment drives local invasion," *Cancer Res*, vol. 73, no. 5, pp. 1524-1535, 2013.

## Chapter 3: Characterization of Breast Cancer Cell Response to Chemotherapeutics in Dynamic Stiffened Hydrogels<sup>3</sup>

### 3.1 INTRODUCTION

The ECM is a major component of the cellular microenvironment that facilitates many basic cellular functions<sup>1</sup> due to its dynamic and transmutable nature<sup>2</sup>. Cells alter their surrounding ECM by changing its composition, through synthesis or degradation of ECM components, or architecture, through cross-linking via covalent and noncovalent modifications<sup>2</sup>. Synthesis of ECM components occurs locally. For example, in developing mammary glands, the fibroblasts surrounding epithelium will synthesize and deposit collagen I, one of the most abundant ECM proteins in mammary gland tissue<sup>3</sup>. Degradation of ECM components is largely directed by the matrix metalloproteinases (MMPs)<sup>4,5</sup> with help from adamalysins<sup>6-9</sup>, meprins<sup>10</sup>, Ser proteases<sup>11,12</sup>, cathepsins<sup>13</sup>, heparanases<sup>4</sup>, and sulphatases<sup>4</sup>. Cells will also align collagen fibers and other structural ECM components through integrin-ECM interactions. It is this interplay of ECM degradation, synthesis, and rearrangement that maintains the ECM in a dynamic state and forms the basis for a reciprocal relationship between cells and the matrix microenvironment.

Numerous diverse experimental approaches have been developed to recreate specific aspects of the ever-changing ECM. Vincent et al.<sup>14</sup> describe a method whereby cells are seeded on a coverslip island in the middle of a PDMS hydrogel to simulate a change in substrate stiffness and composition. During preparation of the hydrogel, the coverslip is placed on top of the partially gelled PDMS, allowing a small amount of PDMS to creep over the edge of the coverslip and form an interface between the glass and hydrogel<sup>14,15</sup>. This enabled the researchers to study how cells respond to changes in substrate stiffness and the cellular mechanics that are involved with these processes.

---

<sup>3</sup> Portions of this chapter were adapted from M. H. Joyce, C. Lu, E. R. James, R. Hegab, S. C. Allen, L. J. Suggs and A. Brock, "Phenotypic Basis for Matrix Stiffness-Dependent Chemoresistance of Breast Cancer Cells to Doxorubicin," *Front Oncol*, vol. 8, p. 337, 2018. A. B. and M. J. were responsible for the planning of the study and writing of the manuscript; C. L., E. J., M. J., R. H., and S. A. conducted the experiments; all authors were involved with the analysis of the manuscript.



Guvendiren & Burdick<sup>16</sup> developed a methacrylated hyaluronic acid (MeHA) hydrogel system capable of dynamically stiffening through UV irradiation. This system allows for the initial formation of a hydrogel through addition of dithiothreitol (DTT), which serves to crosslink some of the methacrylates present in the MeHA solution. Additional stiffening comes through UV irradiation of a photoinitiator (Irgacure 2959) that releases free radicals which crosslink the remaining methacrylate groups. Using this system, the researchers were able to form hydrogels ranging in stiffness from ~3 kPa to ~100 kPa through addition of DTT only, and used UV-induced stiffening to dynamically stiffen hydrogels from ~3 kPa to ~30 kPa.

Gillette et al.<sup>17</sup> combined two natural polymers – collagen I and alginate – to design a hydrogel system that could be dynamically stiffened or softened through the addition of calcium chloride (CaCl) or sodium citrate, respectively. Collagen and alginate were combined to form the initial hydrogel within a PDMS mold placed on a glass slide; a thin aluminum oxide or cellulose membrane was placed over the hydrogel to allow ions to pass through, but prevents passage of larger alginate polymer chains. To dynamically stiffen hydrogels after the initial seeding, a 60 mM calcium chloride solution was pipetted onto the membrane to diffuse through to the hydrogel and induce crosslinking of alginate polymers. Similarly, to soften the hydrogel, a 5% w/v sodium citrate solution can be washed over the membrane to allow for diffusion through to the alginate hydrogel and chelation of the calcium crosslinking alginate polymers.

These are but a few of the methods that researchers have employed to study how a dynamic ECM will impact cellular responses. While each of these methods has its own strengths and limitations, they, as well as others, have aided the discovery of therapeutic targets and treatment options to mitigate tumor progression.

Tumors stiffen as they progress, and this presents issues for treatment options by limiting drug diffusion to targeted tissues and exerting environmental pressures that facilitate further disease progression. Potential therapeutic options that are currently being explored include use of collagenase, collagen<sup>18-20</sup> or hyaluronic acid<sup>21-24</sup> synthesis inhibitors, and integrin inhibitors<sup>25</sup>. These methods have traditionally been employed as a means to soften tissue and thereby increase

drug diffusivity; however studies focused on cell-ECM interactions also suggest that such changes in the cells' microenvironment may be sufficient to transition tumor cells to a more drug sensitive state<sup>25,26</sup>.

Previous studies observed how cells adapt to changes in their ECM, but the system developed by Stowers et al.<sup>27</sup> is uniquely adapted to study the effects of dynamic ECM stiffness. Liposomes loaded with ionic calcium and gold nanorods (20% total volume) are added to 4% alginate (1.6% final concentration, 40% total volume; ProNova UP MVG), 5 – 20mM calcium carbonate (5% total volume), cells (5% total volume), 10 – 40mM D-(+)-Gluconic acid  $\delta$ -lactone (5% total volume), and Matrigel (25% total volume; VWR International) (as in chapter 2) then stimulated with NIR light to induce further hydrogel stiffening. This occurs because exposure to NIR light causes the gold nanorods to undergo surface plasmon resonance and heat the lipid layer close to its gel-to-fluid phase transition at 41°C, allowing the ionic calcium to leak out of liposomes and form additional cross-links with nearby alginate polymers. We therefore sought to use this platform to investigate our hypothesis that the physical forces from a stiffening microenvironment would increase breast cancer resistance to chemotherapeutic treatment. In addition, we hypothesized that varying the exposure time of cells to stiffened ECM would attenuate this stiffness-dependent drug response. The ability to dynamically stiffen the ECM surrounding breast cancer cell cultures in situ, without requiring cells to be removed from a specific hydrogel environment and reseeded in a different environment, made this alginate hydrogel system an ideal platform to test our hypotheses.

## **3.2 MATERIALS AND METHODS**

### **3.2.1 Liposome preparation**

Liposomes were prepared using the interdigitation-fusion method described by Ahl et al.<sup>28</sup>. 1,2-dipalmitoyl-sn-glycero-3-phosphocholine (DPPC, Avanti, 850355P/C) was diluted in chloroform (Fisher Scientific, CAS: 67-66-3) at 25 mg/mL and rotary evaporation (150 mbar vacuum, ~60 rpm, 55 °C, 15 m) was used to coat a round-bottom flask with thin layers of lipids.

After 15 m incubation on the rotary evaporator, the newly formed lipid cake was placed in a desiccator overnight to ensure complete evaporation of any residual chloroform. The lipid cake was rehydrated with 2 mL ultra-pure water and placed on a rotator for 30 m to ensure hydration of the entire lipid cake. The solution was then sonicated via sonic probe (60% amplitude for 10 m) to form small unilaminar vesicles. At this point, the lipid solution was passed through a 0.22  $\mu\text{m}$  filter (Millipore, SLGS033SB) and 424  $\mu\text{L}$  of 100% ethanol (Fisher Scientific, CAS: 64-17-5) was added to form interdigitated sheets. Gold nanorods and 500mM calcium chloride (Sigma-Aldrich, C1016) was added and allowed to incubate at 55 °C for 2 hours with gentle agitation every 30 m to ensure encapsulation of cargo into newly forming liposomes. After incubation, a series of washes with 300 mM sodium chloride (Fisher Scientific, 7647-14-5) plus 1 mM HEPES (Sigma-Aldrich, H3375) was performed to remove any free-floating nanorods or calcium.

### **3.2.2 Hydrogel preparation**

Hydrogels were prepared using similar methods described in chapter 2, with the addition of liposomes to the gel mixture. The following were combined in the order listed, with thorough mixing after each new item added to the gel mixture: 4% alginate (Pronova UP MVG; 40% total volume, 1.6% final concentration), 5 – 20 mM  $\text{CaCO}_3$  (5% total volume), liposomes loaded 500 mM  $\text{CaCl}_2$  plus AuNRs (20% total volume), cells (8 million – 16 million cells/mL; 5% total volume), 10 – 40 mM D-(+)-Gluconic acid  $\delta$ -lactone (Sigma-Aldrich, G4750; 5% total volume), and Matrigel (VWR International, 47743-715; 25% total volume). 50  $\mu\text{L}$  of the final mixture was pipetted into each well of a 96-well plate (Falcon, REF: 353072) and placed in an incubator (37°C, 5%  $\text{CO}_2$ ) for 1 h to promote gelation. 100  $\mu\text{L}$  of culture media was added to each well and cultures were returned to the incubator for cell growth and maintenance.

### **3.2.3 Dynamic stiffening of alginate hydrogels**

Prior to exposing samples to near infrared light, all media was aspirated from each sample to minimize light scattering. A Lasermate (IML808-2500FLAM4A) set at 2.0 W was used to

irradiate samples for 45 s each. After irradiating the final sample, 100  $\mu$ L of fresh culture media was added to each culture well and the samples were returned to the cell incubator (37 °C, 5% CO<sub>2</sub>) for routine growth and maintenance.

### 3.2.4 Statistical analysis

A two-tailed Student's t-test assuming unequal variance was used to compare samples, and a p-value of less than 0.05 was used to determine statistical significance. Microsoft Excel Solver was used to fit cell viability data to a sigmoidal function to generate LD50 curves.

## 3.3 RESULTS

Cells were cultured in an alginate-Matrigel hydrogel platform, as described in Stowers et al.<sup>27</sup>, which uses calcium-loaded liposomes to drive cross-linking following exposure to near-infrared (NIR) light. Cells were initially cultured in hydrogels for 3 days to begin formation of spheroid micro-structures (**Fig. 3.1a**). Hydrogels were stiffened via NIR triggered cross-linking (**Fig. 3.1b,c**), and cells were cultured for 3 additional days before treatment with doxorubicin for 48 h (**Fig. 3.1a**). MDA-MB-231 cultures that were grown in dynamically stiffened hydrogels had a significant decrease in sensitivity to doxorubicin for cultures that were stiffened from 450 Pa to 1,600 Pa (LD50 = 10  $\mu$ M in 450 Pa static cultures vs. LD50 = 80  $\mu$ M in cultures stiffened from 50 Pa to 1,600 Pa;  $p = 0.004$ ; **Fig. 3.2a**) as well as those stiffened from 2,000 Pa to 3,000 Pa (LD50 = 32  $\mu$ M in 2,000 Pa static cultures vs. LD50 = 185  $\mu$ M in cultures stiffened from 2,000 Pa to 3,000 Pa,  $p = 0.014$ ) compared to their static hydrogel counterparts (**Fig. 3.2a**). This relationship was not observed in MCF7 (**Fig. 3.2b**); there was no statistically significant difference in sensitivity to doxorubicin for cultures stiffened from 450 Pa to 1,600 Pa (LD50 = 6  $\mu$ M in 450 Pa static cultures vs. LD50 = 13  $\mu$ M in cultures stiffened from 450 Pa to 1,600 Pa;  $p = 0.143$ ) or 2,000 Pa to 3,000 Pa (LD50 = 12  $\mu$ M in 2,000 Pa static cultures vs. LD50 = 17  $\mu$ M in cultures stiffened from 2,000 Pa to 3,000 Pa;  $p = 0.492$ ) when compared to static cultures.

The time between dynamic stiffening of hydrogel cultures and treatment with doxorubicin was varied to determine if cells undergo adaptation to stiffened ECM that may alter drug sensitivity. Cells were cultured in hydrogels for 3 days to allow formation of micro-structures before being exposed to NIR to induce dynamic stiffening. Cultures were then maintained 24, 72, or 120 h in the stiffened ECM before treatment with doxorubicin. Resistance to doxorubicin peaked in MDA-MB-231 cells that were treated 72 h post-stiffening with an LD50 of 80  $\mu\text{M}$  for cultures stiffened from 450 to 1,600 Pa and 185  $\mu\text{M}$  for cultures stiffened from 2,000 to 3,000 Pa (**Fig. 3.2a**). By 120 h post-stiffening, this increase in resistance dropped to 87  $\mu\text{M}$  for cultures stiffened from 450 to 1,600 Pa ( $p = 0.323$ ) and 71  $\mu\text{M}$  for cultures stiffened from 2,000 to 3,000 Pa ( $p = 0.021$ ). We hypothesize that the stiffening from 2,000 Pa to 3,000 Pa elicits an acute response from MDA-MB-231 cells that results in an increased resistance to doxorubicin, which is shown at the 72 h acclimation time-point. However, our data suggests this response equilibrates by the 120 h acclimation time-point. Sensitivity of 231 to doxorubicin was greatest at 24 h post-stiffening with LD50 measures of 5  $\mu\text{M}$  for cultures stiffened from 450 to 1,600 Pa and 3  $\mu\text{M}$  for cultures stiffened from 2,000 to 3,000 Pa.

MCF7 cultures behaved inversely to their MDA-MB-231 counterparts (**Fig. 3.2b**). Peak resistance for MCF7 cultures was observed following 24 h acclimation in the stiff gels, with an LD50 of 26  $\mu\text{M}$  for cultures stiffened from 450 to 1,600 Pa and 16  $\mu\text{M}$  for cultures stiffened from 2,000 to 3,000 Pa. Resistance progressively decreased to LD50 values of 13  $\mu\text{M}$  ( $p = 0.154$ ) and 8  $\mu\text{M}$  ( $p = 0.104$ ) for cultures stiffened from 450 to 1,600 Pa and 17  $\mu\text{M}$  ( $p = 0.834$ ) and 7  $\mu\text{M}$  ( $p = 0.072$ ) for cultures stiffened from 2,000 to 3,000 Pa at 72 h and 120 h acclimation, respectively. However, when comparing across different lengths of acclimation periods, these decreases in resistance were not statistically significant.

Dynamic stiffening had a significant difference for every acclimation duration tested with MDA-MB-231 cultures as determined by a Student's t-test with  $p < 0.05$  denoting significance. This suggests that the duration of exposure to a particular set of ECM microenvironmental stiffness conditions contributes to resistance to doxorubicin in these cells.

### 3.4 DISCUSSION

Herein we describe how we used an alginate system coupled with calcium-loaded liposomes to simulate the stiffening of the tissue microenvironment that is observed in breast cancer progression. Similar to our results from chapter 2, we observed that MDA-MB-231 cells have increased resistance to doxorubicin following dynamic stiffening of their ECM. Slight increases in resistance were seen in similar MCF7 cultures, however these results were not shown to be statistically significant. We believe that similar mechanisms govern the stiffness-dependent resistance seen in dynamically stiffened hydrogels and static hydrogels, namely, those that underlie phenotypic expressions driving the mesenchymal and epithelial characteristics of each cell line. Interestingly, we found that dynamically stiffening hydrogels increased the resistance of MDA-MB-231 cells more than just placing them in a static hydrogel of similar stiffness alone (**Fig. 3.2a**).

To further investigate this effect, we varied the time between dynamically stiffening the hydrogel and subsequent exposure to the chemotherapeutic agent doxorubicin (**Fig. 3.1a**). We observed that MDA-MB-231 cultures were more sensitive to doxorubicin when only given 24 h to acclimate to the dynamically stiffened hydrogels. In sharp contrast, their resistance to doxorubicin peaked when given 72 h acclimation time between stiffening and drug exposure. MDA-MB-231 cultures given 120 h acclimation time were not as resistant to doxorubicin as the 72 h acclimation time group, but they were still more resistant than their static hydrogel counterparts. Thus, we believe that there is an acute cellular response directing MDA-MB-231 cells into a highly resistant state between 24 – 72 h post-stiffening, but that this response is at least partially equilibrated by 120 h post-stiffening. MCF7 cultures had the highest observed resistance to doxorubicin when given only 24 h acclimation time post-stiffening, however only hydrogels stiffened from 2,000 Pa to 3,000 Pa for 72 h and 120 h acclimation periods were found to be statistically significantly different for the dynamically stiffened MCF7 cultures. Given that MCF7 cultures did not vary significantly within acclimation time groups, and only displayed small changes in resistance after the 24 h acclimation point, we believe this bolsters our findings from chapter 2 that the MCF7 cell line does not have a stiffness-dependent response to doxorubicin.

### **3.5 CONCLUSIONS**

In this section, we have shown that the MDA-MB-231 cell line exhibits a stiffness-dependent resistance to doxorubicin and that drug resistance is affected by the duration of time that cells are exposed to an environment of a particular ECM stiffness. The MCF7 cell line, on the other hand, was not observed to share this stiffness-dependent resistance to doxorubicin, nor was it shown to be significantly affected by the duration of exposure to ECM stiffness. Taken together, this suggests that not all breast cancer cells will be significantly affected by stiffening of their ECM, but some subtypes may have their resistance to doxorubicin significantly increased by the tissue stiffening that occurs with breast cancer progression.

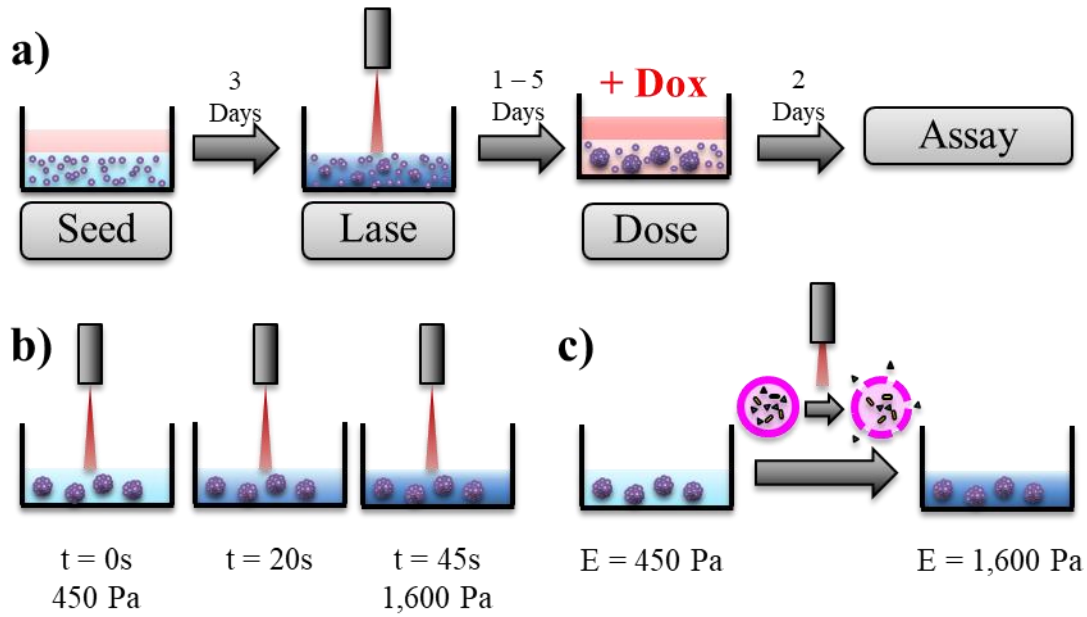


**Fig. 3.1 – An alginate hydrogel platform was used to dynamically stiffen hydrogels to mimic progressive ECM stiffening. a)** Cells were seeded into hydrogels and cultured for 3 days before dynamic stiffening with NIR light. After stiffening, cultures were given 1 – 5 days to acclimate to the new stiffness of the hydrogel before being exposed to doxorubicin for 2 days (48 h). Following treatment with doxorubicin, viability assays were performed to determine doxorubicin resistance. **b)** 450 Pa hydrogels were exposed to NIR light for 45 s to achieve ECM stiffness similar to 2,000 Pa static hydrogels. The same technique was used to stiffen 2,000 Pa hydrogels to 3,000 Pa. **c)** NIR light induces surface plasmon resonance in encapsulated gold nanorods (gold) to heat liposomes (pink) close to their gel-to-liquid transition temperature. This causes calcium (green) to leak from the liposomes and form additional alginate cross-links, thereby stiffening the hydrogel. The above figure was adapted from Joyce et al.<sup>26</sup>.



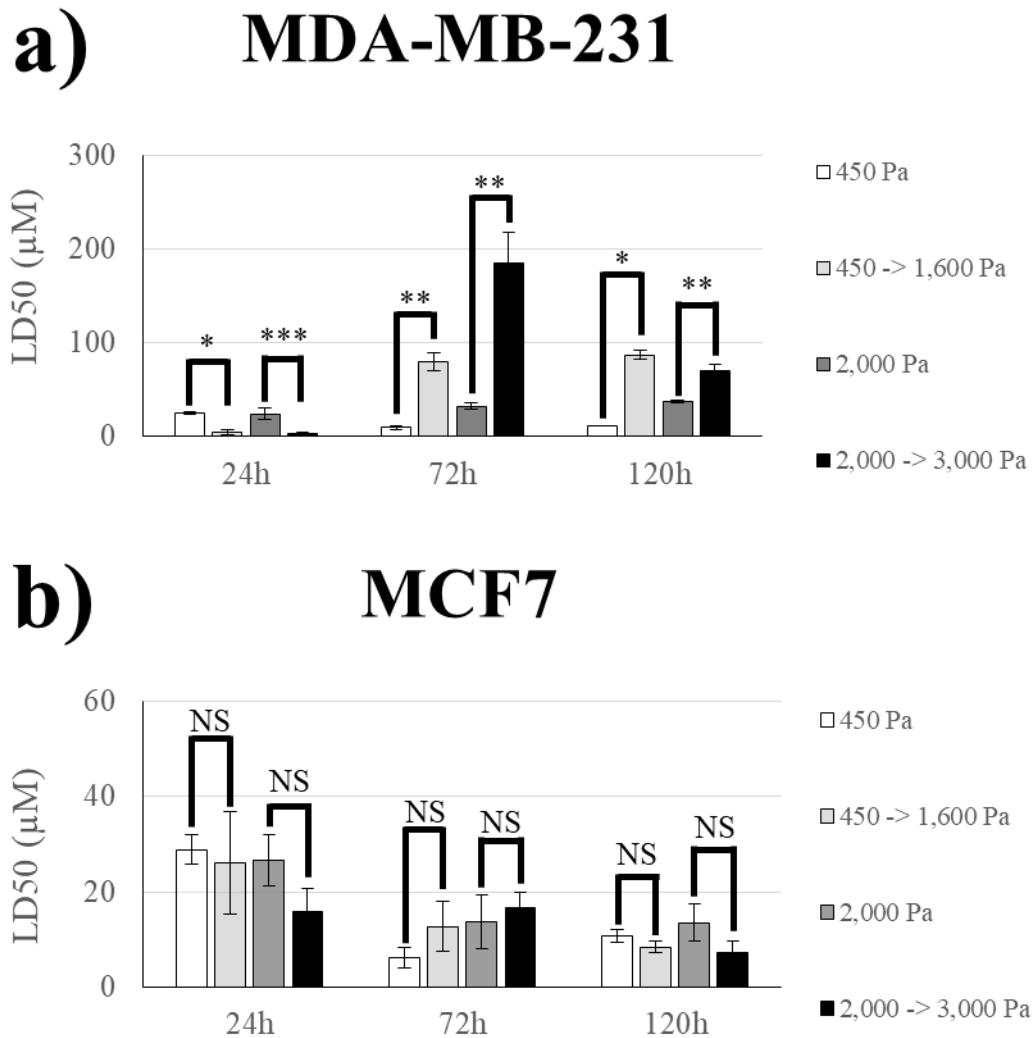


**Fig. 3.2 – MDA-MB-231 cultures have an acclimation-dependent increase in resistance to doxorubicin.** a) MDA-MB-231 and b) MCF7 cells were cultured in hydrogels with an initial stiffness of 450 Pa or 2,000 Pa for 3 days. On day 3, hydrogels either remained static (450 Pa or 2,000 Pa) or were stiffened (450 -> 1,600 Pa or 2,000 -> 3,000 Pa) using NIR light. Samples were then given 24 h to 120 h to acclimate to the hydrogel stiffness before 48 h treatment with doxorubicin. MDA-MB-231 cells showed a higher resistance to doxorubicin as hydrogel stiffness increased and this stiffness-dependent resistance was found to be partially dependent on duration of exposure to hydrogel stiffness. Comparable MCF7 samples did not show any significant change in resistance to doxorubicin across hydrogel stiffness or acclimation time. The above figure was adapted from Joyce et al.<sup>26</sup>. \*p-value < 0.01; \*\*p-value < 0.02; \*\*\*p-value < 0.03; NS = not significant, p-value > 0.05

1. R. Hynes, "The extracellular matrix: Not just pretty fibrils," *Science*, vol. 326, pp. 1216-1219, 2009.
2. W. Daley, S. Peters and M. Larsen, "Extracellular matrix dynamics in development and regenerative medicine," *J Cell Sci*, vol. 121, pp. 255-264, 2008.
3. E. T. Goddard, R. C. Hill, A. Barrett, C. Betts, Q. Guo, O. Maller, V. F. Borges, K. C. Hansen and P. Schedin, "Quantitative extracellular matrix proteomics to study mammary and liver tissue microenvironments," *International Journal of Biochemistry and Cell Biology*, vol. 81, pp. 223-232, 2017.
4. P. Lu, K. Takai, V. Weaver and Z. Werb, "Extracellular matrix degradation and remodeling in development and disease," *Cold Spring Harb Perspect Biol*, vol. 3, no. 12, pp. 1-24, 2011.
5. T. Cawston and D. Young, "Proteinases involved in matrix turnover during cartilage and bone breakdown," *Cell Tissue Res*, vol. 339, no. 1, pp. 221-235, 2010.
6. L. Hite, J. Shannon, J. Bjarnason and J. Fox, "Sequence of a cDNA clone encoding the zinc metalloproteinase hemorrhagic toxin e from *Crotalus atrox*: evidence for signal, zymogen, and disintegrin-like structures," *Biochemistry*, vol. 31, no. 27, pp. 6203-6211, 1992.
7. K. Kuno, N. Kanada, E. Nakashima, F. Fujiki, F. Ichimura and K. Matsushima, "Molecular cloning of a gene encoding a new type of metalloproteinase-disintegrin family protein with thrombospondin motifs as an inflammation associated gene," *J Biol Chem*, vol. 272, no. 1, pp. 556-562, 1997.
8. G. Murphy, "The ADAMs: signalling scissors in the tumour microenvironment," *Nat Rev Cancer*, vol. 8, no. 12, pp. 929-941, 2008.
9. J. White, "ADAMs: modulators of cell-cell and cell-matrix interactions," *Curr Opin Cell Biol*, vol. 15, no. 5, pp. 598-606, 2003.
10. M. Kruse, C. Becker, D. Lottaz, D. Köhler, I. Yiallourous, H. Krell, E. Sterchi and W. Stöcker, "Human meprin alpha and beta homo-oligomers: cleavage of basement membrane proteins and sensitivity to metalloprotease inhibitors," *Biochem J*, vol. 378, pp. 383-389, 2004.
11. H. Smith and C. Marshall, "Regulation of cell signalling by uPAR," *Nat Rev Mol Cell Biol*, vol. 11, no. 1, pp. 23-36, 2010.
12. A. Bonnefoy and C. Legrand, "Proteolysis of subendothelial adhesive glycoproteins (fibronectin, thrombospondin, and von Willebrand factor) by plasmin, leukocyte cathepsin G, and elastase," *Thromb Res*, vol. 98, no. 4, pp. 323-332, 2000.
13. M. Mohammed and B. Sloane, "Cysteine cathepsins: multifunctional enzymes in cancer," *Nat Rev Cancer*, vol. 6, no. 10, pp. 764-775, 2006.

14. L. G. Vincent, Y. S. Choi, B. Alonso-Latorre, J. C. Álamó and A. J. Engler, "Mesenchymal Stem Cell Durotaxis Depends on Substrate Stiffness Gradient Strength," *Biotechnol J*, vol. 8, no. 4, pp. 472-484, 2013.
15. G. J. Goreczny, D. B. Wormer and C. E. Turner, "A Simplified System for Evaluating Cell Mechanosensing and Durotaxis In Vitro," *J Vis Exp*, no. 102, p. e52949, 2015.
16. M. Guvendiren and J. A. Burdick, "Stiffening hydrogels to probe short- and long-term cellular responses to dynamic mechanics," *Nature Communications*, vol. 3, pp. 792-799, 2012.
17. B. M. Gillette, J. A. Jensen, M. Wang, J. Tchao and S. K. Sia, "Dynamic Hydrogels: Switching of 3D Microenvironments Using Two-Component Naturally Derived Extracellular Matrices," *Advanced Materials*, vol. 22, pp. 686-691, 2010.
18. B. Diop-Frimpong, V. Chauhan, S. Krane, Y. Boucher and R. Jain, "Losartan Inhibits Collagen I Synthesis and Improves the Distribution and Efficacy of Nanotherapeutics in Tumors," *Proc Natl Acad Sci USA*, vol. 108, no. 7, pp. 2909-2914, 2011.
19. V. Chauhan, J. Martin, H. Liu, D. Lacorre, S. Jain, S. Kozin, T. Stylianopoulos, A. Mousa, X. Han, P. Adstamongkonkul, Z. Popovic, P. Huang, M. Bawendi, Y. Boucher and R. Jain, "Angiotensin Inhibition Enhances Drug Delivery and Potentiates Chemotherapy by Decompressing Tumour Blood Vessels," *Nat Commun*, vol. 4, p. 2516, 2013.
20. J. Liu, S. Liao, B. Diop-Frimpong, W. Chen, S. Goel, K. Naxerova, M. Ancukiewicz, Y. Boucher, R. Jain and L. Xu, "TGF-Blockade Improves the Distribution and Efficacy of Therapeutics in Breast Carcinoma by Normalizing the Tumor Stroma," *Proc Natl Acad Sci USA*, vol. 109, no. 41, pp. 16618-16623, 2012.
21. H. Morohashi, A. Kon, M. Nakai, M. Yamaguchi, I. Kakizaki, S. Yoshihara, M. Sasaki and K. Takagaki, "Study of Hyaluronan Synthase Inhibitor, 4-Methylumbelliferone Derivatives on Human Pancreatic Cancer Cell (KP1-NL)," *Biochem Biophys Res Commun*, vol. 345, no. 4, pp. 1454-1459, 2006.
22. T. Saito, D. Tamura, T. Nakamura, Y. Makita, H. Ariyama, K. Komiyama, T. Yoshihara and R. Asano, "4-Methylumbelliferone Leads to Growth Arrest and Apoptosis in Canine Mammary Tumor Cells," *Oncol Rep*, vol. 29, no. 1, pp. 335-342, 2013.
23. H. Nakazawa, S. Yoshihara, D. Kudo, H. Morohashi, I. Kakizaki, A. Kon, K. Takagaki and M. Sasaki, "4-Methylumbelliferone, a Hyaluronan Synthase Suppressor, Enhances the Anticancer Activity of Gemcitabine in Human Pancreatic Cancer Cells," *Cancer Chemother Pharmacol*, vol. 57, no. 2, pp. 165-170, 2006.
24. A. Kohli, S. Kivimäe, M. Tiffany and F. Szoka, "Improving the Distribution of Doxil in the Tumor Matrix by Depletion of Tumor Hyaluronan," *J Controlled Release*, vol. 191, no. 1-2, pp. 105-114, 2014.

25. C. J. Lovitt, T. B. Shelper and V. M. Avery, "Doxorubicin resistance in breast cancer cells is mediated by extracellular matrix proteins," *BMC Cancer*, vol. 18, no. 1, p. 41, 2018.
26. M. H. Joyce, C. Lu, E. R. James, R. Hegab, S. C. Allen, L. J. Suggs and A. Brock, "Phenotypic Basis for Matrix Stiffness-Dependent Chemoresistance of Breast Cancer Cells to Doxorubicin," *Front Oncol*, vol. 8, p. 337, 2018.
27. R. S. Stowers, S. C. Allen and L. J. Suggs, "Dynamic phototuning of 3D hydrogel stiffness," *Proceedings of the National Academy of Sciences*, vol. 112, no. 7, pp. 1953-1958, 2015.
28. P. Ahl, L. Chen, W. Perkins, S. Minchey, L. Boni, T. Taraschi and A. Janoff, "Interdigitation-fusion: a new method for producing lipid vesicles of high internal volume," *Biochim Biophys Acta*, vol. 1195, no. 2, pp. 237-244, 1994.
29. K. T. Dicker, L. A. Gurski, S. Pradhan-Bhatt, R. L. Witt, M. C. Farach-Carson and X. Jia, "Hyaluronan: A Simple Polysaccharide with Diverse Biological Functions," *Acta Biomater*, vol. 10, no. 4, pp. 1558-1570, 2014.

## Chapter 4: Molecular Characterization of Breast Cancer Cells Cultured in Soft and Stiff Hydrogels<sup>4</sup>

### 4.1 INTRODUCTION

Metastasis complicates disease treatment and decreases patient survivability, as the spread of tumors presents new locations that must be treated and these new locations will have different microenvironments that can influence resistance to treatment. Tumor metastasis occurs when cells from the primary tumor migrate to new locations and establish tertiary tumors. This process has been intensely studied in hopes of discovering methods to prevent or reduce the disease spreading through a patient's body. For breast cancer cells, this process has been well characterized (see<sup>1-3</sup> for more thorough reviews on the subject). Generally speaking, cells from a primary breast tumor will transition to a state where they are much more motile in a process called Epithelial-to-Mesenchymal transition (EMT). This transition is characterized by a loss of cell-cell adhesions, change from cuboidal to spindle shape, and increased expression of genes facilitating cell migration. For breast cancer, there have been six critical pathways identified that drive EMT: TGF- $\beta$  (transforming growth factor-  $\beta$ ), Wnt, Notch, Hippo, Hedgehog, and receptor tyrosine kinase pathways<sup>2</sup>. Our studies focused on three of these such pathways which are known to play a significant role in breast cancer initiation and metastasis.

TGF- $\beta$  is a secreted protein that regulates key cellular processes including apoptosis, proliferation, and differentiation<sup>4</sup>. In very early stages of tumor development TGF- $\beta$  signaling functions as a tumor suppressor, but as the disease progresses the TGF- $\beta$  pathway has been shown to support tumor growth and metastasis through the induction of EMT<sup>5</sup>. Secreted TGF- $\beta$  will bind to cell surface receptors and form complexes with Smad proteins which, when phosphorylated,

---

<sup>4</sup> Portions of this chapter were adapted from M. H. Joyce, C. Lu, E. R. James, R. Hegab, S. C. Allen, L. J. Suggs and A. Brock, "Phenotypic Basis for Matrix Stiffness-Dependent Chemoresistance of Breast Cancer Cells to Doxorubicin," *Front Oncol*, vol. 8, p. 337, 2018. A. B. and M. J. were responsible for the planning of the study and writing of the manuscript; C. L., E. J., M. J., R. H., and S. A. conducted the experiments; all authors were involved with the analysis of the manuscript.

Portions of this chapter include data that is currently in preparation for publication.

will translocate to the nucleus to drive transcription of target genes such as ZEB1/2, SNAIL1/2, and TWIST1.

The Wnt pathway drives EMT through the downregulation of E-cadherin and up-regulation of Snail (SNAIL)<sup>6</sup>, SLUG (SNAIL2)<sup>7</sup>, and TWIST<sup>8</sup> transcription factors. This can occur through the canonical  $\beta$ -catenin dependent pathway<sup>9</sup> or the non-canonical planar cell polarity and Wnt/Ca<sup>2+</sup> pathways<sup>10</sup>. DiMeo et al. highlighted the necessity of Wnt signaling in EMT by demonstrating that over-expression of DKK1 (negative regulator of the Wnt pathway) was sufficient to decrease tumor formation in mice and reduce expression of EMT markers Slug and Twist<sup>11</sup>. A study of 158 invasive breast cancer samples showed that 99% of the samples examined had alterations in at least one antagonist Wnt pathway, further highlighting its clinical significance as a therapeutic target<sup>12</sup>.

The Hippo pathway is a tumor suppressor pathway that contributes to tissue growth, differentiation, and regeneration. Yes-associated protein (YAP) and tafazzin (TAZ) are two oncogenes that make up part of the core transcriptional components, and both are highly regulated by the Hippo pathway. Phosphorylation of YAP/TAZ by LATS1/2 kinase suppresses their activity by causing them to accumulate in the cytoplasm of the cell where they undergo proteasome degradation<sup>13</sup>. Activation and subsequent nuclear translocation of YAP/TAZ due to inactivation of the Hippo pathway has been shown to lead to EMT<sup>14-16</sup> and increased proliferation<sup>17-19</sup>. Recent work has described how YAP/TAZ activation is mediated by the stiffness of their ECM through JNK<sup>20-22</sup>, RHO<sup>23,24</sup>, and integrin-mediated adhesion pathways<sup>23,25,26</sup>. Given cells in the mammary gland are already sensitive to ECM stiffness, they are an ideal platform to study YAP/TAZ induced EMT<sup>27-29</sup>.

In this chapter, we sought to molecularly characterize the changes that occur when culturing mammary adenocarcinoma cells in soft (450 Pa) and stiff (2,000 Pa) ECM. Our studies focused on changes in markers of EMT due to recent findings that have found links between cells that have undergone EMT and increased chemoresistance in different tumor types.

## **4.2 MATERIALS AND METHODS**

### **4.2.1 Staining for EMT markers**

Samples were fixed with a 15 min. exposure to 4% paraformaldehyde at room temperature. Blocking and permeabilization buffer (0.1% Triton X-100 and 1% bovine serum albumin [BSA] diluted in 1xPBS) was added to each sample and incubated at room temperature for 1 h. Following this, samples were incubated with primary antibody against YAP (Santa Cruz, sc-101199) or actin (Phalloidin488, Thermofisher, A12379) for 1 h at room temperature. Cell nuclei were stained with 300 nM DAPI (ThermoFisher, D1306) for 30 m at room temperature before being imaged on a Zeiss confocal or EVOS epifluorescent microscope.

### **4.2.2 Quantitative real-time PCR**

Total RNA was extracted using the RNeasy Mini Kit (Qiagen, 74104, Hilden, Germany) and was reverse-transcribed using the High-Capacity cDNA Reverse Transcription Kit (Applied Biosystems, 4368814) according to the manufacturer's instructions. Quantitative PCR was performed using the PowerUp SYBR Green Master Mix (Applied Biosystems, A25743) with 20 ng cDNA input in 20  $\mu$ l reaction volume run on a ViiA7 Real-Time PCR system (Applied Biosciences). B2M (beta-2-microglobulin) expression level was used for normalization as a housekeeping gene. The primers for beta-2-microglobulin (HK-B2M), Vimentin (VHPS-9912; Vimentin), and CDH1 (VHPS-1738; E-Cadherin) were designed and synthesized by RealTimePrimers.com ([www.realtimprimers.com](http://www.realtimprimers.com)). Delta CT ( $\Delta$ CT) values for each sample were first normalized to the B2M house-keeping gene, and expression levels were analyzed pair-wise comparing samples cultured in 2,000 Pa hydrogels to the same cell type cultured in 450 Pa hydrogels.

### 4.2.3 Statistical Analysis and Mathematical Modeling

A two-tailed Student's t-test assuming unequal variance was used to compare samples, and a p-value of less than 0.05 was used to determine statistical significance. MatLab was used for plot generation and curve fitting.

## 4.3 RESULTS

### 4.3.1 Expression of EMT Markers

Quantitative real-time PCR was performed using a panel of well-known markers of EMT to evaluate how stiffness of the ECM would affect MDA-MB-231 and MCF7 cell state (**Fig. 4.1a**). We found that expression of E-Cadherin was decreased in both MDA-MB-231 ( $p = 0.037$ ) and MCF7 ( $p = 0.120$ ) cells cultured in 2,000 Pa hydrogels versus their 450 Pa counterparts (**Fig. 4.1b**), however only the MDA-MB-231 cells showed a statistically significant difference in expression with hydrogel stiffness. Decreased expression of E-Cadherin is a well-known marker of EMT, thus further supporting our findings that the stiffer hydrogels promote transition towards a mesenchymal phenotype. MCF7 cells cultured on 2,000 Pa hydrogels showed an increase in SNAIL1 ( $p = 0.069$ , **Fig. 4.1c**) and SLUG ( $p = 0.006$ , **Fig. 4.1d**) with a decrease in ZEB1 ( $p = 0.445$ , **Fig. 4.1e**) and vimentin ( $p = 0.004$ , **Fig. 4.1f**) expression compared to similar cultures grown in 450 Pa hydrogels. MDA-MB-231 samples cultured in 2,000 Pa hydrogels showed a decrease in all SNAIL1 ( $p = 0.001$ , **Fig. 4.1c**), SLUG ( $p = 0.017$ , **Fig. 4.1d**), ZEB1 ( $p = 0.002$ , **Fig. 4.1e**), and vimentin ( $p = 0.018$ , **Fig. 4.1f**) additional markers tested when compared to their 450 Pa counterparts.

We took the same data and normalized all samples to the epithelial model (MCF7) cultured on the softest stiffness (450 Pa) (**Fig. 4.2a**). What we found was that there were significant differences in expression between our mesenchymal (MDA-MB-231) and epithelial (MCF7) cell models for all genes tested. Expression of E-Cadherin was much higher in MCF7 cultures and culturing the highly epithelial MCF7 cells in 2,000 Pa hydrogels was not sufficient to decrease



their expression of E-Cadherin to similar levels seen in MDA-MB-231 cells cultured in either 450 Pa ( $p = 0.002$ ) or 2,000 Pa ( $p = 0.002$ ) hydrogels (**Fig. 4.2b**). SNAIL1 expression was also found to be higher in MCF7 cultures compared to MDA-MB-231 ( $p = 0.002$  for 450 Pa and  $p = 0.0002$  for 2,000 Pa hydrogels, **Fig. 4.2c**). SLUG ( $p = 0.0003$  for 450 Pa and  $p = 0.002$  for 2,000 Pa hydrogels, **Fig. 4.2d**), ZEB1 ( $p = 0.0004$  for 450 Pa and  $p = 0.0001$  for 2,000 Pa hydrogels, **Fig. 4.2e**), and Vimentin ( $p = 0.0005$  for 450 Pa and  $p = 0.0001$  for 2,000 Pa hydrogels, **Fig. 4.2f**) all had higher overall expression in MDA-MB-231 cultures and were found to decrease with expression ( $p = 0.017$  for SLUG,  $p = 0.002$  for ZEB1,  $p = 0.018$  for vimentin) as stiffness increased. SLUG was shown to increase with stiffness ( $p = 0.006$ , **Fig. 4.2d**) for MCF7 cultures, but expression of ZEB1 (**Fig. 4.2e**) and vimentin (**Fig. 4.2f**) did not show a statistically significant difference between 450 Pa and 2,000 Pa cultures.

#### 4.3.2 Increasing hydrogel stiffness leads to nuclear localization of YAP

Samples grown on 450 or 2,000 Pa hydrogels were stained with YAP antibodies as a marker of mesenchymal phenotype. High levels of YAP nuclear localization confirmed that 231 cultures (**Fig. 4.3a**) exhibited higher markers of mesenchymal phenotype than their MCF7 (**Fig. 4.3b**) counterparts. The mean fluorescent intensity (MFI) of YAP-labeled nuclei was MFI = 930 a.u. in 231 cells cultured in 450 Pa hydrogels and MFI = 2,030 a.u. for the same cells cultured in 2000 Pa hydrogels. Given the 231 cells grown on 2,000 Pa hydrogels showed higher levels of YAP nuclear localization than similar cultures on 450 Pa hydrogels ( $p = 1.36E-22$ ), we believe that a stiffer ECM promotes the mesenchymal phenotype for these cells. Similar findings were observed in MCF7 cultures, but to a much lesser extent (MFI = 22 a.u. for cells cultured in 450 Pa hydrogels and MFI = 28 a.u. for cells cultured in 2,000 Pa hydrogels,  $p = 0.0001$ ).

#### 4.3.3 Mathematical models suggests stiffness-induced resistance to doxorubicin is not fully explained by changes in proliferation rates

MDA-MB-231 cells expressing nuclear localized red fluorescent protein were cultured in 450 Pa, 900 Pa, 1,400 Pa, or 2,000 Pa hydrogels ( $n = 11$  for all groups) seeded in a 96-well plate

and imaged every 4 h to track cell growth. Cells were cultured for 6 days to collect growth dynamics data (**Fig. 4.4**). All cultures were then exposed to 10  $\mu$ M doxorubicin for 48 h, before the drug was replaced with standard growth medium and monitored for an additional 5 days (11 d, 262 h total, **Fig. 4.5**). Growth trajectories ( $g_{\text{eff}}$ ) were calculated by fitting cell count data from time points 48 h – 152 h to a single exponential growth model (**Fig. 4.6a,b**). Post-treatment growth trajectories ( $k_{\text{eff}}$ ) were calculated similarly, by fitting cell count data from time points 152 h – 262 h to a single exponential death model (**Fig. 4.6a,b**). Our results from this show that the growth rate of MDA-MB-231 cells is inversely correlated with hydrogel stiffness (**Fig. 4.6c**). Using the same data, we modeled how sensitivity to doxorubicin would be affected by a two-population model that accounted for cells expressing both the epithelial and mesenchymal phenotype with the option to transition between the two states (**Fig. 4.7a**). Here we set the mesenchymal growth rate ( $g_m = 0.0013$  cells per hour) and the transition from mesenchymal-to-epithelial rate ( $k_{me} = 0.0013$ ) to allow us to fit for the epithelial growth rate ( $g_e = 0.0335$ ) and transition rate from epithelial-to-mesenchymal phenotype ( $k_{em}$ ) (**Fig. 4.7b**). Our model showed that the transition rate from epithelial-to-mesenchymal phenotype ( $k_{em}$ ) increased with hydrogel stiffness (**Fig. 4.7c**). We were then able to calculate drug sensitivity (**Fig. 4.8a**) by fitting the equations shown in **Fig. 4.8b** to find the average death rate ( $d_E$  and  $d_M$ ) of each phenotype following treatment with doxorubicin. Our results show that cells expressing the epithelial phenotype are more sensitive to doxorubicin than cells expressing a mesenchymal phenotype (**Fig. 4.8c**).

#### 4.4 DISCUSSION

Previous studies have shown links between EMT and increased resistance to certain chemotherapeutics. We sought to see if this was true for breast cancer cells treated with doxorubicin, a drug with clinical relevance to this disease known to induce chemotherapeutic resistance. To this end, we cultured breast cancer cells known to exhibit the epithelial (MCF7) and mesenchymal (MDA-MB-231) phenotypes in hydrogels that mimicked the stiffness of ECM ranging from healthy mammary tissue (450 Pa) to early stage breast tumor (2,000 Pa). Using

quantitative real-time PCR, we found that SNAIL1 and SLUG increase with ECM stiffness in MCF7 cells, but ZEB1 and vimentin decrease with ECM stiffness. This, paired with the fact that expression of all markers examined decreased for MDA-MB-231 cells, suggests that matrix stiffness alone may not be sufficient to fully induce EMT in certain breast cancer cells. Both cell lines showed loss of cell-cell adhesions, and MCF7 cells upregulated expression of additional negative regulators of E-cadherin (SNAIL1 and SLUG). However, neither MDA-MB-231 nor MCF7 cells showed increased expression of ZEB1 or vimentin. ZEB1 has recently been shown to induce chemoresistance in breast cancer cells through activation of ataxia-telangiectasia mutated (ATM) kinase<sup>30</sup>, however our results suggest that this is not the mechanism governing the stiffness-dependent resistance seen in the MDA-MB-231 samples.

A recent study looking at partial EMT in pancreatic ductal adenocarcinoma (PDAC), breast cancer, and colorectal cancer cell lines showed that cells classified as having undergone partial EMT did not always show a significant decrease in expression of E-cadherin, rather they re-localized it from the membrane to the interior of the cell<sup>31</sup>. Knowing this, we turned our attention to another marker of EMT – nuclear localization of YAP. YAP nuclear localization and subsequent loss of E-cadherin are classical markers of cells undergoing EMT, so we cultured MCF7 and MDA-MB-231 cells in 450 Pa and 2,000 Pa to examine how ECM stiffness would affect YAP nuclear localization. We found that both cell lines showed higher nuclear localization of YAP when cultured in stiffer hydrogels. Similar findings were found by Rice et al.<sup>32</sup> in pancreatic ductal adenocarcinoma cells grown in hydrogels of increasing stiffness. Thus, this further supports our hypothesis that ECM stiffness increases breast cancer cell resistance to doxorubicin through partial induction of EMT.

#### **4.5 CONCLUSION**

We found that quantitative analysis of EMT-associated gene expression suggests that ECM stiffness alone is not sufficient to induce MCF7 cells to fully undergo EMT or to prompt further EMT in MDA-MB-231 cells. Our results find that the decreased expression of ZEB1 in MDA-

MB-231 cells suggests that the stiffness-dependent resistance these cells displayed in chapter 2 and chapter 3 is likely not due to ZEB1 activation of ATM. Mathematical modeling of MDA-MB-231 response to doxorubicin points towards a link between EMT rate and ECM stiffness as the driver of the observed stiffness-dependent resistance.

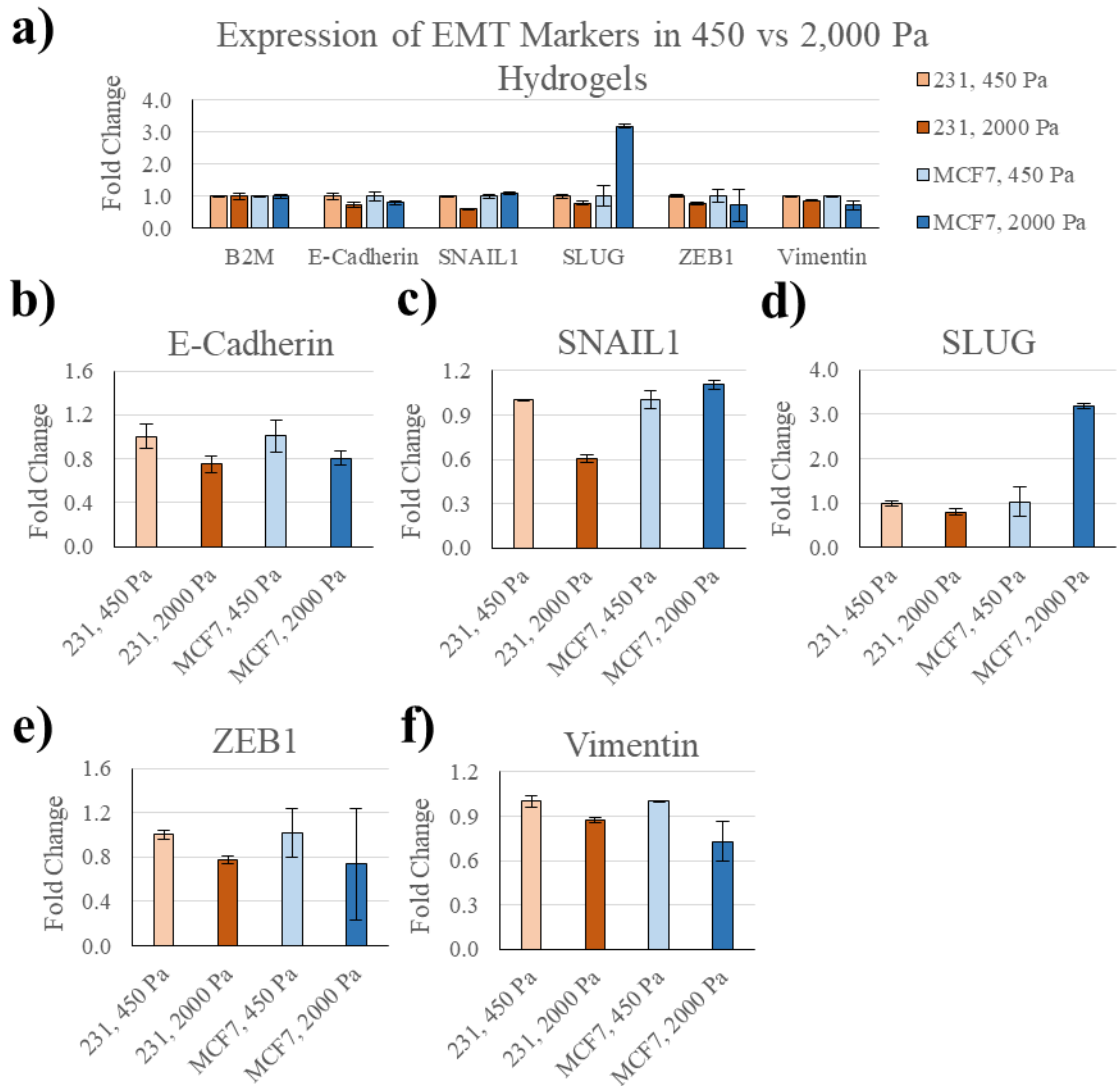


**Fig. 4.1 – Expression of EMT markers suggests ECM stiffness promotes hybrid cell state in MDA-MB-231 and MCF7 cells.** **a)** The expression of five EMT-related genes was examined in MDA-MB-231 (231)/MCF7 cells cultured in 450 Pa vs 2,000 Pa hydrogels using quantitative PCR (qPCR). Cells were cultured in hydrogels for 6 days before RNA was isolated from samples and prepared for qPCR. All primers were normalized to the beta-2-microglobulin (B2M) house-keeping gene. **b)** E-cadherin expression was shown to decrease when both cell lines were cultured in 2,000 Pa hydrogels vs 450 Pa hydrogels, though only the MDA-MB-231 ( $p = 0.037$ ) cultures showed a significant decrease whereas the MCF7 ( $p = 0.120$ ) cultures did not. **c)** SNAIL1 expression was shown to significantly decrease for MDA-MB-231 samples ( $p = 0.001$ ), and while expression increased in MCF7 cultures ( $p = 0.069$ ) it was not found to be statistically significant. **d)** Expression of SLUG (SNAIL2) was shown to significantly decrease for MDA-MB-231 cultures ( $p = 0.017$ ), but increase 3-fold for MCF7 cultures ( $p = 0.006$ ). **e)** ZEB1 was shown to have less expression in MDA-MB-231 cells ( $p = 0.002$ ), but were not shown to be statistically different for MCF7 cells ( $p = 0.445$ ) cultured in stiffer hydrogels. **f)** Expression of vimentin was found to be significantly decreased for both MDA-MB-231 ( $p = 0.018$ ) and MCF7 ( $p = 0.004$ ) cells cultured in 2,000 Pa hydrogels compared to their counterparts cultured in 450 Pa hydrogels.

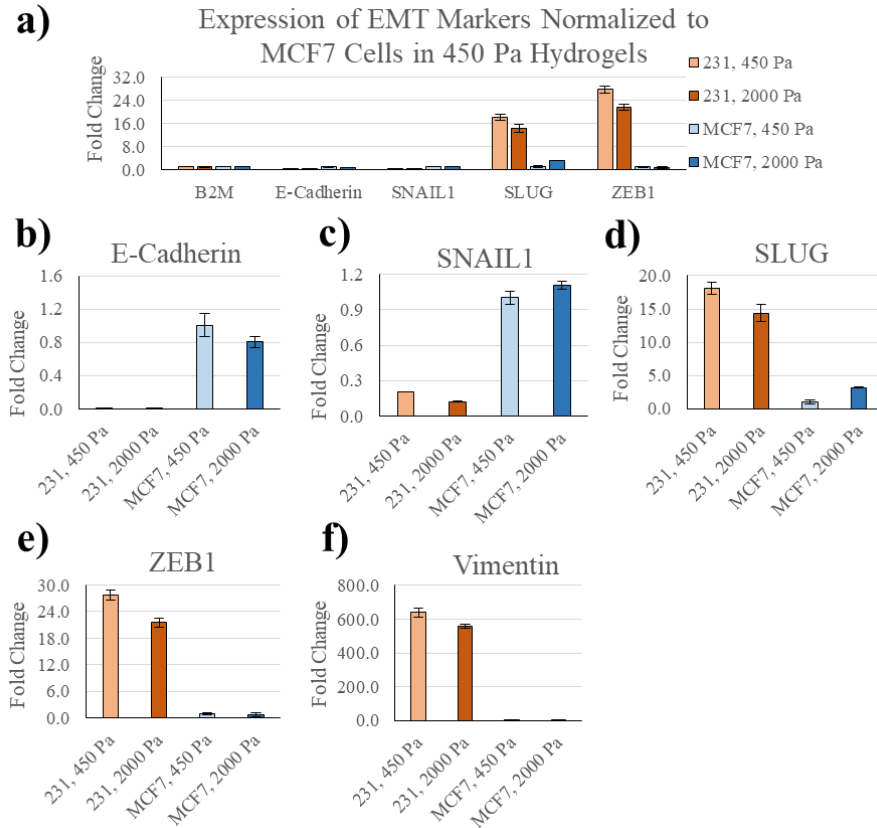
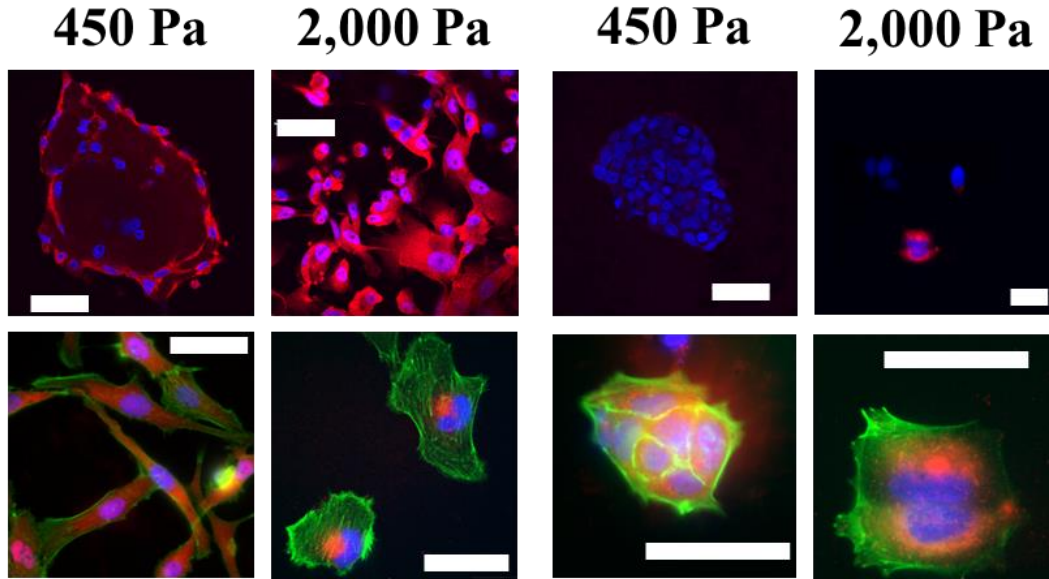


**Fig. 4.2 – Expression of EMT markers compared to epithelial cells on soft hydrogels.** **a)** The expression of five EMT-related genes was examined in MDA-MB-231 (231)/MCF7 cells cultured in 450 Pa vs 2,000 Pa hydrogels using quantitative PCR (qPCR). All primers were normalized to the beta-2-microglobulin (B2M) house-keeping gene and compared against the MCF7 cells cultured in 450 Pa hydrogels. **b)** E-cadherin expression is much higher in MCF7 cells for both 450 Pa ( $p = 0.007$ ) and 2,000 Pa ( $p = 0.002$ ) hydrogels. **c)** SNAIL1 expression overall is much lower in MDA-MB-231 cultures ( $p = 0.002$  for 450 Pa and  $p = 0.0002$  for 2,000 Pa hydrogels). SNAIL1 further decreases in MDA-MB-231 cultures ( $p = 0.001$ ) as stiffness increases but increases with stiffness in MCF7 cultures ( $p = 0.069$ ). **d)** Expression of SLUG (SNAIL2) is much higher in MDA-MB-231 cultures ( $p = 0.0003$  for 450 Pa and  $p = 0.002$  for 2,000 Pa hydrogels). Again, SLUG further decreases in MDA-MB-231 cultures ( $p = 0.017$ ) as stiffness increases but increases with stiffness in MCF7 cultures ( $p = 0.006$ ). **e)** ZEB1 expression is much higher in MDA-MB-231 cultures overall ( $p = 0.0004$  for 450 Pa and  $p = 0.0001$  for 2,000 Pa hydrogels). Here we observe a stiffness-dependent decrease in ZEB1 for both MDA-MB-231 ( $p = 0.002$ ) and MCF7 ( $p = 0.445$ ), though differences in MCF7 cultures were not found to be statistically significant. **f)** Vimentin is dramatically more expressed in MDA-MB-231 cultures ( $p = 0.0005$  for 450 Pa and  $p = 0.0001$  for 2,000 Pa hydrogels). A stiffness-dependent decrease in vimentin was observed in both MDA-MB-231 ( $p = 0.018$ ) and MCF7 ( $p = 0.076$ ) cultures, though the difference in MCF7 cultures was not significant.

a) MDA-MB-231

b) MCF7

### YAP Nuclear Localization



### Quantification of YAP Nuclear Localization

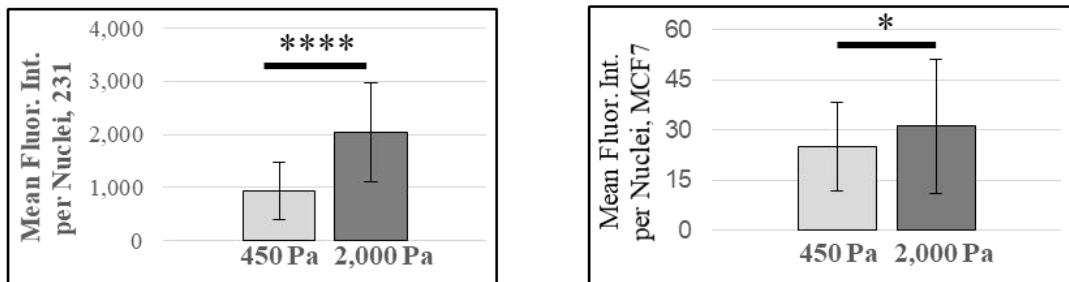


**Fig. 4.3 – Stiffer ECM increases nuclear localization of YAP and decreases expression of E-Cadherin.** a) MDA-MB-231 and b) MCF7 cells were cultured on 450 Pa or 2,000 Pa hydrogels for 3 days before fixation and staining with YAP (red) and actin (phalloidin-488, green) antibodies, as well as DAPI (blue). Images were captured using confocal microscopy and analysis was done in ImageJ to determine nuclear localization of YAP ( $n = 123$  for MDA-MB-231 cells cultured in 450 Pa hydrogels,  $n = 119$  for MDA-MB-231 cells cultured in 2,000 Pa hydrogels,  $n = 72$  for MCF7 cells cultured in 450 Pa hydrogels,  $n = 90$  for MCF7 cells cultured in 2,000 Pa hydrogels). There is a stiffness-dependent increase in nuclear localization of YAP for both MDA-MB-231 ( $p = 1.38E-22$ ) and MCF7 ( $p = 0.02$ ) cultures, though the increase in MCF7 cultures is small. MDA-MB-231 cultures showed significantly higher expression of nuclear YAP compared to similar MCF7 cultures ( $p = 2.37E-37$  for 450 Pa and  $p = 4.44E-46$  for 2,000 Pa). Scale bar = 50  $\mu$ m. \* $p$ -value < 0.05; \*\*\*\* $p$ -value < 0.001

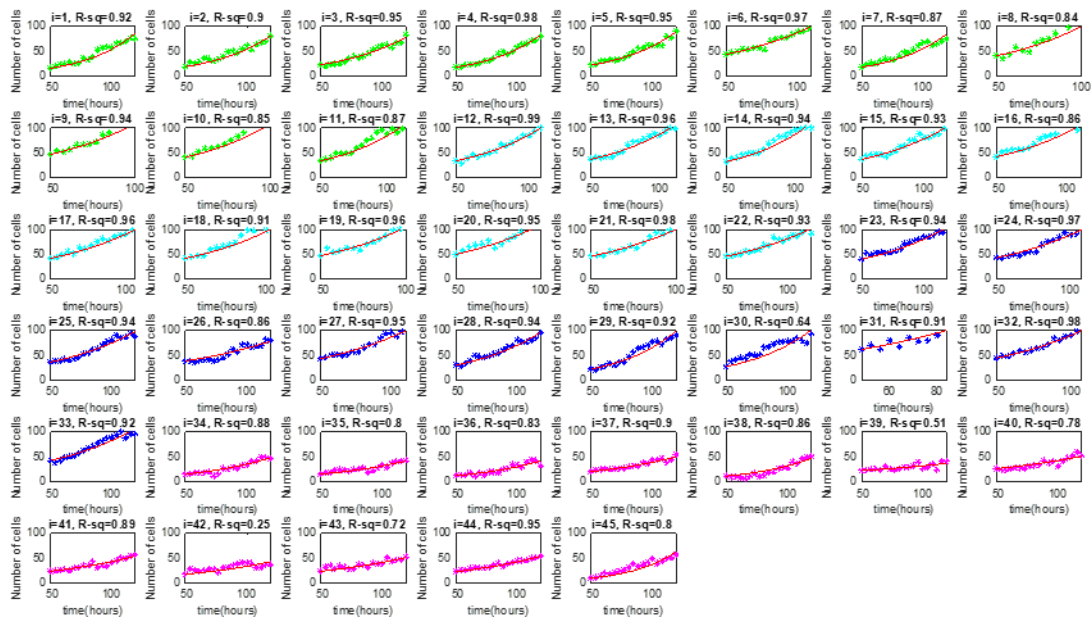


**Fig. 4.4 – Growth dynamics of MDA-MB-231 cells in hydrogels of varying stiffness before treatment with doxorubicin.** MDA-MB-231 cells were seeded into 450 (green), 900 (cyan), 1400 (blue), or 2000 (pink) Pa hydrogels and cultured for 6 days in an Incucyte S3 incubator. Images were collected every 4 h and cells were counted using the S3 on-board software.



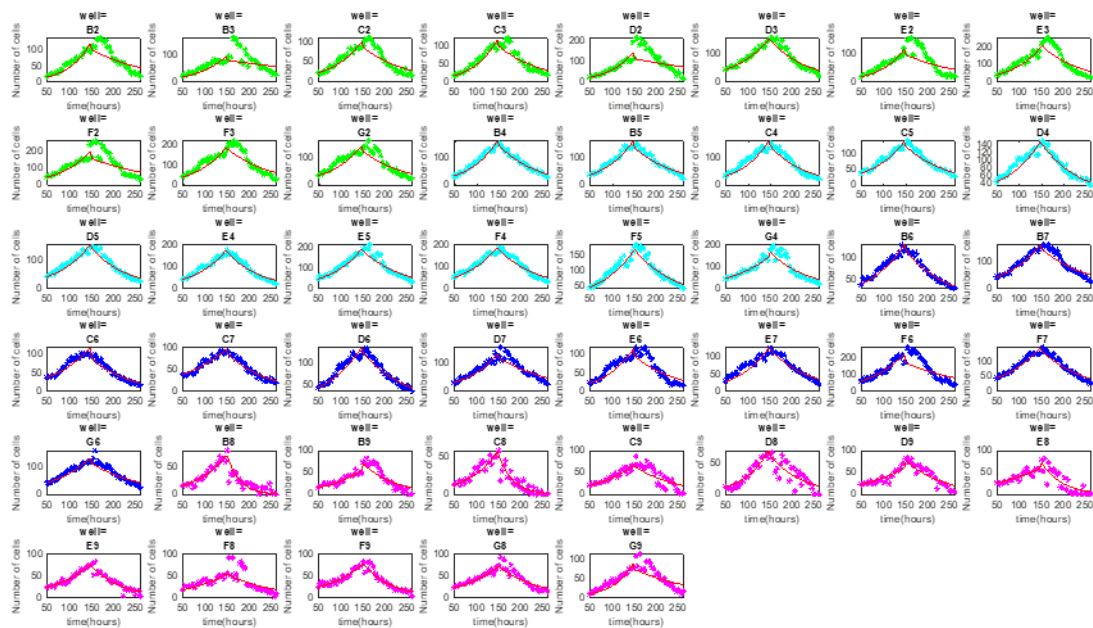


**Fig. 4.5 – Growth dynamics of MDA-MB-231 cells in hydrogels of varying stiffness following treatment with doxorubicin.** Following 6 days of standard growth in 450 (green), 900 (cyan), 1400 (blue), or 2000 (pink) Pa hydrogels, cells were exposed to 10  $\mu$ M doxorubicin for 48 h. Cultures were monitored for an additional 5 days to collect growth dynamics information following treatment with doxorubicin. Images were collected every 4 h in an Incucyte S3 incubator and cells were counted using the S3 on-board software.

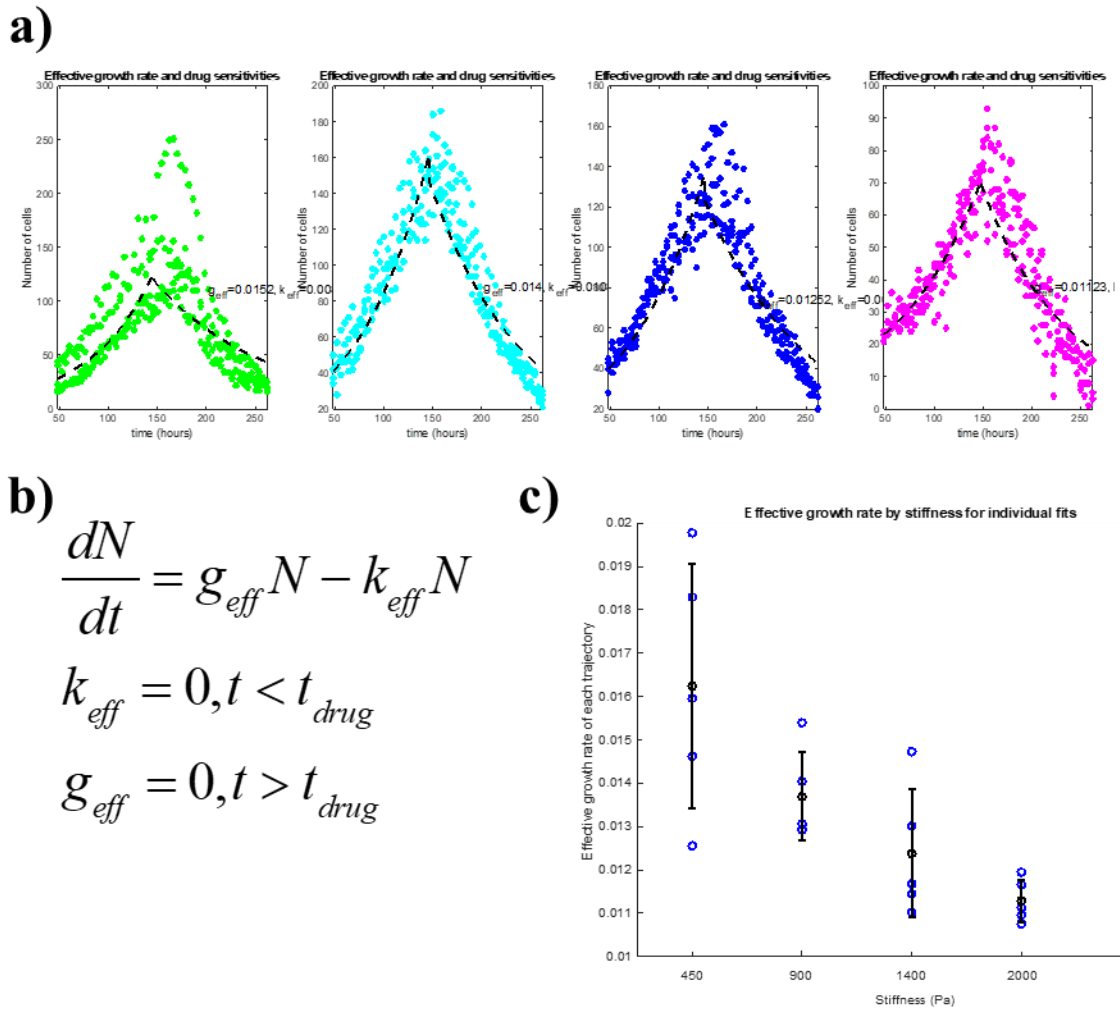


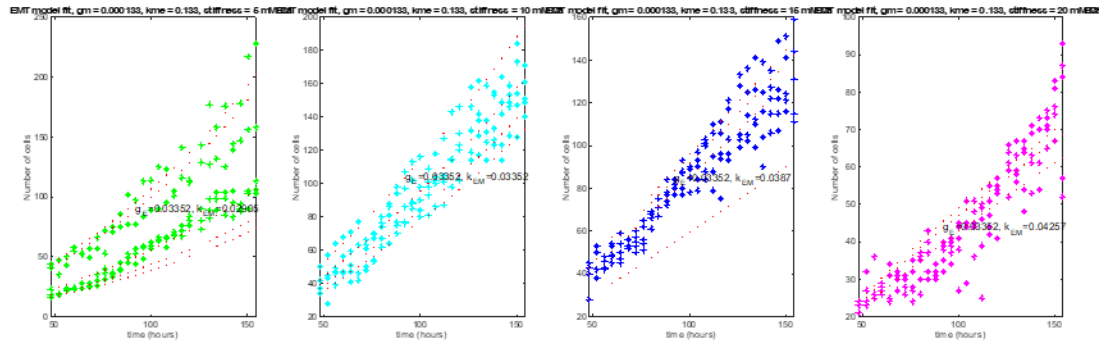
**Fig. 4.6 – Proliferation rate of MDA-MB-231 cells decreases with increased hydrogel stiffness.** a) Data collected between 48 h and 152 h time points was fit to b) a single exponential growth model to calculate the effective growth rate for cultures pre-treatment. The cell count data from 152 h to 262 h time points, was fit to a single exponential death model to calculate the effective growth rate of cells following 48 h exposure to doxorubicin. c) Our results show that growth rate of MDA-MB-231 cells decreases as the stiffness of the hydrogel increases. The error bars shown represent the 95% confidence interval,  $n = 5$  for each hydrogel stiffness.

a)

$$\frac{dE}{dt} = g_E E - k_{EM}(\sigma)E + k_{ME}M$$

$$\frac{dM}{dt} = g_M M + k_{EM}(\sigma)E - k_{ME}M$$

b)



c)

### Transition Rate from Epithelial to Mesenchymal Phenotype In Hydrogels

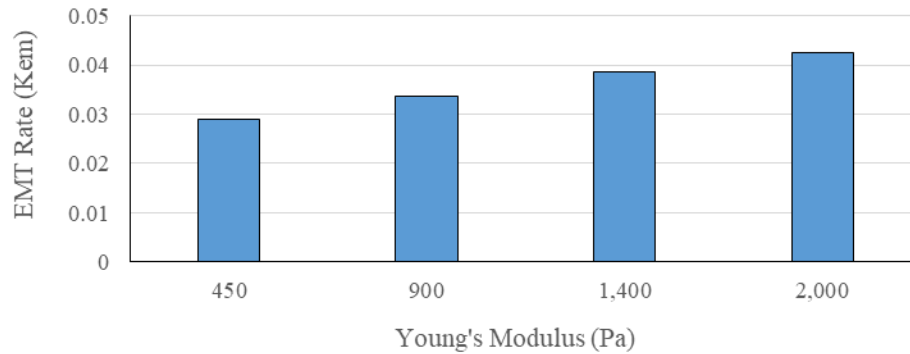


**Fig. 4.7 – Fitting data to a two-population EMT model shows rate of EMT increases with hydrogel stiffness.** **a)** Growth data collected from the Incucyte S3 was fit to a two-population model that assumed populations of epithelial (E) and mesenchymal (M) were present and that they could transition from one E to M ( $k_{EM}$ ) or vice-versa ( $k_{ME}$ ). **b)** Assuming a mesenchymal growth rate ( $g_M$ ) of 0.0013 cells per hour and  $k_{ME}$  of 0.0013, we fit the data to calculate epithelial growth rate ( $g_E$ ) and  $k_{EM}$ . **c)** Our mathematical model shows that the rate of transition from E to M ( $k_{EM}$  or EMT) increases with hydrogel stiffness.

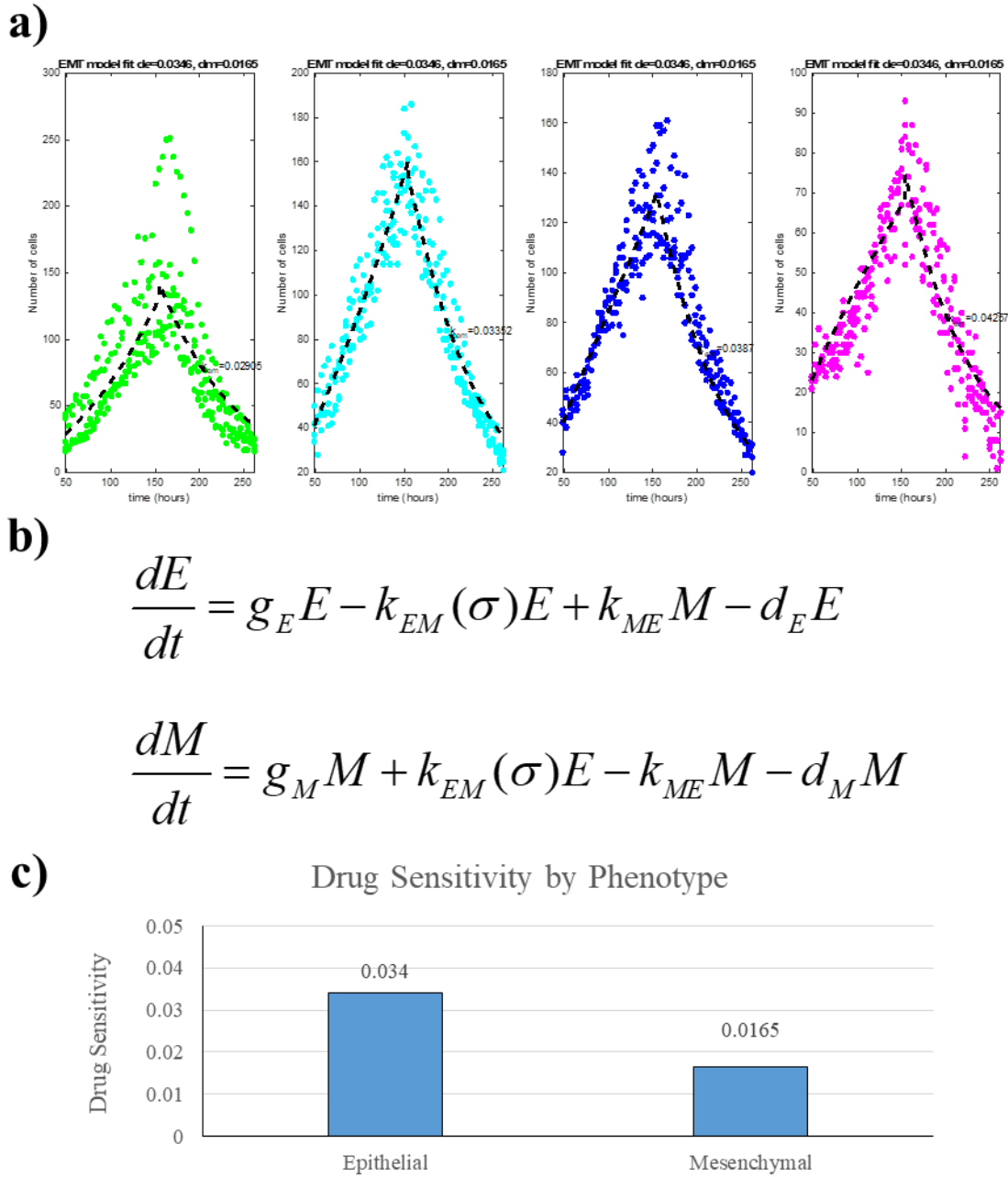


**Fig. 4.8 – Cells with mesenchymal phenotype have a lower death rate in response to treatment with doxorubicin. a)** We fit our data to the equations in **b)** using previously calculated variables to determine the sensitivity of epithelial (E) and mesenchymal (M) populations to doxorubicin. **c)** Our model shows that mesenchymal cells are more resistant to doxorubicin. This suggests that cells undergoing transitioning from E to M ( $k_{EM}$  or EMT) would have a survival advantage and increase the overall resistance of the cell entire population.

1. Y. Wu, M. Sarkissyan and J. V. Vadgama, "Epithelial-Mesenchymal Transition and Breast Cancer," *Journal of Clinical Medicine*, vol. 5, no. 2, 2016.
2. M. Fedele, L. Cerchia and G. Chiappetta, "The Epithelial-to-Mesenchymal Transition in Breast Cancer: Focus on Basal-Like Carcinomas," *Cancers (Basel)*, vol. 9, no. 10, p. 134, 2017.
3. F. Liu, L.-N. Gu, B.-E. Shan, C.-Z. Geng and M.-X. Sang, "Biomarkers for EMT and MET in breast cancer: An update," *Oncology Letters*, vol. 12, no. 6, pp. 4869-4876, 2016.
4. J. Massagué, S. W. Blain and R. S. Lo, "TGF $\beta$  Signaling in Growth Control, Cancer, and Heritable Disorders," *Cell*, vol. 103, no. 2, pp. 295-309, 2000.
5. J. Massagué, "TGF $\beta$  in Cancer," *Cell*, vol. 134, no. 2, pp. 215-230, 2008.
6. J. Yook, X. Li, I. Ota, C. Hu, H. Kim, N. Kim, S. Cha, J. Ryu, Y. Choi, J. Kim, E. Fearon and S. Weiss, "A Wnt-Axin2-GSK3 $\beta$  cascade regulates Snail1 activity in breast cancer cells," *Nat Cell Biol*, vol. 8, no. 12, pp. 1398-1406, 2006.
7. M. Conacci-Sorrell, I. Simcha, T. Ben-Yedidia, J. Blechman, P. Savagner and A. Ben-Ze'ev, "Autoregulation of E-cadherin expression by cadherin-cadherin interactions: the roles of beta-catenin signaling, Slug, and MAPK," *J Cell Biol*, vol. 163, no. 4, pp. 847-857, 2003.
8. L. Howe, O. Watanabe, J. Leanard and A. Brown, "Twist is up-regulated in response to Wnt1 and inhibits mouse mammary cell differentiation," *Cancer Res*, vol. 63, no. 8, pp. 1906-1913, 2003.
9. H. Clevers, "Wnt/beta-catenin signaling in development and disease," *Cell*, vol. 127, no. 3, pp. 469-480, 2006.
10. S. Pohl, N. Brook, M. Agostino, F. Arfuso, A. Kumar and A. Dharmarajan, "Wnt signaling in triple-negative breast cancer," *Oncogenesis*, vol. 6, no. 4, p. e310, 2017.
11. T. DiMeo, K. Anderson, P. Phadke, C. Fan, C. Perou, S. Naber and C. Kuperwasser, "A novel lung metastasis signature links Wnt signaling with cancer cell self-renewal and epithelial-mesenchymal transition in basal-like breast cancer," *Cancer Res*, vol. 69, no. 13, pp. 5364-5373, 2009.
12. N. Mukherjee, N. Bhattacharya, N. Alam, A. Roy, S. Roychoudhury and C. K. Panda, "Subtype-specific alterations of the Wnt signaling pathway in breast cancer: Clinical and prognostic significance," *Cancer Science*, vol. 103, no. 2, pp. 210-220, 2012.
13. K. Harvey, X. Zhang and D. Thomas, "The Hippo pathway and human cancer," *Nat Rev Cancer*, vol. 13, no. 4, pp. 246-257, 2013.
14. D. D. Shao, W. Xue, E. B. Krall, A. Bhutkar, F. Piccioni, X. Wang, A. C. Schinzel, S. Sood, J. Rosenbluh, J. W. Kim, Y. Zwang, T. M. Roberts, D. E. Root, T. Jacks and W.

- C. Hahn, "KRAS and YAP1 converge to regulate EMT and tumor survival," *Cell*, vol. 158, no. 1, pp. 171-184, 2014.
15. J. Lamar, P. Stern, H. Liu, J. Schindler, Z. Jiang and R. Hynes, "The Hippo pathway target, YAP, promotes metastasis through its TEAD-interaction domain," *Proc Natl Acad Sci USA*, vol. 109, no. 37, pp. 2441-2450, 2012.
  16. D. Chen, Y. Sun, Y. Wei, P. Zhang, A. Rezaeian and J. Teruya-Feldstein, "LIFR is a breast cancer metastasis suppressor upstream of the Hippo-YAP pathway and a prognostic marker," *Nat Med*, vol. 18, pp. 1511-1517, 2012.
  17. O. M, J. Zhang, G. Smolen, B. Muir, W. Li, D. Sgroi, C. Deng, J. Brugge and D. Haber, "Transforming properties of YAP, a candidate oncogene on the chromosome 11q22 amplicon," *Proc Natl Acad Sci USA*, vol. 103, no. 33, pp. 12405-12410, 2006.
  18. S. Piccolo, M. Cordenonsi and S. Dupont, "Molecular pathways: YAP and TAZ take center stage in organ growth and tumorigenesis," *Clin Cancer Res*, vol. 19, pp. 4925-4930, 2013.
  19. M. Aragona, T. Panciera, A. Manfrin, S. Giullitti, F. Michielin and N. Elvassore, "A mechanical checkpoint controls multicellular growth through YAP/TAZ regulation by actin-processing factors," *Cell*, vol. 154, pp. 1047-1059, 2013.
  20. V. Codelia, G. Sun and K. Irvine, "Regulation of YAP by Mechanical Strain through Jnk and Hippo Signaling," *Curr Biol*, vol. 24, pp. 2012-2017, 2014.
  21. C.-L. Chen, M. Schroeder, M. Kango-Singh, C. Tao and G. Halder, "Tumor suppression by cell competition through regulation of the Hippo pathway," *Proc Natl Acad Sci USA*, vol. 109, pp. 484-489, 2011.
  22. G. Sun and K. Irvine, "Regulation of Hippo signaling by Jun kinase signaling during compensatory cell proliferation and regeneration, and in neoplastic tumors," *Dev Biol*, vol. 350, pp. 139-151, 2011.
  23. S. Dupont, L. Morsut, M. Aragona, E. Enzo, S. Giullitti and M. Cordenonsi, "Role of YAP/TAZ in mechanotransduction," *Nature*, vol. 474, pp. 179-183, 2011.
  24. B. Zhao, L. Li, L. Wang, C.-Y. Wang, J. Yu and K.-L. Guan, "Cell detachment activates the Hippo pathway via cytoskeleton reorganization to induce anoikis," *Genes Dev*, vol. 26, pp. 54-68, 2012.
  25. A. Bonnefoy and C. Legrand, "Proteolysis of subendothelial adhesive glycoproteins (fibronectin, thrombospondin, and von Willebrand factor) by plasmin, leukocyte cathepsin G, and elastase," *Thromb Res*, vol. 98, no. 4, pp. 323-332, 2000.
  26. K.-I. Wada, K. Itoga, T. Okano, S. Yonemura and H. Sasaki, "Hippo pathway regulation by cell morphology and stress fibers," *Development*, vol. 138, pp. 3907-3914, 2011.

27. C. DuFort, M. Paszek and V. Weaver, "Balancing forces: architectural control of mechanotransduction," *Nat Rev Mol Cell Biol*, vol. 12, pp. 308-319, 2011.
28. C. Nelson and M. Bissell, "Of extracellular matrix, scaffolds, and signaling: tissue architecture regulates development, homeostasis, and cancer," *Annu Rev Cell Dev Biol*, vol. 22, pp. 287-309, 2006.
29. P. Schedin and P. Keely, "Mammary gland ECM remodeling, stiffness, and mechanosignaling in normal development and tumor progression," *Cold Spring Harb Perspect Biol*, vol. 3, p. a003228, 2011.
30. X. Zhang, Z. Zhang, Q. Zhang, Q. Zhang, P. X. R. Sun, G. Ren and S. Yang, "ZEB1 confers chemotherapeutic resistance to breast cancer by activating ATM," *Cell Death & Disease*, vol. 9, pp. 57-72, 2018.
31. N. M. Aiello, R. Maddipati, R. J. Norgard, D. Balli, J. Li, S. Yuan, T. Yamazoe, T. Black, A. Sahmoud, E. E. Furth, D. Bar-Sagi and B. Z. Stanger, "EMT Subtype Influences Epithelial Plasticity and Mode of Cell Migration," *Developmental Cell*, vol. 45, pp. 681-695, 2018.
32. A. J. Rice, E. Cortes, D. Lachowski, B. Cheung, S. Karim, J. Morton and A. del Río Hernández, "Matrix stiffness induces epithelial–mesenchymal transition and promotes chemoresistance in pancreatic cancer cells," *Oncogenesis*, vol. 6, no. 7, p. e352, 2017.

## Appendix



Cell Type	Stiffness (Pa)	LD50 ( $\mu$ M)	Std Dev. ( $\mu$ M)
231	450	9.59	1.87
	450 $\rightarrow$ 1,600	79.99	9.54
	2,000	32.24	3.45
	2,000 $\rightarrow$ 3,000	184.97	32.28
	Monolayer	26.57	2.91
MCF7	450	6.02	2.19
	450 $\rightarrow$ 1,600	12.68	5.18
	2,000	12.07	6.88
	2,000 $\rightarrow$ 3,000	16.60	3.26
	Monolayer	4.44	2.00

Cell Type	Stiffness (Pa)	LD50 ( $\mu$ M)	Std Dev. ( $\mu$ M)
231	450 $\rightarrow$ Monolayer	14.23	0.65
	2,000 $\rightarrow$ Monolayer	11.24	2.34
MCF7	450 $\rightarrow$ Monolayer	1.55	0.61
	2,000 $\rightarrow$ Monolayer	3.33	2.44

**Table A1 – Doxorubicin sensitivity for MCF7 and 231 across culture conditions.** Dose response curves of 231 and MCF7 cells cultured in static hydrogels, dynamic hydrogels, and monolayer culture conditions following 48h exposure to Doxorubicin. Live and Dead cells were counted using a Nexcelom Cellometer with AOPI stain.

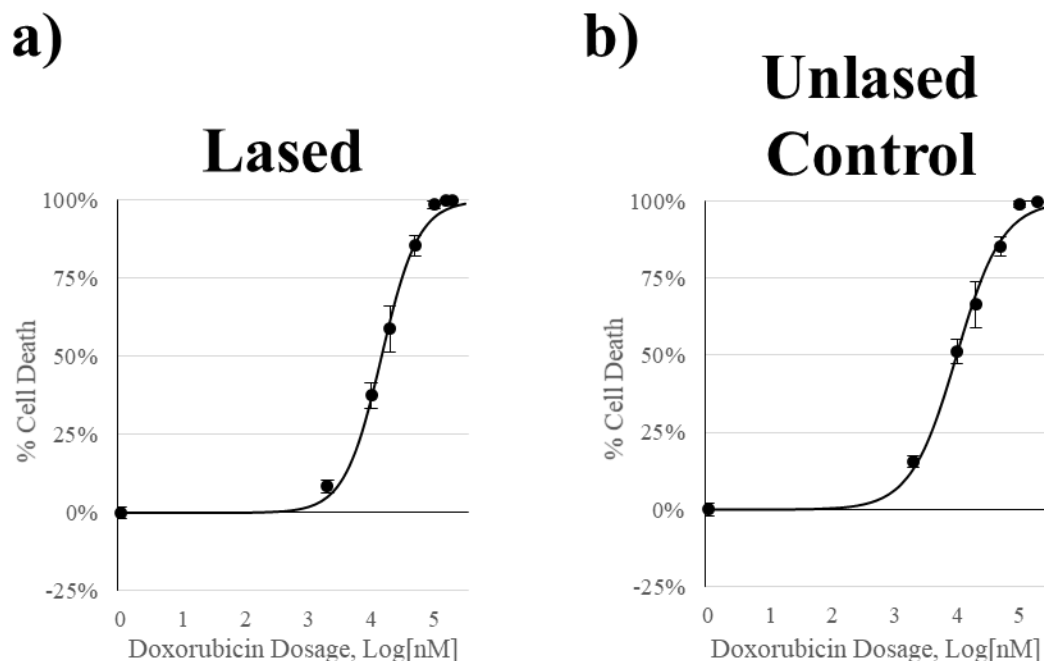


**Fig. A1 – Exposure to Near Infrared (NIR) light does not significantly affect response to doxorubicin.** MDA-MB-231 cells were cultured as a monolayer (2D) on tissue culture plastic before being exposed to NIR light for 45 s. Samples were cultured an additional 2 days after lasing prior to treatment with doxorubicin. Staining with acridine orange/propidium iodide (AOPI) was used to quantify the ratio of live/dead cells. **a)** Cells that were exposed to NIR light did not show a significant difference ( $p = 0.064$ ) in resistance to doxorubicin compared to **b)** control samples that were not exposed to NIR light.  $n = 3$

## References

### CHAPTER 1

1. C. Frantz, K. M. Stewart and V. M. Weaver, "The Extracellular Matrix at a Glance," *Journal of Cell Science*, vol. 123, no. 24, pp. 4195 LP-4200, 2010.
2. T. F. Lisenmayer, "Collagen," in *Cell Biology of Extracellular Matrix*, E. D. Hay, Ed., New York, Plenum Press, 1991, pp. 7-44.
3. R. Timpl, "Structure and biological activity of basement membrane proteins," *Eur J Biochem*, vol. 180, no. 3, pp. 487-502, 1989.
4. E. Ruoslahti, E. G. Hayman, M. Pierschbacher and E. Engvall, "Fibronectin: purification, immunochemical properties, and biological activities," *Methods Enzymol*, vol. 82, pp. 803-831, 1982.
5. R. O. Hynes, *Fibronectins*, New York: Springer-Verlag, 1990.
6. K. M. Yamada, "Fibronectin and other cell interactive glycoproteins," in *Cell Biology of Extracellular Matrix*, E. D. Hay, Ed., New York, Plenum Press, 1991, pp. 111-146.
7. M. J. Brennan, A. Oldberg, M. D. Pierschbacher and E. Ruoslahti, "Chondroitin/dermatan sulfate proteoglycan in human fetal membranes. Demonstration of an antigenically similar proteoglycan in fibroblast," *Journal of Biological Chemistry*, vol. 259, no. 22, pp. 13742-13750, 1984.
8. B. Voss, J. Glössl, Z. Cully and H. Kresse, "Immunocytochemical investigation on the distribution of small chondroitin sulfate-dermatan sulfate proteoglycan in the human," *Journal of Histochemistry and Cytochemistry*, vol. 34, no. 8, pp. 1013-1019, 1986.
9. L. Cöster, I. Carlstedt, S. Kendall, A. Malmström, A. Schmidtchen and L.-Å. Fransson, "Structure of proteoheparan sulfates from fibroblasts. Confluent and proliferating fibroblasts produce at least three types of proteoheparan sulfates with functionally different core proteins," *Journal of Biological Chemistry*, vol. 261, no. 26, pp. 12079-12088, 1986.
10. A. Heremans, B. V. D. Schueren, B. D. Cock, M. Paulsson, J.-J. Cassiman, H. V. D. Berghe and G. David, "Matrix- associated heparan sulfate proteoglycan: core protein-specific monoclonal antibodies decorate the pericellular matrix of connective tissue cells and the stromal side of basement membranes," *Journal of Cell Biology*, vol. 109, pp. 3199-3211, 1989.
11. J. Perry, S. Tam, K. Zheng, Y. Sado, H. Dobson, B. Jefferson, R. Jacobs and P. S. Thorner, "Type IV collagen induces podocytic features in bone marrow stromal stem cells in vitro," *J Am Soc Nephrol*, vol. 17, pp. 66-76, 2006.

12. R. Jayadev and D. R. Sherwood, "Basement membranes," *Current Biology*, vol. 27, no. 6, pp. R207-R211, 2017.
13. E. Poschl, U. Schlotzer-Schrehardt, B. Brachvogel, K. Saito, Y. Ninomiya and U. Mayer, "Collagen IV is essential for basement membrane stability but dispensable for initiation of its assembly during early development," *Development*, vol. 131, pp. 1619-1628, 2004.
14. J. H. Miner, C. Li, J. L. Mudd, G. Go and A. E. Sutherland, "Compositional and structural requirements for laminin and basement membranes during mouse embryo implantation and gastrulation," *Development*, vol. 131, pp. 2247-2256, 2004.
15. A. C. Erickson and J. R. Couchman, "Still more complexity in mammalian basement membranes," *J Histochem Cytochem*, vol. 48, pp. 1291-1306, 2000.
16. A. E. Chung, L. J. Dong, C. Wu and M. E. Durkin, "Biological functions of entactin," *Kidney Int*, vol. 43, pp. 13-19, 1993.
17. P. D. Yurchenco and J. J. O'Rear, "Basal lamina assembly," *Curr Opin Cell Biol*, vol. 6, pp. 674-681, 1994.
18. M. Paulsson, "Basement membrane proteins: structure, assembly, and cellular interactions," *Crit Rev Biochem Mol Biol*, vol. 27, pp. 93-127, 1992.
19. J. Nageotte and L. Guyon, "Reticulin," *American Journal of Pathology*, vol. 6, no. 6, pp. 631-653, 1930.
20. C. W. Oatley, "The early history of the scanning electron microscope," *Journal of Applied Physics*, vol. 53, no. 2, pp. R1-R13, 1982.
21. T. M. Weiss, "Small Angle Scattering: Historical Perspective and Future Outlook," in *Biological Small Angle Scattering: Techniques, Strategies and Tips*, vol. 1009, B. Chaudhuri, I. Muñoz, S. Qian and V. Urban, Eds., Singapore, Springer, Singapore, 2017, pp. 1-10.
22. R. S. Bear, "Long x-ray diffraction spacings of collagen," *J Am Chem Soc*, vol. 64, no. 3, pp. 727-727, 1942.
23. C. E. Hall, M. A. Jakus and F. O. Schmitt, "Electron microscope observations of collagen," *J Am Chem Soc*, vol. 64, no. 5, pp. 1234-1234, 1942.
24. F. O. Schmitt, J. Gross and J. H. Highberger, "A new particle type in certain connective tissue extracts," *Proc Natl Acad Sci USA*, vol. 39, no. 6, pp. 459-470, 1953.
25. A. Rich and F. H. C. Crick, "The structure of collagen," *Nature*, vol. 176, pp. 593-595, 1955.
26. G. N. Ramachandran and G. Kartha, "Structure of collagen," *Nature*, vol. 176, pp. 593-595, 1955.

27. P. Cowan, S. McGavin and A. North, "The polypeptide chain configuration of collagen," *Nature*, vol. 176, no. 4492, pp. 1062-1064, 1955.
28. R. Orkin, P. Gehron, E. McGoodwin, G. Martin, T. Valentine and R. Swarm, "A murine tumor producing a matrix of basement membrane," *J Exp Med*, vol. 145, no. 1, pp. 204-220, 1977.
29. R. Timpl, H. Rohde, P. G. Robey, S. I. Rennard, J.-M. Foidart and G. R. Martin, "Laminin - A Glycoprotein from Basement Membranes," *Journal of Biological Chemistry*, vol. 254, no. 19, pp. 9933-9937, 1979.
30. S. Baker and J. Southgate, "Towards control of smooth muscle cell differentiation in synthetic 3D scaffolds," *Biomaterials*, vol. 29, no. 23, pp. 3357-3366, 2008.
31. M. Bissell, H. Hall and G. Parry, "How does the extracellular matrix direct gene expression?," *J Theor Biol*, vol. 99, no. 1, pp. 31-68, 1982.
32. N. Boudreau, C. Myers and M. Bissell, "From laminin to lamin: regulation of tissue-specific gene expression by the ECM," *Trends Cell Biol*, vol. 5, no. 1, pp. 1-4, 1995.
33. D. Ingber, "Extracellular matrix and cell shape: potential control points for inhibition of angiogenesis," *J Cell Biochem*, vol. 47, no. 3, pp. 236-241, 1991.
34. H. Lodish, A. Berk and S. Zipursky, "Collagen: The Fibrous Proteins of the Matrix," in *Molecular Cell Biology*, New York, W. H. Freeman, 2000.
35. A. R. Gillies and R. L. Lieber, "Structure and Function of the Skeletal Muscle Extracellular Matrix," *Muscle Nerve*, vol. 44, no. 3, pp. 318-331, 2011.
36. H. Cui, C. Freeman, G. A. Jacobson and D. H. Small, "Proteoglycans in the central nervous system: Role in development, neural repair, and Alzheimer's disease," *IUBMB Life*, vol. 65, no. 2, pp. 108-120, 2013.
37. B. Alberts, A. Johnson and J. Lewis, "The Extracellular Matrix of Animals," in *Molecular Biology of the Cell*, New York, Garland Science, 2002.
38. H. O. Gautier, A. J. Thompson, S. Achouri, D. E. Koser, K. Holtzmann, E. Moeendarbary and K. Franze, "Atomic force microscopy-based force measurements on animal cells and tissues," in *Biophysical Methods in Cell Biology*, E. K. Paluch, Ed., Elsevier, 2015, pp. 211-235.
39. G. Binnig, C. Quate and C. Gerber, "Atomic force microscope," *Physical Review Letters*, vol. 56, no. 9, pp. 930-933, 1986.
40. G. Thomas, N. A. Burnham, T. A. Camesano and Q. Wen, "Measuring the Mechanical Properties of Living Cells Using Atomic Force Microscopy," *J Vis Exp*, vol. 76, p. e50497, 2013.

41. Y. K. Mariappan, K. J. Glaser and R. L. Ehman, "Magnetic Resonance Elastography: A Review," *Clin Anat*, vol. 23, no. 5, pp. 497-511, 2010.
42. S. Nam, K. H. Hu, M. J. Butte and O. Chaudhuri, "Strain-enhanced stress relaxation impacts nonlinear elasticity in collagen gels," *Proc Natl Acad Sci USA*, vol. 113, no. 20, pp. 5492-5497, 2016.
43. X. Zhao, N. Huebsch, D. J. Mooney and Z. Suo, "Stress-relaxation behavior in gels with ionic and covalent crosslinks," *J Appl Phys*, vol. 107, no. 6, p. 063509, 2010.
44. X. Zhao, "Multi-scale multi-mechanism design of tough hydrogels: building dissipation into stretchy networks," *Soft Matter*, vol. 10, pp. 672-687, 2014.
45. A. E. Brown, R. I. Litvinov, D. E. Discher, P. K. Purohit and J. W. Weisel, "Multiscale Mechanics of Fibrin Polymer: Gel Stretching with Protein Unfolding and Loss of Water," *Science*, vol. 325, no. 5941, pp. 741-744, 2009.
46. C.-S. Han, S. H. Sanei and F. Alisafaei, "On the origin of indentation size effects and depth dependent mechanical properties of elastic polymers," *J Polym Eng*, vol. 36, no. 1, pp. 103-111, 2015.
47. O. Chaudhuri, "Viscoelastic hydrogels for 3D cell culture," *Biomaterials Science*, vol. 5, pp. 480-1490, 2017.
48. G. Davis and D. Senger, "Endothelial extracellular matrix: biosynthesis, remodeling, and functions during vascular morphogenesis and neovessel stabilization," *Circ Res*, vol. 97, no. 11, pp. 1093-1107, 2005.
49. V. Gupta and K. J. Grande-Allen, "Effects of static and cyclic loading in regulating extracellular matrix synthesis by cardiovascular cells," *Cardiovascular Research*, vol. 72, no. 3, pp. 375-383, 2006.
50. S. Y. N. Takahashi, K. Tobe, T. Kadowaki and Y. Yazaki, "Pulsatile stretch activates mitogen-activated protein kinase (MAPK) family members and focal adhesion kinase (p125FAK) in cultured rat cardiac myocytes," *Biochem Biophys Res Commun*, vol. 259, no. 1, pp. 8-14, 1999.
51. M. Wong, M. Siegrist and K. Goodwin, "Cyclic tensile strain and cyclic hydrostatic pressure differentially regulate expression of hypertrophic markers in primary chondrocytes," *Bone*, vol. 33, no. 4, pp. 685-693, 2003.
52. D. Discher, P. Janmey and Y. Wang, "Tissue cells feel and respond to the stiffness of their substrate," *Science*, vol. 310, pp. 1139-1143, 2005.
53. L. Flanagan, Y. Ju, B. Marg, M. Osterfield and P. Janmey, "Neurite branching on deformable substrates," *Neuroreport*, vol. 13, pp. 2411-2415, 2002.

54. P. Georges, W. Miller, D. Meaney, E. Sawyer and P. Janmey, "Matrices with compliance comparable to that of brain tissue select neuronal overglial growth in mixed cortical cultures," *Biophysical Journal*, vol. 90, pp. 3012-3018, 2006.
55. X. Jiang, P. Georges, B. Li, Y. Du, M. Kutzing, M. Previtera, N. Langrana and B. Firestein, "Cell growth in response to mechanical stiffness is affected by neuron-astroglia interactions," *The Open Neuroscience Journal*, vol. 1, pp. 7-14, 2007.
56. F. Jiang, B. Yurke, B. Firestein and N. Langrana, "Neurite outgrowth on a DNA crosslinked hydrogel with tunable stiffnesses," *Annals of Biomedical Engineering*, vol. 36, pp. 1565-1579, 2008.
57. K. Franze, J. Gerdemann, M. Weick, T. Betz, S. Pawlizak, M. Lakadamyali, J. Bayer, K. Rillich, M. Gogler, Y. Lu, A. Reichenback, P. Janmey and J. Kas, "Neurite branch retraction is caused by a threshold-dependent mechanical impact," *Biophysical Journal*, vol. 97, pp. 1883-1890, 2009.
58. D. Bray, "Axonal growth in response to experimentally applied mechanical tension," *Developmental Biology*, vol. 102, pp. 379-389, 1984.
59. D. Van Essen, "A tension-based theory of morphogenesis and compact wiring in the central nervous system," *Nature*, vol. 385, pp. 313-318, 1997.
60. S. Heidemann and R. Buxbaum, "Mechanical tension as a regulator of axonal development," *Neurotoxicology*, vol. 15, pp. 95-107, 1994.
61. A. Naba, O. M. Pearce, A. D. Rosario, D. Ma, H. Ding, V. Rajeeve, P. R. Cutillas, F. R. Balkwill and R. O. Hynes, "Characterization of the Extracellular Matrix of Normal and Diseased Tissues Using Proteomics," *Journal of Proteome Research*, vol. 16, no. 8, pp. 3083-3091, 2017.
62. F. A. Duck, "Mechanical Properties of Tissue," in *Physical Properties of Tissues: A Comprehensive Reference Work*, San Diego, Academic Press Limited, 1990, pp. 137-165.
63. A. Sarvazyan, A. Skovoroda, S. Emelianov, J. Fowlkes, J. Pipe, R. Adler, R. Buxton and P. Carson, "Biophysical Bases of Elasticity Imaging," in *Acoustical Imaging*, Boston, Springer, 1995, pp. 223-240.
64. T. Rozario and D. DeSimone, "The extracellular matrix in development and morphogenesis: a dynamic view," *Dev Biol*, vol. 341, pp. 126-140, 2010.
65. K. Tsang, M. Cheung, D. Chan and K. Cheah, "The development roles of the extracellular matrix: beyond structure to regulation," *Cell Tissue Res*, vol. 339, pp. 93-110, 2010.

66. S. Venkatesh, M. Yin, J. Glockner, N. Takahashi, P. Araoz, J. Talwalkar and R. Ehman, "MR elastography of liver tumors: preliminary results," *AJR Am J Roentgenol*, vol. 190, no. 6, pp. 1534-1540, 2008.
67. M. Yin, J. Talwalkar, K. Glaser, A. Manduca, R. Grimm, P. Rossman, J. Fidler and R. Ehman, "Assessment of hepatic fibrosis with magnetic resonance elastography," *Clin Gastroenterol Hepatol*, vol. 5, no. 10, pp. 1207-1213, 2007.
68. R. Wright, "Elastic tissue of normal and emphysematous lungs: a tridimensional histologic study," *Am J Pathol*, vol. 39, pp. 355-367, 1961.
69. P. Chrzanowski, S. Keller and J. Cerreta, "Elastin content of normal and emphysematous lung parenchyma," *Am J Med*, vol. 69, pp. 351-359, 1980.
70. M. Merrilees, P. Ching and B. Beaumont, "Changes in elastin, elastin binding protein and versican in alveoli in chronic obstructive pulmonary disease," *Respir Res*, vol. 9, p. 41, 2008.
71. J. van Straaten, W. Coers and J. Noordhoek, "Proteoglycan changes in the extracellular matrix of lung tissue from patients with pulmonary emphysema," *Mod Pathol*, vol. 12, pp. 697-705, 1999.
72. R. Annoni, T. Lanças, R. Tanigawa, M. Matsushita, S. Fernezlian, A. Bruno, L. Silva, P. Roughley, S. Battaglia, M. Dolhnikoff, P. Hiemstra, P. Sterk, K. Rabe and T. Mauad, "Extracellular matrix composition in COPD," *Eur Respir J*, vol. 40, pp. 1362-1373, 2012.
73. D. Butcher, T. Alliston and V. Weaver, "A tense situation: forcing tumor progression," *Nat Rev Cancer*, vol. 9, pp. 108-122, 2009.
74. K. R. Levental, H. Yu, L. Kass, J. N. Lakins, M. Egeblad, J. T. Erler, S. F. Fong, K. Csiszar, A. Giaccia, W. Weninger, M. Yamauchi, D. L. Gasser and V. M. Weaver, "Matrix crosslinking forces tumor progression by enhancing integrin signaling," *Cell*, vol. 139, no. 5, pp. 891-906, 2009.
75. R. Jain, J. Martin and T. Stylianopoulos, "The Role of Mechanical Forces in Tumor Growth and Therapy," in *Annual Review of Biomedical Engineering*, Vol 16, M. Yarmush, Ed., Palo Alto, Annual Reviews, 2014, pp. 321-346.
76. O. De Wever, P. Demetter, M. Mareel and M. Bracke, "Stromal myofibroblasts are drivers of invasive cancer growth," *Int J Cancer*, vol. 123, pp. 2229-2238, 2008.
77. K. Kessenbrock, V. Plaks and Z. Werb, "Matrix metalloproteinases: regulators of the tumor microenvironment," *Cell*, vol. 141, pp. 52-67, 2010.
78. F. T. Bosman and I. Stamenkovic, "Functional structure and composition of the extracellular matrix," *Journal of Pathology*, vol. 200, no. 4, pp. 423-428, 2003.
79. J. Erler and V. Weaver, "Three-dimensional context regulation of metastasis," *Clin Exp Metastasis*, vol. 26, pp. 35-49, 2009.



80. M. Paszek and V. Weaver, "The tension mounts: mechanics meets morphogenesis and malignancy," *J Mammary Gland Biol Neoplasia*, vol. 9, pp. 325-342, 2004.
81. M. Paszek, N. Zahir, K. Johnson, J. Lakins, G. Rozenberg, A. Gefen, C. Reinhart-King, S. Margulies, M. Dembo, D. Boettiger, D. Hammer and V. Weaver, "Tensional homeostasis and the malignant phenotype," *Cancer Cell*, vol. 8, no. 3, pp. 241-254, 2005.
82. Insua-Rodríguez and T. Oskarsson, "The extracellular matrix in breast cancer," *Advanced Drug Delivery Reviews*, vol. 97, pp. 51-55, 2016.
83. T. Oskarsson, "Extracellular matrix components in breast cancer progression and metastasis," *The Breast*, vol. 22, no. Supplement 2, pp. S66-S72, 2013.
84. A. Lochter and M. Bissell, "Involvement of extracellular matrix constituents in breast cancer," *Semin Cancer Biol*, vol. 6, pp. 165-173, 1995.
85. P. Lu, K. Takai, V. Weaver and Z. Werb, "Extracellular matrix degradation and remodeling in development and disease," *Cold Spring Harb Perspect Biol*, vol. 3, no. 12, 2011.
86. P. Schedin, J. O'Brien, M. Rudolph, T. Stein and V. Borges, "Microenvironment of the involuting mammary gland mediates mammary cancer progression," *J Mammary Gland Biol Neoplasia*, vol. 12, pp. 71-82, 2007.
87. J. O'Brien, L. Vanderlinden, P. Schedin and K. Hansen, "Rat mammary extracellular matrix composition and response to ibuprofen treatment during postpartum involution by differential GeLC-MS/MS analysis," *J Proteome Res*, vol. 11, pp. 4894-4905, 2012.
88. P. Schedin, "Pregnancy-associated breast cancer and metastasis," *Nat Rev Cancer*, vol. 6, pp. 281-291, 2006.
89. M. Duffy, T. Maguire, A. Hill, E. McDermott and N. O'Higgins, "Metalloproteinases: role in breast carcinogenesis, invasion and metastasis," *Breast Cancer Res*, vol. 2, no. 4, pp. 252-257, 2000.
90. T. Gudjonsson, L. Ronnov-Jessen, R. Villadsen, F. Rank, M. Bissell and O. Petersen, "Normal and tumor-derived myoepithelial cells differ in their ability to interact with luminal breast epithelial cells for polarity and basement membrane deposition," *J Cell Sci*, vol. 115, pp. 39-50, 2002.
91. H. Chong, C. Tan, R. Huang and N. Tan, "Matricellular proteins: a sticky affair with cancers," *Journal of Oncology*, vol. 2012, pp. 1-17, 2012.
92. A. Yee, M. Akens, B. Yang, J. Finkelstein, P. Zheng, Z. Deng and B. Yang, "The effect of versican G3 domain on local breast cancer invasiveness and bony metastasis," *Breast Cancer Res*, vol. 9, p. R47, 2007.

93. M. Leivonen, J. Lundin, S. Nordling, K. von Boguslawski and C. Haglund, "Prognostic value of syndecan-1 expression in breast cancer," *Oncology*, vol. 67, pp. 11-18, 2004.
94. K. Matsuda, H. Maruyama, F. Guo, J. Kleeff, J. Itakura, Y. Matsumoto, A. Lander and M. Korc, "Glypican-1 is overexpressed in human breast cancer and modulates the mitogenic effects of multiple heparin-binding growth factors in breast cancer cells," *Cancer Res*, vol. 61, pp. 5562-5569, 2001.
95. M. Barton, R. Harris and S. Fletcher, "The rational clinical examination. Does this patient have breast cancer? The screening clinical breast examination: should it be done? How?," *JAMA*, vol. 282, no. 13, pp. 1270-1280, 1999.
96. D. Elias, L. Sideris, M. Pocard, T. de Baere, C. Dromain, N. Lassau and P. Lasser, "Incidence of unsuspected and treatable metastatic disease associated with operable colorectal liver metastases discovered only at laparotomy (and not treated when performing percutaneous radiofrequency ablation)," *Ann Surg Oncol*, vol. 12, no. 4, pp. 298-302, 2005.
97. P. L. Jones, J. Crack and M. Rabinovitch, "Regulation of tenascin-C, a Vascular Smooth Muscle Cell Survival Factor that Interacts with the  $\alpha$ V $\beta$ 3 Integrin to Promote Epidermal Growth Factor Receptor Phosphorylation and Growth," *J Cell Biol*, vol. 139, pp. 279-293, 1997.
98. C. D. Roskelley, A. Srebrow and M. J. Bissell, "A hierarchy of ECM-mediated signalling regulates tissue-specific gene expression," *Current Opinion in Cell Biology*, vol. 7, pp. 736-747, 1995.
99. A. Fullár, J. Dudás, L. Oláh, P. Hollósi, Z. Papp, G. Sobel, K. Karászi, S. Paku, K. Baghy and I. Kovalszky, "Remodeling of extracellular matrix by normal and tumor-associated fibroblasts promotes cervical cancer progression," *BMC Cancer*, vol. 15, pp. 256-271, 2015.
100. American Cancer Society, "Cancer Facts & Figures 2018," American Cancer Society, Atlanta, 2018.
101. H. Verheul and H. Pinedo, "Clinical implications of drug resistance," in *Drug Resistance in the Treatment of Cancer*, H. Pinedo and G. Giaccone, Eds., Cambridge, Cambridge University Press, 2006, pp. 199-231.
102. A. Prahallad, "Unresponsiveness of colon cancer to BRAF(V600E) inhibition through feedback activation of EGFR," *Nature*, vol. 483, pp. 100-103, 2012.
103. C. Sun, L. Wang, S. Huang, G. Heynen, A. Prahallad, C. Robert, J. Haanen, C. Blank, J. Wesseling, S. Willems, D. Zecchin, S. Hobor, P. Bajpe, C. Liefink, C. Mateus, S. Vagner, W. Grenrum, I. Hofland, A. Schlicker, L. Wessels, R. Beijersbergen and e. al, "Reversible and adaptive resistance to BRAF(V600E) inhibition in melanoma," *Nature*, vol. 508, no. 7494, pp. 118-122, 2014.

104. J. Riordan and V. Ling, "Genetic and biochemical characterization of multidrug resistance," *Pharmacol Ther*, vol. 28, no. 1, pp. 51-75, 1985.
105. L. Liu, "DNA topoisomerase poisons as antitumor drugs," *Annu Rev Biochem*, vol. 58, pp. 351-375, 1989.
106. S. Hasegawa, T. Abe, S. Naito, S. Kotoh, J. Kumazawa, D. Hipfner, R. Deeley and S. K. M. Cole, "Expression of multidrug resistance-associated protein (MRP), MDR1 and DNA topoisomerase II in human multidrug-resistant bladder cancer cell lines," *Br J Cancer*, vol. 71, no. 5, pp. 907-913, 1995.
107. K. Brasseur, N. Gévry and E. Asselin, "Chemoresistance and targeted therapies in ovarian and endometrial cancers," *Oncotarget*, vol. 8, pp. 4008-4042, 2017.
108. C. Lu and A. Shervington, "Chemoresistance in gliomas," *Mol Cell Biochem*, vol. 312, pp. 71-80, 2008.
109. E. A. O'Reilly, L. Gubbins, S. Sharma, R. Tully, M. H. Z. Guang, K. Weiner-Gorzel, J. McCaffrey, M. Harrison, F. Furlong, M. Kell and A. McCann, "The fate of chemoresistance in triple negative breast cancer (TNBC)," *BBA Clinical*, vol. 3, pp. 257-275, 2015.
110. D. Gewirtz, "A critical evaluation of the mechanisms of action proposed for the antitumor effects of the anthracycline antibiotics adriamycin and daunorubicin," *Biochem Pharmacol*, vol. 57, pp. 727-741, 1999.
111. K. Tewey, T. Rowe, L. Yang, B. Halligan and L. Liu, "Adriamycin-induced DNA damage mediated by mammalian DNA topoisomerase-II," *Science*, vol. 226, pp. 466-468, 1984.
112. J. Doroshow, "Role of hydrogen peroxide and hydroxyl radical formation in the killing of Ehrlich tumor cells by anticancer quinones," *Proc Natl Acad Sci USA*, vol. 83, pp. 4514-4518, 1986.
113. S. Fogli, P. Nieri and M. Breschi, "The role of nitric oxide in anthracycline toxicity and prospects for pharmacologic prevention of cardiac damage," *FASEB J*, vol. 18, pp. 664-675, 2004.
114. F. Yaqub, "Mechanism of action of anthracycline drugs," *The Lancet Oncology*, vol. 14, no. 8, p. e296, 2013.
115. U. Germann, "P-glycoprotein: a mediator of multidrug resistance in tumour cells," *Eur J Cancer*, vol. 32A, pp. 927-944, 1996.
116. S. Cole, G. Bhardwaj, J. Gerlach, J. Mackie, C. Grant, K. Almquist, A. Stewart, E. Kurz, A. Duncan and R. Deeley, "Overexpression of a transporter gene in a multidrug-resistant human lung cancer cell line," *Science*, vol. 258, no. 5088, pp. 1650-1654, 1992.

117. S. Lal, A. Mahajan, W. Chen and B. Chowbay, "Pharmacogenetics of target genes across doxorubicin disposition pathway: a review," *Curr Drug Metab*, vol. 11, pp. 115-128, 2010.
118. L. Young, B. Campling, S. Cole, R. Deeley and J. Gerlach, "Multidrug resistance proteins MRP3, MRP1, and MRP2 in lung cancer: correlation of protein levels with drug response and messenger RNA levels," *Clin Cancer Res*, vol. 7, pp. 1798-1804, 2001.
119. S. Singhal, J. Singhal, R. Sharma, S. Singh, P. Zimniak and Y. A. S. Awasthi, "Role of RLIP76 in lung cancer doxorubicin resistance: I. The ATPase activity of RLIP76 correlates with doxorubicin and 4-hydroxynonenal resistance in lung cancer cells.," *Int J Oncol*, vol. 22, no. 2, pp. 365-375, 2003.
120. D. Burgess, J. Doles, L. Zender, W. Xue, B. Ma, W. McCombie, G. Hannon, S. Lowe and M. Hemann, "Topoisomerase levels determine chemotherapy response in vitro and in vivo," *Proc Natl Acad Sci USA*, vol. 105, no. 26, pp. 9053-9058, 2008.
121. C. Oakman, E. Moretti, F. Galardi, L. Santarpia and L. A. Di, "The role of topoisomerase-IIalpha and HER-2 in predicting sensitivity to anthracyclines in breast cancer patients," *Cancer Treat Rev*, vol. 35, pp. 662-667, 2009.
122. K. Pritchard, H. Messersmith, L. Elavathil, M. Trudeau, F. O'Malley and B. Dhesy-Thind, "HER-2 and topoisomerase II as predictors of response to chemotherapy," *J Clin Oncol*, vol. 26, pp. 736-744, 2008.
123. B. A. Weaver, "How Taxol/paclitaxel kills cancer cells," *Mol Biol Cell*, vol. 25, no. 18, pp. 2677-2681, 2014.
124. R. Yusuf, Z. Duan, D. Lamendola, R. Penson and M. Seiden, "Paclitaxel Resistance: Molecular Mechanisms and Pharmacologic Manipulation," *Current Cancer Drug Targets*, vol. 3, no. 1, pp. 1-19, 2005.
125. T. Strobel, L. Swanson, S. Korsmeyer and S. Cannistra, "BAX Enhances Paclitaxel-Induced Apoptosis through a p53-Independent Pathway," *Proc Natl Acad Sci USA*, vol. 93, pp. 14094-14099, 1996.
126. T. Strobel, Y. Tai, S. Korsmeyer and S. Cannistra, "BAD Partly Reverses Paclitaxel Resistance in Human Ovarian Cancer Cells," *Oncogene*, vol. 17, pp. 2419-2427, 1998.
127. D. Luo, S. Cheng, H. Xie and Y. Xie, "Effects of Bcl-2 and Bcl-XL Protein Levels On Chemoresistance Of Hepatoblastoma Hepg2 Cell Line," *Biochem Cell Biol*, vol. 78, pp. 119-126, 2000.
128. B. Ogretmen and A. Safa, "Down-Regulation of Apoptosis-Related Bcl-2 but not Bcl-Xl or Bax Proteins in Multidrug-Resistant MCF-y/Adr Human Breast Cancer Cells," *Int J Cancer*, vol. 67, pp. 608-614, 1996.

129. Z. Duan, D. Lamendola, R. Penson, K. Kronish and M. Seiden, "Overexpression of IL-6 but not IL-8 Increases Paclitaxel Resistance of u-2os Human Osteosarcoma Cells," *Cytokine*, vol. 17, pp. 234-242, 2002.
130. S. Song, M. Wientjes, Y. Gan and J. Au, "Fibroblast Growth Factors: An Epigenetic Mechanism of Broad Spectrum Resistance to Anticancer Drugs," *Proc Natl Acad Sci USA*, vol. 97, pp. 8658-8663, 2000.
131. D. Yu and M. Hung, "Role of ErbB2 in Breast Cancer Chemosensitivity," *Bioessays*, vol. 22, pp. 673-680, 2000.
132. J. Mendelsohn and J. Baselga, "The EGF Receptor Family as Targets for Cancer Therapy," *Oncogene*, vol. 19, pp. 6550-6565, 2000.
133. F. Aoudjit and K. Vuori, "Integrin Signaling Inhibits Paclitaxel-Induced Apoptosis in Breast Cancer Cells," *Oncogene*, vol. 20, pp. 4995-5004, 2001.
134. K. Luker, C. Pica, R. Schreiber and D. Piwnica-Worms, "Overexpression of IRF9 Confers Resistance to Antimicrotubule Agents in Breast Cancer Cells," *Cancer Res*, vol. 61, pp. 6540-6547, 2001.
135. E. Dolci, R. Abramson, Y. Xuan, J. Siegfried, K. Yuenger, D. Yassa and T. Tritton, "Anomalous Expression Of P-Glycoprotein in Highly Drug-Resistant Human KB Cells," *Int J Cancer*, vol. 54, pp. 302-308, 1993.
136. P. Cesaro, E. Raiteri, M. Demoz, R. Castino, F. Baccino, G. Bonelli and C. Isidoro, "Expression of protein kinase C beta1 confers resistance to TNFalpha- and paclitaxel-induced apoptosis in HT-29 colon carcinoma cells," *Int J Cancer*, vol. 93, no. 2, pp. 179-184, 2001.
137. G. Ajabnoor, T. Crook and H. Coley, "Paclitaxel resistance is associated with switch from apoptotic to autophagic cell death in MCF-7 breast cancer cells," *Cell Death and Disease*, vol. 3, no. 1, p. e260, 2012.
138. D. Hanahan and R. Weinberg, "The hallmarks of cancer," *Cell*, vol. 100, pp. 57-70, 2000.
139. D. Hanahan and R. Weinberg, "Hallmarks of cancer: the next generation," *Cell*, vol. 144, pp. 646-674, 2011.
140. M. Pickup, J. Mouw and V. Weaver, "The extracellular matrix modulates the hallmarks of cancer," *EMBO Rep*, vol. 15, no. 12, pp. 1243-1253, 2014.
141. V. Weaver, O. Petersen, F. Wang, C. Larabell, P. Briand, C. Damsky and M. Bissell, "Reversion of the Malignant Phenotype of Human Breast Cells in Three-Dimensional Culture and In Vivo by Integrin Blocking Antibodies," *Journal of Cell Biology*, vol. 137, no. 1, pp. 231-245, 1997.

142. P. Provenzano, D. Inman, K. Eliceiri, J. Knittel, L. Yan, C. Rueden, J. White and P. Keely, "Collagen density promotes mammary tumor initiation and progression," *BMC Medicine*, vol. 6, no. 11, 2008.
143. P. Provenzano, D. Inman, K. Eliceiri and P. Keely, "Matrix density-induced mechanoregulation of breast cell phenotype, signaling and gene expression through a FAK-ERK linkage," *Oncogene*, vol. 28, no. 49, pp. 4326-4343, 2009.
144. J.-W. Shin and D. J. Mooney, "Shin, J.-W., & Mooney, D. J. (2016). Extracellular matrix stiffness causes systematic variations in proliferation and chemosensitivity in myeloid leukemias," *Proceedings of the National Academy of Sciences of the United States of America*, vol. 113, no. 43, pp. 12126-12131, 2016.
145. H. Abu-Tayeh, K. Weidenfeld, A. Zhilin-Roth, S. Schif-Zuck, S. Thaler, C. Cotarelo, T. Tan, J. Thiery, J. Green, G. Klorin, E. Sabo, J. Sleeman, M. Tzukerman and D. Barkan, "'Normalizing' the malignant phenotype of luminal breast cancer cells via alpha(v)beta(3)-integrin," *Cell Death and Disease*, vol. 7, p. e2491, 2016.
146. S. Carey, K. Martin and C. Reinhart-King, "Three-dimensional collagen matrix induces a mechanosensitive invasive epithelial phenotype," *Scientific Reports*, vol. 7, p. 42088, 2017.
147. S. Gopal, L. Veracini, D. Grall, C. Butori, S. Schaub, S. Audebert, L. Camoin, E. Baudalet, A. Radwanska, S. Divonne, S. Violette, P. Weinreb, S. Rekima, M. Ilie, A. Sudaka, P. Hofman and E. Obberghen-Schilling, "Fibronectin-guided migration of carcinoma collectives," *Nature Communications*, vol. 8, p. 14105, 2017.
148. S. Zusiak, R. Nossal and D. Sackett, "Multiwell Stiffness Assay for the Study of Cell Responsiveness to Cytotoxic Drugs," *Biotechnology and Bioengineering*, vol. 111, no. 2, pp. 396-403, 2014.
149. A. Rice, E. Cortes, D. Lachowski, B. Cheung, S. Karim, J. Morton and A. d. R. Hernández, "Matrix stiffness induced epithelial-mesenchymal transition and promotes chemoresistance in pancreatic cancer cells," *Oncogenesis*, vol. 6, p. e352, 2017.
150. T. Moroishi, C. Hansen, K. Guan and S. Diego, "The emerging roles of YAP and TAZ in cancer," *Nat Rev Cancer*, vol. 15, pp. 73-79, 2015.
151. J. M. Lamar, P. Stern, H. Liu, J. W. Schindler, Z.-G. Jiang and R. O. Hynes, "The Hippo pathway target, YAP, promotes metastasis through its TEAD-interaction domain," *PNAS*, vol. 109, no. 37, pp. E2441-E2450, 2012.
152. Y. Liu, K. He, Y. Hu, X. Guo, D. Wang, W. Shi, J. Li and J. Song, "YAP modulates TGF-beta1-induced simultaneous apoptosis and EMT through upregulation of the EGF receptor," *Scientific Reports*, vol. 7, p. 45523, 2017.
153. C. Badouel and H. McNeill, "SnapShot: The Hippo Signaling Pathway," *Cell*, vol. 145, no. 3, pp. 484-484, 2011.

154. D. Pan, "The Hippo Signaling Pathway in Development and Cancer," *Dev Cell*, vol. 19, no. 4, pp. 491-505, 2010.
155. H. J. J. van Rensburg and X. Yang, "The roles of the Hippo pathway in cancer metastasis," *Cellular Signalling*, vol. 28, pp. 1761-1772, 2016.
156. W. Lehmann, D. Mossmann, J. Kleemann, K. Mock, C. Meisinger, T. Brummer, R. Herr, S. Brabletz, M. P. Stemmler and T. Brabletz, "ZEB1 turns into a transcriptional activator by interacting with YAP1 in aggressive cancer types," *Nat Comm*, vol. 7, pp. 1-15, 2016.

## CHAPTER 2

1. T. Rozario and D. W. DeSimone, "The extracellular matrix in development and morphogenesis: A dynamic view," *Developmental Biology*, vol. 341, no. 2010, pp. 126-140, 2010.
2. S. L. Bowers, I. Banerjee and T. A. Baudino, "The Extracellular Matrix: At the Center of it All," *J Mol Cell Cardiol*, vol. 48, no. 3, pp. 474-482, 2010.
3. C. Bonnans, J. Chou and Z. Werb, "Remodelling the extracellular matrix in development and disease," *Nat Rev Mol Cell Biol*, vol. 15, no. 12, pp. 786-801, 2014.
4. P. Jones, J. Crack and M. Rabinovitch, "Regulation of tenascin-C, a Vascular Smooth Muscle Cell Survival Factor that Interacts with the  $\alpha$ V $\beta$ 3 Integrin to Promote Epidermal Growth Factor Receptor Phosphorylation and Growth," *J Cell Biol*, vol. 139, pp. 279-293, 1997.
5. C. Roskelley, A. Srebrow and M. Bissell, "A hierarchy of ECM-mediated signalling regulates tissue-specific gene expression," *Current Opinion in Cell Biology*, vol. 7, pp. 736-747, 1995.
6. A. Fullár, J. Dudás, L. Oláh, P. Hollósi, Z. Papp, G. Sobel, K. Karászi, S. Paku, K. Baghy and I. Kovalszky, "Remodeling of extracellular matrix by normal and tumor-associated fibroblasts promotes cervical cancer progression," *BMC Cancer*, vol. 15, pp. 256-271, 2015.
7. S. Caliri and J. Burdick, "A Practical Guide to Hydrogels for Cell Culture," *Nat Methods*, vol. 13, no. 5, pp. 405-414, 2016.
8. P. Provenzano, D. Inman, K. Eliceiri, J. Knittel, L. Yan, C. Rueden, J. White and P. Keely, "Collagen density promotes mammary tumor initiation and progression," *BMC Med*, p. 11, 2008.
9. V. McCormack and S. dos Santos, "Breast density and parenchymal patterns as markers of breast cancer risk: a meta-analysis," *Cancer Epidemiol Biomarkers Prev*, pp. 1159-1169, 2006.

10. N. Boyd, G. Lockwood, J. Byng, D. Tritchler and M. Yaffe, "Mammographic densities and breast cancer risk," *Cancer Epidemiol Biomarkers Prev*, pp. 1133-1144, 1998.
11. N. Boy, L. Martin, J. Stone, C. Greenberg, S. Minkin and M. Yaffe, "Mammographic densities as a marker of human breast cancer risk and their use in chemoprevention," *Curr Oncol Rep*, pp. 314-321, 2001.
12. N. Boyd, G. Dite, J. Stone, A. Gunasekara, D. English, M. McCredie, G. Giles, D. Tritchler, A. Chiarelli, M. Yaffe and J. Hopper, "Heritability of mammographic density, a risk factor for breast cancer," *N Engl J Med*, pp. 886-894, 2002.
13. H. Kleinman and G. Martin, "Matrigel: basement membrane matrix with biological activity," *Semin Cancer Biol.*, vol. 15, pp. 378-386, 2005.
14. B. Toole, "Hyaluronan in morphogenesis," *Semin Cell Dev Biol*, vol. 12, no. 2, pp. 79-87, 2001.
15. B. Toole, "Hyaluronan: from extracellular glue to pericellular cue," *Nat Rev Cancer*, vol. 4, no. 7, pp. 528-539, 2004.
16. R. Stern, Ed., *Hyaluronan in cancer biology*, 1st ed., San Diego, CA: Elsevier, 2009.
17. K. Dicker, L. Gurski, S. Pradhan-Bhatt, R. Witt, M. Farach-Carson and X. Jia, "Hyaluronan: a simple polysaccharide with diverse biological functions," *Acta Biomater.*, vol. 10, no. 4, pp. 1558-1570, 2014.
18. J. Burdick and D. Glenn, "Hyaluronic Acid Hydrogels for Biomedical Applications," *Adv Mater*, vol. 23, no. 12, pp. H41-H56, 2011.
19. S. Khetan, M. Guvendiren, W. Legant, D. Cohen, C. CS and J. Burdick, "Degradation-mediated cellular traction directs stem cell fate in covalently crosslinked three-dimensional hydrogels," *Nat Mater*, vol. 12, no. 5, pp. 458-465, 2013.
20. M. Guvendiren and J. Burdick, "Stiffening hydrogels to probe short- and long-term cellular responses to dynamic mechanics," *Nat Commun*, vol. 3, p. 792, 2012.
21. S. Mooney and J. Shin, "Extracellular matrix stiffness causes systematic variations in proliferation and chemosensitivity in myeloid leukemias.," *Proceedings of the National Academy of Sciences of the United States of America*, pp. 12126-12131, 2016.
22. S. Zustiak, R. Nossal and D. Sackett, "Multiwell Stiffness Assay for the Study of Cell Responsiveness to Cytotoxic Drugs," *Biotechnology and Bioengineering*, vol. 111, no. 2, pp. 396-403, 2014.
23. R. Stowers, S. Allen and L. Suggs, "Dynamic phototuning of 3D hydrogel stiffness," *Proceedings of the National Academy of Sciences*, pp. 1953-1958, 2015.
24. X. Wang and H. G. Spencer, "Calcium alginate gels: formation and stability in the presence of an inert electrolyte," *Polymer*, vol. 39, no. 13, pp. 2759-2764, 1998.



25. N. Genes, J. Rowley, D. Mooney and L. Bonassar, "Effect of substrate mechanics on chondrocyte adhesion to modified alginate surfaces," *Archives of Biochemistry and Biophysics*, vol. 422, no. 2, pp. 161-167, 2004.
26. M. Wästfelt, B. Fadeel and J. Henter, "A journey of hope: Lessons learned from studies on rare diseases and orphan drugs," *J Intern Med*, vol. 260, pp. 1-10, 2006.
27. Y. Uchida, S. Tanaka, A. Aihara, R. Adikrisna, K. Yoshitake, S. Matsumura, Y. Mitsunori, A. Murakata, N. Noguchi, T. Irie, A. Kudo, N. Nakamura, P. Lai and S. Arii, "Analogy between sphere forming ability and stemness of human hepatoma cells," *Oncol Rep*, vol. 24, no. 5, pp. 1147-1151, 2010.
28. H. Dhiman, A. Ray and A. Panda, "Three-dimensional chitosan scaffold-based MCF-7 cell culture for the determination of the cytotoxicity of tamoxifen," *Biomaterials*, vol. 26, pp. 979-986, 2005.
29. V. Estrella, T. Chen, M. Lloyd, J. Wojtkowiak, H. Cornnell, A. Ibrahim-Hashim, K. Bailey, Y. Balagurunathan, J. Rothberg, B. Sloane, J. Johnson, R. Gatenby and R. Gillies, "Acidity generated by the tumor microenvironment drives local invasion," *Cancer Res*, vol. 73, no. 5, pp. 1524-1535, 2013.
30. D. T. Butcher, T. Alliston and V. M. Weaver, "A tense situation: forcing tumour progression," *Nature Reviews Cancer*, vol. 9, pp. 108-122, 2009.
31. O. Tacar, P. Sriamornsak and C. Dass, "Doxorubicin: an update on anticancer molecular action, toxicity and novel drug delivery systems," *Journal of Pharmacy and Pharmacology*, vol. 65, pp. 157-170, 2012.
32. M. Jordan and L. Wilson, "Microtubules as a target for anticancer drugs," *Nat. Rev. Cancer*, vol. 4, no. 4, pp. 356-265, 2004.
33. C. Walczak and R. Heald, "Mechanisms of mitotic spindle assembly and function," in *International Review of Cytology*, vol. 265, K. W. Jeon, Ed., San Diego, California: Elsevier, 2008, pp. 111-158.
34. E. Nogales, S. Wolf, I. Khan, R. Luduena and K. Downing, "Structure of tubulin at 6. 5Å and location of the taxol-binding site," *Nature*, vol. 375, pp. 424-427, 1995.
35. E. Nogales, "Structural insights into microtubule function," *Annu. Rev. Biochem.*, vol. 69, pp. 277-302, 2000.
36. B. Long and C. Fairchild, "Paclitaxel inhibits progression of mitotic cells to G1 phase by interference with spindle formation without affecting other microtubule functions during anaphase and telephase," *Cancer Res*, vol. 54, no. 16, pp. 4355-4361, 1994.
37. M. Jordan, K. Wendell, S. Gardiner, W. Derry, H. Copp and L. Wilson, "Mitotic block induced in HeLa cells by low concentrations of paclitaxel (Taxol) results in abnormal mitotic exit and apoptotic cell death," *Cancer Res*, vol. 56, no. 4, pp. 816-825, 1996.

38. J.-W. Shin and D. J. Mooney, "Shin, J.-W., & Mooney, D. J. (2016). Extracellular matrix stiffness causes systematic variations in proliferation and chemosensitivity in myeloid leukemias," *Proceedings of the National Academy of Sciences of the United States of America*, vol. 113, no. 43, pp. 12126-12131, 2016.
39. C. J. Lovitt, T. B. Shelper and V. M. Avery, "Doxorubicin resistance in breast cancer cells is mediated by extracellular matrix proteins," *BMC Cancer*, vol. 18, no. 1, p. 41, 2018.
40. V. Estrella, T. Chen, M. Lloyd, J. Wojtkowiak, H. Cornnell, A. Ibrahim-Hashim, K. Bailey, Y. Balagurunathan, J. Rothberg, B. Sloane, J. Johnson, R. Gatenby and R. Gillies, "Acidity generated by the tumor microenvironment drives local invasion," *Cancer Res*, vol. 73, no. 5, pp. 1524-1535, 2013.

### CHAPTER 3

1. R. Hynes, "The extracellular matrix: Not just pretty fibrils," *Science*, vol. 326, pp. 1216-1219, 2009.
2. W. Daley, S. Peters and M. Larsen, "Extracellular matrix dynamics in development and regenerative medicine," *J Cell Sci*, vol. 121, pp. 255-264, 2008.
3. E. T. Goddard, R. C. Hill, A. Barrett, C. Betts, Q. Guo, O. Maller, V. F. Borges, K. C. Hansen and P. Schedin, "Quantitative extracellular matrix proteomics to study mammary and liver tissue microenvironments," *International Journal of Biochemistry and Cell Biology*, vol. 81, pp. 223-232, 2017.
4. P. Lu, K. Takai, V. Weaver and Z. Werb, "Extracellular matrix degradation and remodeling in development and disease," *Cold Spring Harb Perspect Biol*, vol. 3, no. 12, pp. 1-24, 2011.
5. T. Cawston and D. Young, "Proteinases involved in matrix turnover during cartilage and bone breakdown," *Cell Tissue Res*, vol. 339, no. 1, pp. 221-235, 2010.
6. L. Hite, J. Shannon, J. Bjarnason and J. Fox, "Sequence of a cDNA clone encoding the zinc metalloproteinase hemorrhagic toxin e from *Crotalus atrox*: evidence for signal, zymogen, and disintegrin-like structures," *Biochemistry*, vol. 31, no. 27, pp. 6203-6211, 1992.
7. K. Kuno, N. Kanada, E. Nakashima, F. Fujiki, F. Ichimura and K. Matsushima, "Molecular cloning of a gene encoding a new type of metalloproteinase-disintegrin family protein with thrombospondin motifs as an inflammation associated gene," *J Biol Chem*, vol. 272, no. 1, pp. 556-562, 1997.
8. G. Murphy, "The ADAMs: signalling scissors in the tumour microenvironment," *Nat Rev Cancer*, vol. 8, no. 12, pp. 929-941, 2008.

9. J. White, "ADAMs: modulators of cell-cell and cell-matrix interactions," *Curr Opin Cell Biol*, vol. 15, no. 5, pp. 598-606, 2003.
10. M. Kruse, C. Becker, D. Lottaz, D. Köhler, I. Yiallourous, H. Krell, E. Sterchi and W. Stöcker, "Human meprin alpha and beta homo-oligomers: cleavage of basement membrane proteins and sensitivity to metalloprotease inhibitors," *Biochem J*, vol. 378, pp. 383-389, 2004.
11. H. Smith and C. Marshall, "Regulation of cell signalling by uPAR," *Nat Rev Mol Cell Biol*, vol. 11, no. 1, pp. 23-36, 2010.
12. A. Bonnefoy and C. Legrand, "Proteolysis of subendothelial adhesive glycoproteins (fibronectin, thrombospondin, and von Willebrand factor) by plasmin, leukocyte cathepsin G, and elastase," *Thromb Res*, vol. 98, no. 4, pp. 323-332, 2000.
13. M. Mohammed and B. Sloane, "Cysteine cathepsins: multifunctional enzymes in cancer," *Nat Rev Cancer*, vol. 6, no. 10, pp. 764-775, 2006.
14. L. G. Vincent, Y. S. Choi, B. Alonso-Latorre, J. C. Álamo and A. J. Engler, "Mesenchymal Stem Cell Durotaxis Depends on Substrate Stiffness Gradient Strength," *Biotechnol J*, vol. 8, no. 4, pp. 472-484, 2013.
15. G. J. Goreczny, D. B. Wormer and C. E. Turner, "A Simplified System for Evaluating Cell Mechanosensing and Durotaxis In Vitro," *J Vis Exp*, no. 102, p. e52949, 2015.
16. M. Guvendiren and J. A. Burdick, "Stiffening hydrogels to probe short- and long-term cellular responses to dynamic mechanics," *Nature Communications*, vol. 3, pp. 792-799, 2012.
17. B. M. Gillette, J. A. Jensen, M. Wang, J. Tchao and S. K. Sia, "Dynamic Hydrogels: Switching of 3D Microenvironments Using Two-Component Naturally Derived Extracellular Matrices," *Advanced Materials*, vol. 22, pp. 686-691, 2010.
18. B. Diop-Frimpong, V. Chauhan, S. Krane, Y. Boucher and R. Jain, "Losartan Inhibits Collagen I Synthesis and Improves the Distribution and Efficacy of Nanotherapeutics in Tumors," *Proc Natl Acad Sci USA*, vol. 108, no. 7, pp. 2909-2914, 2011.
19. V. Chauhan, J. Martin, H. Liu, D. Lacorre, S. Jain, S. Kozin, T. Stylianopoulos, A. Mousa, X. Han, P. Adstamongkonkul, Z. Popovic, P. Huang, M. Bawendi, Y. Boucher and R. Jain, "Angiotensin Inhibition Enhances Drug Delivery and Potentiates Chemotherapy by Decompressing Tumour Blood Vessels," *Nat Commun*, vol. 4, p. 2516, 013.
20. J. Liu, S. Liao, B. Diop-Frimpong, W. Chen, S. Goel, K. Naxerova, M. Ancukiewicz, Y. Boucher, R. Jain and L. Xu, "TGF-Blockade Improves the Distribution and Efficacy of Therapeutics in Breast Carcinoma by Normalizing the Tumor Stroma," *Proc Natl Acad Sci USA*, vol. 109, no. 41, pp. 16618-16623, 2012.

21. H. Morohashi, A. Kon, M. Nakai, M. Yamaguchi, I. Kakizaki, S. Yoshihara, M. Sasaki and K. Takagaki, "Study of Hyaluronan Synthase Inhibitor, 4-Methylumbelliferone Derivatives on Human Pancreatic Cancer Cell (KP1-NL)," *Biochem Biophys Res Commun*, vol. 345, no. 4, pp. 1454-1459, 2006.
22. T. Saito, D. Tamura, T. Nakamura, Y. Makita, H. Ariyama, K. Komiyama, T. Yoshihara and R. Asano, "4-Methylumbelliferone Leads to Growth Arrest and Apoptosis in Canine Mammary Tumor Cells," *Oncol Rep*, vol. 29, no. 1, pp. 335-342, 2013.
23. H. Nakazawa, S. Yoshihara, D. Kudo, H. Morohashi, I. Kakizaki, A. Kon, K. Takagaki and M. Sasaki, "4-Methylumbelliferone, a Hyaluronan Synthase Suppressor, Enhances the Anticancer Activity of Gemcitabine in Human Pancreatic Cancer Cells," *Cancer Chemother Pharmacol*, vol. 57, no. 2, pp. 165-170, 2006.
24. A. Kohli, S. Kivimäe, M. Tiffany and F. Szoka, "Improving the Distribution of Doxil in the Tumor Matrix by Depletion of Tumor Hyaluronan," *J Controlled Release*, vol. 191, no. 1-2, pp. 105-114, 2014.
25. C. J. Lovitt, T. B. Shelper and V. M. Avery, "Doxorubicin resistance in breast cancer cells is mediated by extracellular matrix proteins," *BMC Cancer*, vol. 18, no. 1, p. 41, 2018.
26. M. H. Joyce, C. Lu, E. R. James, R. Hegab, S. C. Allen, L. J. Suggs and A. Brock, "Phenotypic Basis for Matrix Stiffness-Dependent Chemoresistance of Breast Cancer Cells to Doxorubicin," *Front Oncol*, vol. 8, p. 337, 2018.
27. R. S. Stowers, S. C. Allen and L. J. Suggs, "Dynamic phototuning of 3D hydrogel stiffness," *Proceedings of the National Academy of Sciences*, vol. 112, no. 7, pp. 1953-1958, 2015.
28. P. Ahl, L. Chen, W. Perkins, S. Minchey, L. Boni, T. Taraschi and A. Janoff, "Interdigitation-fusion: a new method for producing lipid vesicles of high internal volume," *Biochim Biophys Acta*, vol. 1195, no. 2, pp. 237-244, 1994.
29. K. T. Dicker, L. A. Gurski, S. Pradhan-Bhatt, R. L. Witt, M. C. Farach-Carson and X. Jia, "Hyaluronan: A Simple Polysaccharide with Diverse Biological Functions," *Acta Biomater*, vol. 10, no. 4, pp. 1558-1570, 2014.

## CHAPTER 4

1. Y. Wu, M. Sarkissyan and J. V. Vadgama, "Epithelial-Mesenchymal Transition and Breast Cancer," *Journal of Clinical Medicine*, vol. 5, no. 2, 2016.
2. M. Fedele, L. Cerchia and G. Chiappetta, "The Epithelial-to-Mesenchymal Transition in Breast Cancer: Focus on Basal-Like Carcinomas," *Cancers (Basel)*, vol. 9, no. 10, p. 134, 2017.

3. F. Liu, L.-N. Gu, B.-E. Shan, C.-Z. Geng and M.-X. Sang, "Biomarkers for EMT and MET in breast cancer: An update," *Oncology Letters*, vol. 12, no. 6, pp. 4869-4876, 2016.
4. J. Massagué, S. W. Blain and R. S. Lo, "TGF $\beta$  Signaling in Growth Control, Cancer, and Heritable Disorders," *Cell*, vol. 103, no. 2, pp. 295-309, 2000.
5. J. Massagué, "TGF $\beta$  in Cancer," *Cell*, vol. 134, no. 2, pp. 215-230, 2008.
6. J. Yook, X. Li, I. Ota, C. Hu, H. Kim, N. Kim, S. Cha, J. Ryu, Y. Choi, J. Kim, E. Fearon and S. Weiss, "A Wnt-Axin2-GSK3 $\beta$  cascade regulates Snail1 activity in breast cancer cells," *Nat Cell Biol*, vol. 8, no. 12, pp. 1398-1406, 2006.
7. M. Conacci-Sorrell, I. Simcha, T. Ben-Yedidia, J. Blechman, P. Savagner and A. Ben-Ze'ev, "Autoregulation of E-cadherin expression by cadherin-cadherin interactions: the roles of beta-catenin signaling, Slug, and MAPK," *J Cell Biol*, vol. 163, no. 4, pp. 847-857, 2003.
8. L. Howe, O. Watanabe, J. Leanard and A. Brown, "Twist is up-regulated in response to Wnt1 and inhibits mouse mammary cell differentiation," *Cancer Res*, vol. 63, no. 8, pp. 1906-1913, 2003.
9. H. Clevers, "Wnt/beta-catenin signaling in development and disease," *Cell*, vol. 127, no. 3, pp. 469-480, 2006.
10. S. Pohl, N. Brook, M. Agostino, F. Arfuso, A. Kumar and A. Dharmarajan, "Wnt signaling in triple-negative breast cancer," *Oncogenesis*, vol. 6, no. 4, p. e310, 2017.
11. T. DiMeo, K. Anderson, P. Phadke, C. Fan, C. Perou, S. Naber and C. Kuperwasser, "A novel lung metastasis signature links Wnt signaling with cancer cell self-renewal and epithelial-mesenchymal transition in basal-like breast cancer," *Cancer Res*, vol. 69, no. 13, pp. 5364-5373, 2009.
12. N. Mukherjee, N. Bhattacharya, N. Alam, A. Roy, S. Roychoudhury and C. K. Panda, "Subtype-specific alterations of the Wnt signaling pathway in breast cancer: Clinical and prognostic significance," *Cancer Science*, vol. 103, no. 2, pp. 210-220, 2012.
13. K. Harvey, X. Zhang and D. Thomas, "The Hippo pathway and human cancer," *Nat Rev Cancer*, vol. 13, no. 4, pp. 246-257, 2013.
14. D. D. Shao, W. Xue, E. B. Krall, A. Bhutkar, F. Piccioni, X. Wang, A. C. Schinzel, S. Sood, J. Rosenbluh, J. W. Kim, Y. Zwang, T. M. Roberts, D. E. Root, T. Jacks and W. C. Hahn, "KRAS and YAP1 converge to regulate EMT and tumor survival," *Cell*, vol. 158, no. 1, pp. 171-184, 2014.
15. J. Lamar, P. Stern, H. Liu, J. Schindler, Z. Jiang and R. Hynes, "The Hippo pathway target, YAP, promotes metastasis through its TEAD-interaction domain," *Proc Natl Acad Sci USA*, vol. 109, no. 37, pp. 2441-2450, 2012.

16. D. Chen, Y. Sun, Y. Wei, P. Zhang, A. Rezaeian and J. Teruya-Feldstein, "LIFR is a breast cancer metastasis suppressor upstream of the Hippo-YAP pathway and a prognostic marker," *Nat Med*, vol. 18, pp. 1511-1517, 2012.
17. O. M, J. Zhang, G. Smolen, B. Muir, W. Li, D. Sgroi, C. Deng, J. Brugge and D. Haber, "Transforming properties of YAP, a candidate oncogene on the chromosome 11q22 amplicon," *Proc Natl Acad Sci USA*, vol. 103, no. 33, pp. 12405-12410, 2006.
18. S. Piccolo, M. Cordenonsi and S. Dupont, "Molecular pathways: YAP and TAZ take center stage in organ growth and tumorigenesis," *Clin Cancer Res*, vol. 19, pp. 4925-4930, 2013.
19. M. Aragona, T. Panciera, A. Manfrin, S. Giullitti, F. Michielin and N. Elvassore, "A mechanical checkpoint controls multicellular growth through YAP/TAZ regulation by actin-processing factors," *Cell*, vol. 154, pp. 1047-1059, 2013.
20. V. Codelia, G. Sun and K. Irvine, "Regulation of YAP by Mechanical Strain through Jnk and Hippo Signaling," *Curr Biol*, vol. 24, pp. 2012-2017, 2014.
21. C.-L. Chen, M. Schroeder, M. Kango-Singh, C. Tao and G. Halder, "Tumor suppression by cell competition through regulation of the Hippo pathway," *Proc Natl Acad Sci USA*, vol. 109, pp. 484-489, 2011.
22. G. Sun and K. Irvine, "Regulation of Hippo signaling by Jun kinase signaling during compensatory cell proliferation and regeneration, and in neoplastic tumors," *Dev Biol*, vol. 350, pp. 139-151, 2011.
23. S. Dupont, L. Morsut, M. Aragona, E. Enzo, S. Giullitti and M. Cordenonsi, "Role of YAP/TAZ in mechanotransduction," *Nature*, vol. 474, pp. 179-183, 2011.
24. B. Zhao, L. Li, L. Wang, C.-Y. Wang, J. Yu and K.-L. Guan, "Cell detachment activates the Hippo pathway via cytoskeleton reorganization to induce anoikis," *Genes Dev*, vol. 26, pp. 54-68, 2012.
25. A. Bonnefoy and C. Legrand, "Proteolysis of subendothelial adhesive glycoproteins (fibronectin, thrombospondin, and von Willebrand factor) by plasmin, leukocyte cathepsin G, and elastase," *Thromb Res*, vol. 98, no. 4, pp. 323-332, 2000.
26. K.-I. Wada, K. Itoga, T. Okano, S. Yonemura and H. Sasaki, "Hippo pathway regulation by cell morphology and stress fibers," *Development*, vol. 138, pp. 3907-3914, 2011.
27. C. DuFort, M. Paszek and V. Weaver, "Balancing forces: architectural control of mechanotransduction," *Nat Rev Mol Cell Biol*, vol. 12, pp. 308-319, 2011.
28. C. Nelson and M. Bissell, "Of extracellular matrix, scaffolds, and signaling: tissue architecture regulates development, homeostasis, and cancer," *Annu Rev Cell Dev Biol*, vol. 22, pp. 287-309, 2006.

29. P. Schedin and P. Keely, "Mammary gland ECM remodeling, stiffness, and mechanosignaling in normal development and tumor progression," *Cold Spring Harb Perspect Biol*, vol. 3, p. a003228, 2011.
30. X. Zhang, Z. Zhang, Q. Zhang, Q. Zhang, P. X. R. Sun, G. Ren and S. Yang, "ZEB1 confers chemotherapeutic resistance to breast cancer by activating ATM," *Cell Death & Disease*, vol. 9, pp. 57-72, 2018.
31. N. M. Aiello, R. Maddipati, R. J. Norgard, D. Balli, J. Li, S. Yuan, T. Yamazoe, T. Black, A. Sahmoud, E. E. Furth, D. Bar-Sagi and B. Z. Stanger, "EMT Subtype Influences Epithelial Plasticity and Mode of Cell Migration," *Developmental Cell*, vol. 45, pp. 681-695, 2018.
32. A. J. Rice, E. Cortes, D. Lachowski, B. Cheung, S. Karim, J. Morton and A. del Río Hernández, "Matrix stiffness induces epithelial–mesenchymal transition and promotes chemoresistance in pancreatic cancer cells," *Oncogenesis*, vol. 6, no. 7, p. e352, 2017.